



Estudios de resonancia magnética y técnicas electrofisiológicas para evaluar y predecir la discapacidad en pacientes con esclerosis múltiple

Sara Llufriu Duran

ADVERTIMENT. La consulta d'aquesta tesi queda condicionada a l'acceptació de les següents condicions d'ús: La difusió d'aquesta tesi per mitjà del servei TDX (www.tdx.cat) i a través del Dipòsit Digital de la UB (deposit.ub.edu) ha estat autoritzada pels titulars dels drets de propietat intel·lectual únicament per a usos privats emmarcats en activitats d'investigació i docència. No s'autoritza la seva reproducció amb finalitats de lucre ni la seva difusió i posada a disposició des d'un lloc aliè al servei TDX ni al Dipòsit Digital de la UB. No s'autoritza la presentació del seu contingut en una finestra o marc aliè a TDX o al Dipòsit Digital de la UB (framing). Aquesta reserva de drets afecta tant al resum de presentació de la tesi com als seus continguts. En la utilització o cita de parts de la tesi és obligat indicar el nom de la persona autora.

ADVERTENCIA. La consulta de esta tesis queda condicionada a la aceptación de las siguientes condiciones de uso: La difusión de esta tesis por medio del servicio TDR (www.tdx.cat) y a través del Repositorio Digital de la UB (deposit.ub.edu) ha sido autorizada por los titulares de los derechos de propiedad intelectual únicamente para usos privados emmarcados en actividades de investigación y docencia. No se autoriza su reproducción con finalidades de lucro ni su difusión y puesta a disposición desde un sitio ajeno al servicio TDR o al Repositorio Digital de la UB. No se autoriza la presentación de su contenido en una ventana o marco ajeno a TDR o al Repositorio Digital de la UB (framing). Esta reserva de derechos afecta tanto al resumen de presentación de la tesis como a sus contenidos. En la utilización o cita de partes de la tesis es obligado indicar el nombre de la persona autora.

WARNING. On having consulted this thesis you're accepting the following use conditions: Spreading this thesis by the TDX (www.tdx.cat) service and by the UB Digital Repository (deposit.ub.edu) has been authorized by the titular of the intellectual property rights only for private uses placed in investigation and teaching activities. Reproduction with lucrative aims is not authorized nor its spreading and availability from a site foreign to the TDX service or to the UB Digital Repository. Introducing its content in a window or frame foreign to the TDX service or to the UB Digital Repository is not authorized (framing). Those rights affect to the presentation summary of the thesis as well as to its contents. In the using or citation of parts of the thesis it's obliged to indicate the name of the author.



TESIS DOCTORAL

Estudios de resonancia magnética y técnicas electrofisiológicas
para evaluar y predecir la discapacidad en pacientes con
esclerosis múltiple

Doctorando

SARA LLUFRIU DURAN

Directores

Dr. Albert Saiz Hinarejos

Dra. Yolanda Blanco Morgado

PROGRAMA DOCTORADO MEDICINA

UNIVERSITAT DE BARCELONA

2013

INFORME DE LOS DIRECTORES DE LA TESIS

El Dr. ALBERT SAIZ HINAREJOS, Doctor en Medicina por la Universitat de Barcelona, Coordinador de la Unidad de Neuroinmunología y Esclerosis Múltiple del Servicio de Neurología del Hospital Clínic de Barcelona, y la Dra. YOLANDA BLANCO MORGADO, Doctora en Medicina por la Universitat de Barcelona y Especialista Sénior en Neurología del Servicio de Neurología del Hospital Clínic de Barcelona,

CERTIFICAN:

Que la memoria titulada “Estudios de resonancia magnética y técnicas electrofisiológicas para evaluar y predecir la discapacidad en pacientes con esclerosis múltiple”, presentada por Sara Llufriu Duran para optar al grado de Doctor en Medicina por la Universitat de Barcelona se ha realizado bajo nuestra dirección y cumple todos los requisitos necesarios para ser defendida ante el Tribunal correspondiente.

Firmado,

Dr. Albert Saiz Hinarejos

*Unidad de Neuroinmunología y Esclerosis
Múltiple
Servicio de Neurología
Hospital Clínic de Barcelona*

Dra. Yolanda Blanco Morgado

*Unidad de Neuroinmunología y Esclerosis
Múltiple
Servicio de Neurología
Hospital Clínic de Barcelona*

Barcelona, Septiembre de 2013

Índice

I.	Agradecimientos	7
II.	Presentación	11
III.	Glosario de abreviaturas	15
IV.	Introducción	19
	1. Introducción a la esclerosis múltiple	21
	2. Historia natural	21
	3. Fisiopatología	23
	4. Discapacidad física y cognitiva asociada a la EM	24
	4.1 Condicionantes de la discapacidad	24
	4.2 Disfunción cognitiva	25
	4.3 Escalas de evaluación	26
	5. Biomarcadores	27
	5.1 Estudios electrofisiológicos	28
	5.2 Biomarcadores de imagen en RM	29
	5.2.1 Técnicas de RM convencional	30
	5.2.2 Técnicas de RM no convencional o avanzada	31
	5.2.3 Trabajo de Revisión	35
V.	Hipótesis	45
VI.	Objetivos	49
VII.	Resultados	53
	1. Trabajo 1: T2 hypointense rims and ring-enhancing lesions in MS	55
	2. Trabajo 2: Influence of Corpus Callosum Damage on Cognition and Physical Disability in Multiple Sclerosis: A Multimodal Study	67
	3. Trabajo 3: Cognitive functions in multiple sclerosis: impact of gray matter integrity ..	77
	4. Trabajo 4: MR Spectroscopy Markers of Disease Progression in Multiple Sclerosis (en preparación)	95
VIII.	Discusión	123
IX.	Conclusiones	135
X.	Bibliografía	139

I. Agradecimientos

Esta tesis doctoral es el fruto de años de trabajo y no habría sido posible sin la ayuda de muchas personas, algunas de las cuales cito a continuación.

En primer lugar quiero dar las gracias a los directores de esta tesis que son el pilar fundamental sin el cual no hubiera sido posible llegar a completarla. Al Dr. Albert Saiz, que apostó por un proyecto de futuro, con gran esfuerzo y una implicación máxima. No tengo palabras para agradecerle aquellas horas, que aunque a veces duras, hemos pasado trabajando codo con codo para acabar los artículos. A la Dra. Yolanda Blanco por estar siempre ahí, con su visión práctica y enorme paciencia, apoyándome y siempre disponible ante cualquier duda.

También quiero agradecer al Dr. Graus su apoyo y las sabias recomendaciones que me ha dado a lo largo de estos años. Al Dr. Pablo Villoslada le agradezco las múltiples iniciativas para impulsar la neuroimagen en nuestro centro y la colaboración en los trabajos de esta tesis.

Otra persona absolutamente imprescindible ha sido Eloy Martínez. Ambos empezamos de la nada pero hemos conseguido combinar de una forma eficaz el lenguaje técnico y clínico creando un tandem perfecto. Gracias por su gran implicación y por ponerle una sonrisa a cada dificultad que nos encontrábamos.

A mis compañeras del equipo de EM, María, Montse y Nuria. No sólo compañeras sino amigas, el apoyo mutuo en el trabajo y las risas en las charlas diarias durante las comidas han sido una válvula de escape. Con Iñigo hemos compartido dificultades derivadas de empezar un camino nuevo como la neuroimagen pero las hemos capeado con buen hacer y formando un equipo unido. Elena se ha unido recientemente al equipo y su eficaz organización nos ha ayudado a acelerar los pasos.

El Dr. Josep Valls y Jordi Casanova me introdujeron en el mundo de la electrofisiología. Al Dr. Valls le agradezco su apoyo en el diseño y la realización de los estudios neurofisiológicos, es admirable su capacidad de desarrollar nuevas ideas. A Jordi le agradezco que estuviera siempre disponible, que se sentara conmigo durante horas a analizar los datos, le agradezco sus enormes ganas de ayudar. También quiero dar las gracias al Dr. Joan Santamaría, al Dr. Álex Iranzo y a los técnicos de EMG.

A los radiólogos Joan Berenguer, Nuria Bargalló Teresa Pujol y attia arcia por la ayuda en el diseño de los protocolos de imagen y su implicación en los trabajos de esta tesis, y

AGRADECIMIENTOS

a César Garrido por su ayuda con las nuevas secuencias. También a Carles Falcón por su inestimable asesoramiento técnico.

El Dr. Daniel Pelletier, mi mentor en la UCSF, me acogió en su laboratorio y me permitió participar en un gran proyecto. Esa estancia significó un antes y un después en mi formación.

A Juan, mi amigo y “ex-coR”, quiero darle las gracias por la ayuda que me ofreció en el estudio que trata sobre la cognición y sobretodo por su amistad en los buenos y malos momentos. También a amigos como Laura, Judith, Mircea y Manu con los que he compartido muchos momentos especiales dentro y fuera del hospital.

A Sergi, mi gran apoyo. Admiro su capacidad de trabajo, de sacrificio, su inteligencia, disfruto de sus bromas, de su amor. Él es el contrapunto necesario en mi vida.

A mi familia, sin la que no hubiera conseguido estar donde estoy. Mi madre, que tiene una capacidad de sacrificio por los demás que no he visto en nadie más. Recuerdo como casi convirtió nuestra casa en un monasterio para que yo pudiera preparar el MIR. Mi padre, que siempre ha estado ahí y me ha animado a ser una persona sensible y espiritual. Mi hermano al que quiero muchísimo. Se que él puede conseguir lo que quiera en la vida. Mi abuela Ramona, mujer adelantada a su tiempo, es un honor para mí que ella haya vivido a través de mi vida algunas de las cosas que no pudo hacer por ser mujer. También al resto de mi familia, tanto a los que están como a los que no. Y a mis amigas de siempre, con las que me une una amistad que permite que el tiempo parezca que no haya pasado.

Por último, los pacientes que han participado en los estudios me han mostrado una gran voluntad de superación y una implicación maravillosa. Les agradezco profundamente su buena disponibilidad.

II. Presentación



Esta tesis doctoral se estructura según las directrices de la normativa para la presentación de tesis doctorales como compendio de publicaciones aprobada por la Comisión de Doctorado del Consejo de Gobierno en fecha 24 de Julio de 2008 y modificada el 28 de Abril de 2010, al amparo del régimen previsto en el RD 99/2011 del 28 de Enero.

La presente memoria se basa en cuatro artículos originales y un artículo de revisión que pertenecen a una misma línea de trabajo: el uso de técnicas de resonancia magnética (RM) y electrofisiológicas para evaluar y predecir la discapacidad física o cognitiva en pacientes con esclerosis múltiple (EM). En primer lugar, a través de RM convencional se ha evaluado el comportamiento radiológico de determinados patrones de lesiones cerebrales y su asociación con una peor evolución de la discapacidad. En segundo lugar se ha realizado un estudio multimodal del cuerpo calloso utilizando de forma conjunta técnicas electrofisiológicas con RM avanzada para indagar en el papel de la alteración de dicha estructura sobre la discapacidad física y cognitiva. En tercer lugar se han utilizado diversas técnicas de RM avanzada para evaluar la integridad del tejido cerebral tanto de la sustancia gris como de la sustancia blanca y su relación con el rendimiento de diversas funciones cognitivas. En cuarto lugar, se ha investigado la capacidad de marcadores de desmielinización, daño axonal y astrogliosis en RM avanzada para predecir la discapacidad y la atrofia cerebral a medio plazo. Este último trabajo, actualmente en preparación, fue seleccionado para ser presentado en la “Contemporary Clinical Issues Plenary Session” de la Academia Americana de Neurología celebrada en Nueva Orleans en Abril de 2012.

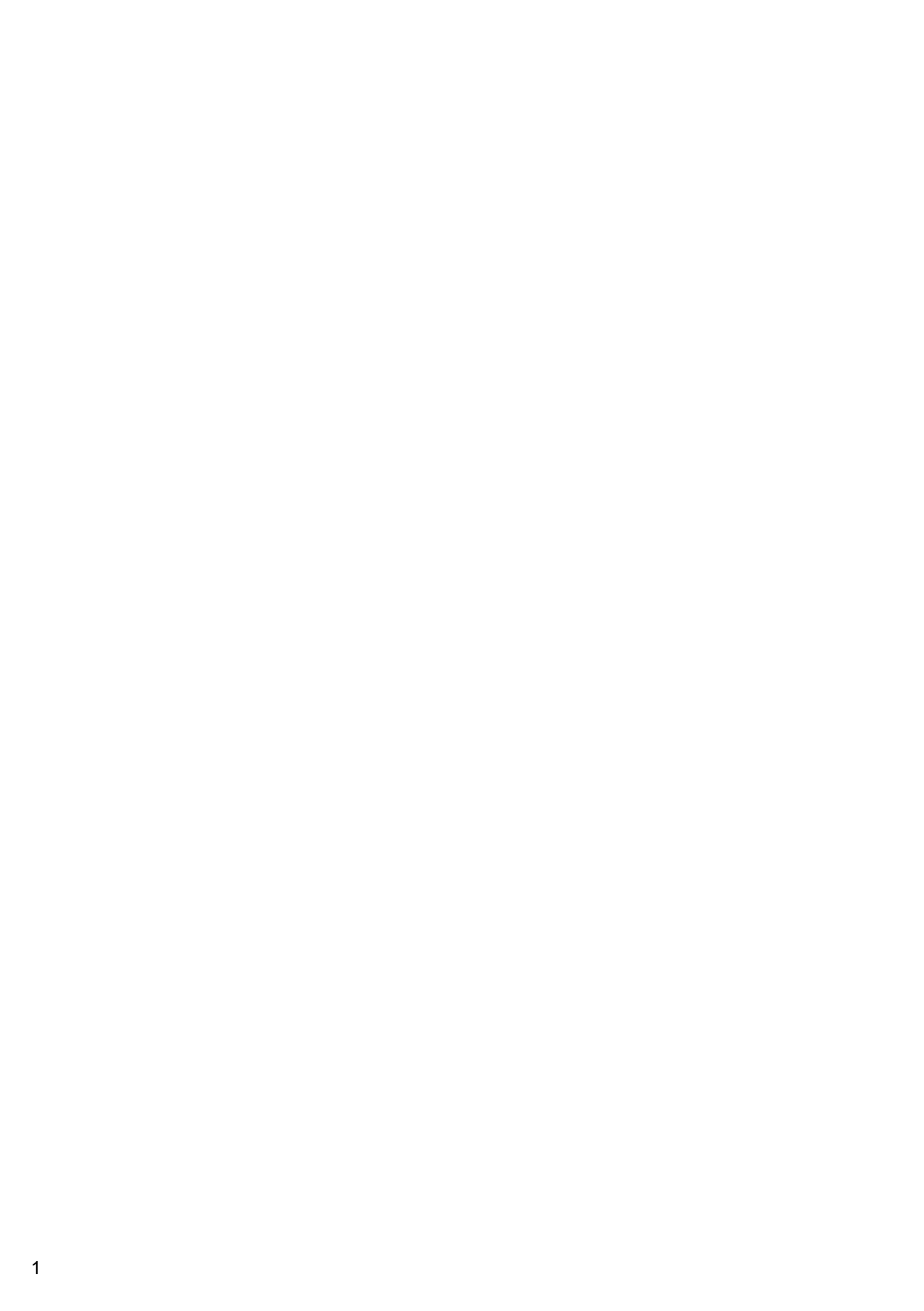
Estos estudios han servido para profundizar en el conocimiento de la fisiopatología de los condicionantes de la discapacidad, y en el avance en la búsqueda de marcadores de RM y electrofisiológicos útiles para evaluar y predecir la discapacidad en la EM.

El presente trabajo ha sido financiado por el Hospital Clínic de Barcelona a través de un Premio Fin de Residencia Emili Letang y por el Institut d’Investigacions Biomèdiques August Pi i Sunyer (IDIBAPS) y el Instituto de Salud Carlos III mediante un contrato Rio Hortega, junto con aportaciones del Instituto de Salud Carlos III a través de los proyectos de la Red Española de Esclerosis Múltiple RD07/0060/0012 (Dr. Albert Saiz y Dr. Francesc Graus) y FIS PS09/00259 (Dr. Pablo Villoslada).

El factor de impacto acumulado de los artículos que componen la presente tesis es de 12.67 según ISI-Web of KnowledgeSM – Journal Citation Reports® de 2012.



III. Glosario de abreviaturas



AF	Anisotropía fraccional
BHE	Barrera hematoencefálica
BOC	Bandas oligoclonales
BPF	Brain parenchymal fraction
BRB-N	Batería Neuropsicológica Repetitiva Breve (siglas en inglés)
CC	Cuerpo calloso
DA	Difusividad axial
DM	Difusividad media
DR	Difusividad radial
DTI	Diffusion tensor imaging
EDSS	Expanded Disability Status Scale
EM	Esclerosis múltiple
EMCD	Esclerosis múltiple clínicamente definida
EMPP	Esclerosis múltiple primariamente progresiva
EMRR	Esclerosis múltiple remitente-recidivante
EMSP	Esclerosis múltiple secundariamente progresiva
FLAIR	Fluid-Attenuated Inversion Recovery
iSP	Ipsilateral silent period
mI	Mioinositol
LCR	Líquido cefalorraquídeo
MSFC	Multiple Sclerosis Functional Composite
MWF	Myelin water fraction
NAA	N-acetil aspartato
PASAT	Paced Auditory Serial Addition Test
PBVC	Percentage of brain parenchymal volume change
PE	Potenciales evocados
RM	Resonancia magnética
SB	Sustancia blanca
SBAN	Sustancia blanca de apariencia normal
SG	Sustancia gris
SNA	Síndrome neurológico aislado
SNC	Sistema nervioso central
SPART	10/36 Spatial Recall Test
SPART-D	10/36 Spatial Delayed Recall Test
SRT	Selective Reminding Test
TMS	Transcranial Magnetic Stimulation
WLG	Word List Generation



IV. Introducción

1. Introducción a la esclerosis múltiple

La esclerosis múltiple (EM) es una enfermedad inflamatoria crónica y neurodegenerativa del sistema nervioso central (SNC) de etiología desconocida aunque probablemente multifactorial en que se combinan una susceptibilidad genética y causas ambientales (Marrie, 2004; Compston and Coles, 2008). Afecta predominantemente a adultos jóvenes, con un pico de incidencia en la tercera década de la vida (Compston and Coles, 2008). Además, es la causa no traumática más frecuente de discapacidad en este grupo poblacional en el mundo occidental y tiene importantes consecuencias en la vida profesional, familiar y social de los enfermos.

La prevalencia de la enfermedad incrementa con la distancia hacia el norte o el sur desde el ecuador (Simpson et al., 2011). En España, los estudios epidemiológicos sitúan la prevalencia en la franja de riesgo medio-alto de desarrollo de la enfermedad (Pugliatti et al., 2006) y parecen indicar que está incrementando, con unos 80 casos/100.000 habitantes en la región de Cataluña en la actualidad (Otero-Romero et al., 2012). Asimismo, la prevalencia a nivel mundial también parece estar aumentando, probablemente a expensas de un mayor incremento en mujeres (Koch-Henriksen and Sorensen, 2010).

2. Historia natural

El 85% de los pacientes inician la enfermedad con un episodio agudo que afecta una (o a veces varias) localizaciones neurológicas, conocido como un síndrome neurológico aislado (SNA) (Confavreux and Vukusic, 2006; Scalfari et al., 2010; Miller et al., 2012). Cuando esto se acompaña de lesiones en la sustancia blanca (SB) detectadas por resonancia magnética (RM) convencional en lugares clínicamente silentes, la proporción de sujetos que presentan un segundo brote de desmielinización es del 82% a lo largo de los siguientes 20 años mientras que en caso de no presentar lesiones la proporción es únicamente del 20% (Fisniku et al., 2008).

El diagnóstico de la enfermedad requiere que la clínica o las lesiones visibles en RM se repitan a lo largo del tiempo y afecten a diferentes regiones del SNC (Polman et al., 2011). Al presentar el segundo brote de la enfermedad el paciente cumple criterios clínicos de esclerosis múltiple remitente-recidivante (EMRR) (Polman et al., 2011). Los nuevos episodios de desmielinización ocurren de forma errática, y la tasa anualizada de brotes suele estar entre 0.3

INTRODUCCIÓN

y 1.7 episodios/año (Inusah et al., 2010). Inicialmente estos episodios de disfunción neurológica o brotes se suelen recuperar de forma completa, pero con el tiempo la recuperación de algunos episodios es incompleta y se acumulan síntomas residuales. Es destacable que el número de episodios, sus manifestaciones clínicas y la capacidad de recuperación son muy variables de un paciente a otro e incluso pueden ser diferentes a lo largo del tiempo en un mismo paciente (Compston and Coles, 2008). Por ello, se considera que la enfermedad es muy heterogénea, tanto en su presentación como en su evolución y en la respuesta terapéutica.

Eventualmente, alrededor del 65% de los pacientes evolucionan a una fase secundariamente progresiva (EMSP) en la cual la discapacidad empeora de forma sostenida independientemente de la presencia de brotes (Compston and Coles, 2008). El tiempo medio que tardan los pacientes en evolucionar a una fase secundariamente progresiva es de unos 19 años (Vukusic and Confavreux, 2003). Puede considerarse que la fase remitente-recidivante y la secundariamente progresiva representan dos estadios clínicos de la misma enfermedad (Leray et al., 2010).

Se calcula que alrededor de un 10% de los pacientes con EM podría presentar una forma benigna y continuar con una discapacidad muy baja tras 20-30 años de enfermedad (Hutchinson, 2012). Sin embargo, el término “benigno” ha sido objeto de debate en los últimos años dado que algunos pacientes que cumplen con esta definición presentan un empeoramiento de su discapacidad de forma tardía, pueden tener disfunción cognitiva o convertir a formas secundariamente progresivas (Portaccio et al., 2009).

Aproximadamente el 10% de los casos presentan un curso progresivo de la discapacidad desde el inicio (Miller et al., 2012). Los pacientes con EM primaria-progresiva (EMPP) empeoran desde el inicio aunque raramente pueden presentar algún brote de forma concomitante. En comparación con pacientes con EMSP inician la enfermedad con una edad mayor, tardan menos en alcanzar una progresión confirmada de la discapacidad y tienen un peor pronóstico funcional (Confavreux and Vukusic, 2006). Estas diferencias clínicas han abierto el debate de si en realidad la EMPP podría ser una enfermedad distinta a las formas recurrentes o si es una forma más del espectro.

3. Fisiopatología

En la EM se produce una infiltración focal en el SNC por linfocitos autorreactivos que lleva a un daño de la mielina y los axones. Al principio de la enfermedad la inflamación es transitoria y existe remielinización (Lassmann, 2008), lo cual caracteriza clínicamente esta primera fase de la enfermedad por episodios transitorios de disfunción neurológica que habitualmente se recuperan. Sin embargo con el tiempo, los cambios patológicos se caracterizan por una activación de la microglia de forma generalizada en el SNC asociada con neurodegeneración extensa y crónica (Frischer et al., 2009; Lassmann et al., 2012; Popescu et al., 2013). El correlato clínico de esta fase tardía es la acumulación progresiva de la discapacidad (Leray et al., 2010). Se ha documentado que la acumulación de la discapacidad persistente a lo largo del tiempo parece ser debida al daño axonal y que la gravedad del daño axonal se correlaciona con el grado de inflamación (Trapp et al., 1998). Aunque en los últimos años han habido grandes avances en el conocimiento de la fisiopatología de la enfermedad, todavía no se conoce con exactitud cuál es la inter-dependencia entre la inflamación focal, la inflamación difusa y la neurodegeneración (Frischer et al., 2009), así como su contribución relativa a los déficits clínicos.

Una de las principales características de la enfermedad es la presencia de lesiones focales en la SB del SNC que pueden visualizarse mediante RM convencional. En los estudios anatopatológicos, las lesiones activas están infiltradas por macrófagos con desechos de mielina, linfocitos y astrocitos reactivos, y aunque existe una preservación parcial de los axones, ya existe daño axonal. Las lesiones crónicas inactivas están bien circunscritas, son hipocelulares, con gliosis fibrilar, pérdida de los axones y los oligodendrocitos son prominentes (Filippi et al., 2012; Popescu et al., 2013).

Se han descrito cuatro patrones distintos de desmielinización en las lesiones focales agudas (Lucchinetti et al., 2000). En el tipo I y II existe desmielinización asociada a inflamación por linfocitos T activados y macrófagos. Además, en el tipo II existe también un depósito de inmunoglobulinas y complemento. Las lesiones de tipo III y IV, en cambio, parecen tener un daño o distrofia primaria de los oligodendrocitos (Lucchinetti et al., 2000). Estos patrones pueden ser heterogéneos entre distintos pacientes pero suelen ser homogéneos entre las múltiples lesiones de un mismo paciente y pueden ser importantes en la evolución de la enfermedad y la respuesta a tratamientos (Lucchinetti et al., 2000).

A nivel de la sustancia gris (SG) las lesiones son áreas focales de desmielinización donde existe una pérdida de oligodendrocitos y axones. Sin embargo, se diferencian de las lesiones de SB en el grado y tipo de inflamación, en que no existe disfunción de la barrera hematoencefálica (BHE) y además puede apreciarse una marcada inflamación meníngea (Calabrese et al., 2009; Calabrese et al., 2010). Las lesiones corticales son difícilmente visibles a través de secuencias de RM convencional debido a los bajos niveles de infiltración por células inflamatorias, a la ausencia de daño de la BHE y a la baja densidad de mielina en las capas corticales superiores, lo cual disminuye el contraste en dichas secuencias (Popescu et al., 2013).

Asimismo, la afectación del tejido cerebral va más allá de las lesiones circunscritas. Existe una afectación difusa del tejido cerebral con daño de la SB (la llamada sustancia blanca de apariencia normal, SBAN) y de la SG. En la SNBA existe gliosis, desmielinización, infiltración por células redondas pequeñas, presencia de macrófagos, activación de la microglia y de los astrocitos (Filippi et al., 2012). En el córtex puede existir pérdida o atrofia neuronal, resultado de una degeneración anterógrada o retrógrada desde lesiones en la SB, SG profunda u otras áreas corticales (Kolasinski et al., 2012).

4. Discapacidad física y cognitiva asociada a la EM

4.1 Condicionantes de la discapacidad

La EM puede causar síntomas motores, sensitivos, de tronco cerebral, manifestaciones cerebelosas, visuales, esfinterianas, cognitivas y neuropsiquiátricas (Cook, 2006). Los síntomas dependerán mayoritariamente de la localización de los brotes, es decir de la inflamación focal. Dichos síntomas llegan a su máximo pocos días tras el inicio del brote y mejoran a lo largo de las siguientes semanas hasta su recuperación total o parcial. La discapacidad en la EM proviene de la recuperación incompleta de los brotes inflamatorios lo cual refleja el balance entre el daño al SNC y el grado de reparación endógena, así como cambios glióticos y neurodegeneración progresiva irreversible (Frohman et al., 2005; Compston and Coles, 2008). Asimismo, parece ser que el sustrato patológico de la discapacidad permanente, aquella que persiste tras 3-6 meses desde el inicio del empeoramiento, es el daño axonal (Bjartmar et al., 2000; Tallantyre et al., 2010). En las formas progresivas de la enfermedad existe un sustrato patológico distinto, con inflamación difusa y neurodegeneración, que condiciona que la discapacidad sea progresiva (Lassmann et al., 2012). En estos casos

predominan los síntomas medulares, aunque también puede manifestarse como afectación progresiva de nervio óptico, cerebro o tronco cerebral (Compston and Coles, 2008).

4.2 Disfunción cognitiva

La disfunción cognitiva puede estar presente desde etapas iniciales de la enfermedad en algunos pacientes y causar dificultades en el ámbito laboral y social. A pesar de ello ha sido una manifestación de la enfermedad que ha recibido poca atención hasta hace relativamente pocos años. La EM puede causar problemas en la atención, la eficiencia del procesamiento de la información, en funciones ejecutivas, memoria de trabajo y memoria episódica (Chiaravalloti and DeLuca, 2008). Es sabido que las principales funciones cognitivas afectadas son la rapidez de procesamiento de la información, el aprendizaje visual y la memoria episódica (Calabrese, 2006; Chiaravalloti and DeLuca, 2008). La prevalencia de la disfunción cognitiva se sitúa entre el 40-70% de los pacientes con EMRR según las series publicadas (Benedict et al., 2006; Patti, 2009).

Uno de los principales condicionantes de la disfunción cognitiva en la EM parece ser la desconexión funcional entre las estructuras corticales y profundas de SG secundaria al daño de los tractos de la SB (Catani and ffytche, 2005). Sin embargo, actualmente hay datos suficientes en la literatura para creer que la afectación de la SG también juega un papel importante en los cambios cognitivos (Morgen et al., 2006; Pirko et al., 2007; Calabrese et al., 2012; Zivadinov and Pirko, 2012).

Varios estudios de neuroimagen han demostrado que el volumen de las lesiones cerebrales se asocia con la disfunción cognitiva en la EM (Filippi et al., 2010). Además, la atrofia cerebral global o en la corteza, que es un marcador de cambios patológicos destructivos, parece relacionarse con cambios en la función cognitiva (Pelletier et al., 2001; Calabrese et al., 2010). Sin embargo, tanto las medidas globales de lesiones como de atrofia no son capaces de explicar de forma completa las alteraciones cognitivas, probablemente en parte porque son medidas de un daño inespecífico global y no dan información topográfica. En ese sentido, estudiar la relación entre atrofia de determinadas estructuras cerebrales elegidas a priori como el cuerpo calloso (CC) (Pelletier et al., 2001; Mesaros et al., 2009) o el tálamo (Benedict et al., 2006; Benedict et al., 2013), o a través de métodos no-apriorísticos que permitan identificar las regiones relevantes para una función cognitiva sin partir de la elección previa de regiones específicas (Calabrese et al., 2010) puede ser útil para ayudar a explicar mejor la disfunción cognitiva en la EM.

Los avances en RM han permitido incrementar el conocimiento de los condicionantes de la disfunción cognitiva (Filippi et al., 2010; Penny et al., 2010). El daño de la integridad del tejido cerebral (Dineen et al., 2009; Roosendaal et al., 2009; Yu et al., 2012) o la presencia de lesiones (Sepulcre et al., 2008; Sepulcre et al., 2009; Rossi et al., 2012), en determinados tractos de SB se asocia con un peor rendimiento en funciones cognitivas específicas, lo cual va a favor de que existe un síndrome de desconexión en la EM. También la integridad tisular de la SG se ha relacionado con el rendimiento cognitivo (Rovaris et al., 2002). Sin embargo, la asociación entre integridad microestructural en SG a nivel regional y el rendimiento cognitivo no se ha evaluado previamente en la EM. Así, la aplicación de nuevas tecnologías de neuroimagen puede aumentar el conocimiento acerca de la asociación entre estructura cerebral y función.

4.3 Escalas de evaluación

La Escala de Discapacidad Ampliada de Kurtzke (Expanded Disability Status Scale, EDSS) es la más utilizada para medir la discapacidad en la EM tanto en la práctica clínica habitual como en ensayos clínicos (Kurtzke, 1983). Tiene en cuenta la gravedad de la afectación de siete sistemas funcionales y la capacidad de deambulación. Sin embargo, esta escala tiene diversas limitaciones como una baja sensibilidad, una excesiva influencia de la afectación motora en puntuaciones elevadas, una distribución bimodal y una baja reproducibilidad en las puntuaciones más bajas de la escala (Comi and Filippi, 2005).

La Multiple Sclerosis Functional Composite (MSFC) es una escala más reciente que se utiliza principalmente en el ámbito de la investigación (Fischer et al., 1999). Es una medida compuesta que incluye tres tests que evalúan la función de las extremidades superiores e inferiores y las habilidades cognitivas. Su valor se expresa en puntuación z, que indica cuantas desviaciones estándares se desvía la medida respecto a la media de una población de referencia. Es una escala continua que se correlaciona altamente con el EDSS (Miller et al., 2000) pero con la ventaja de ser más sensible a los cambios (Comi and Filippi, 2005).

Una de las principales baterías utilizadas para el cribaje de la disfunción cognitiva en pacientes con EM es la Batería Neuropsicológica Repetitiva Breve (BRB-N) (Rao, National Multiple Sclerosis Society, New York 1991). Dicha batería evalúa las siguientes funciones cognitivas:

- Memoria verbal episódica: se evalúa a través del Selective Reminding Test (SRT) que consta de tres subtests distintos.

- Memoria visual: evaluada a través del 10/36 Spatial Recall Test (SPART) y del SPART diferido (SPART-D)
- Atención y rapidez de procesamiento de la información: Paced Auditory Serial Addition Test (PASAT) y Symbol Digit Modalities Test (SDMT)
- Fluencia verbal asociativa: Word List Generation (WLG).

Esta batería tiene la ventaja de ser de fácil y rápida administración (40-45 minutos), ha demostrado su sensibilidad en distintos estudios y se considera como uno de los métodos de referencia para el cribaje de la disfunción cognitiva en la EM (Camp et al., 2005; Sepulcre et al., 2006). Sin embargo, su principal limitación es que no tiene en cuenta los dominios de funciones ejecutivas superiores y el procesamiento espacial (Benedict and Zivadinov, 2011).

5. Biomarcadores

Un biomarcador se refiere a una característica objetiva que puede ser evaluada y medida, pudiendo reflejar un proceso biológico normal, un proceso patológico o una respuesta a una terapia (Biomarker Definitions Working Group, 2001). Pueden usarse como marcadores subrogados, los cuales no sólo presentan una correlación fuerte y clínicamente significativa con una medida clínica sino que también son capaces de informar sobre el efecto de una terapia modificadora de la enfermedad (Prentice, 1989; Modificado 1997).

La identificación de buenos biomarcadores para la EM, una enfermedad extremadamente compleja y heterogénea, ha sido un objetivo importante de la comunidad científica en los últimos años. Aunque se han realizado importantes esfuerzos muy pocos de ellos han sido validados o integrados en la práctica clínica rutinaria (Fernandez et al., 2013). La dificultad para encontrar biomarcadores en la EM se debe a algunas características intrínsecas de la enfermedad (Rajasekharan and Bar-Or, 2012) como el desconocimiento acerca del mecanismo exacto de la misma, la relativa inaccesibilidad del órgano diana y su gran complejidad biológica.

Un metanálisis de múltiples estudios basados en la historia natural de la enfermedad ha identificado los principales biomarcadores clínicos que se asocian con la evolución de la discapacidad y que pueden ser de utilidad pronóstica (Degenhardt et al., 2009). Entre aquellos factores pronósticos negativos, en todos los grupos de pacientes con EM, está el inicio de la fase progresiva y el grado de discapacidad a los 2 y 5 años tras el diagnóstico. En pacientes con EMRR un número elevado de brotes, un intervalo corto entre el primer y segundo brote,

INTRODUCCIÓN

una discapacidad alta a los 5 años del inicio y la afectación de múltiples sistemas funcionales son factores pronósticos negativos (Degenhardt et al., 2009). La actividad inflamatoria en forma de brotes al comienzo de la enfermedad (dos primeros años) está ampliamente aceptada como factor pronóstico (Scalfari et al., 2010). Pero este efecto se mantiene sólo hasta que se alcanza una EDSS de 3-4 puntos; a partir de ese punto, la discapacidad progresiona de manera continua e independiente de los brotes (Leray et al., 2010). Así, debería considerarse esta fase como “ventana terapéutica” donde centrar los esfuerzos terapéuticos y donde más utilidad pueden tener los estudios que buscan marcadores predictivos de la evolución de la enfermedad.

En líquido cefalorraquídeo (LCR) se utiliza de forma rutinaria la determinación de la presencia de bandas oligoclonales (BOC) y el índice de IgG (Stangel et al., 2013). La presencia de BOC de IgG en LCR es muy sensible pero poco específica de la EM. Además de su papel en el apoyo al diagnóstico de la enfermedad, tienen un valor pronóstico en el desarrollo de una EM clínicamente definida tras un SNA (Tintore et al., 2008; Dobson et al., 2013) aunque su valor pronóstico sobre la progresión de la enfermedad no está del todo establecido (Joseph et al., 2009; Siritho and Freedman, 2009; Lourenco et al., 2013). Las BOC de IgM, sin embargo, sí parecen asociarse con formas agresivas de EMRR y con un peor pronóstico (Villar et al., 2003; Garcia-Barragan et al., 2009; Villar et al., 2009) y pueden variar tras iniciar un tratamiento modificador de la enfermedad (Bosca et al., 2010; Villar et al., 2012).

Las nuevas disciplinas llamadas globalmente “ómicas” (transcriptómica, proteómica, lipidómica, metabolómica y epigenómica) tienen un gran potencial para hallar biomarcadores en líquidos biológicos. Desafortunadamente, por el momento ninguna de estas tecnologías ha conseguido encontrar un biomarcador para la EM que sea utilizado en la práctica clínica (Comabella and Racke, 2012).

5.1 Estudios electrofisiológicos

De entre los biomarcadores subclínicos cabe destacar los potenciales evocados (PE) cuya utilidad en la EM radica en que pueden detectar un daño subclínico del SNC si la vía que estudian está afecta o ayudar a confirmar la presencia de un brote en caso de duda. Sin embargo, su sensibilidad para detectar la presencia de lesiones cerebrales y su capacidad pronóstica es mucho menor que la RM (Leocani and Comi, 2008). Posiblemente, la evaluación conjunta de diversas modalidades de PE pueda mejorar dicha capacidad de pronosticar la evolución de la enfermedad (Invernizzi et al., 2011; Margaritella et al., 2012).

Asimismo, es posible evaluar la conectividad interhemisférica a través del CC mediante estudios neurofisiológicos que utilizan la estimulación magnética transcraneal (Transcranial Magnetic Stimulation, TMS). El periodo de silencio ipsilateral (ipsilateral Silent Period, iSP) refleja la inhibición de la actividad motora voluntaria ipsilateral al estímulo que ejerce el TMS (Giovannelli et al., 2009). Parece evaluar la función de fibras transcallosas que median un efecto inhibitorio desde el córtex motor estimulado al córtex motor del hemisferio opuesto aunque podrían también estar implicadas vías más caudales (Jung et al., 2006). Sin embargo, hasta el momento su significado y utilidad en la EM han sido poco estudiados.

5.2 Biomarcadores de imagen en RM

La RM permite estudiar el SNC de una forma incruenta y ha significando un avance importantísimo en la forma de evaluar la EM. Actualmente, es una herramienta esencial para el diagnóstico de la enfermedad y se utiliza de forma rutinaria en el seguimiento clínico de los pacientes. Además, las nuevas técnicas de RM han permitido obtener medidas cuantitativas acerca del daño del tejido cerebral y estudiar la estructura y función con mayor detalle. Todo ello está permitiendo el desarrollo de biomarcadores de imagen en RM, algunos de los cuales se han implementado en la práctica asistencial. Las principales características que debe tener un biomarcador de neuroimagen en la EM se exponen en la tabla 1.

OBJETIVOS	<ul style="list-style-type: none">• Permitir un diagnóstico temprano e incrementar la sensibilidad y especificidad• Ayudar en la decisión terapéutica a ofrecer un pronóstico• Detectar la actividad de la enfermedad para ayudar en la toma de decisiones• Monitorizar la respuesta terapéutica
CARACTERÍSTICAS IDEALES	<ul style="list-style-type: none">• Fiable, con alta sensibilidad y especificidad• Reproducible y cuantitativo• Sensible a cambios en la enfermedad• Se correlaciona y es capaz de predecir medidas clínicas relevantes• No invasivo, simple de llevar a cabo y de interpretar• Validado por estudios patológicos• Da una información global con la posibilidad de extraer información regional
DATOS A MEDIR	<ul style="list-style-type: none">• Naturaleza y gravedad de las alteraciones macroscópicas en la sustancia blanca• Componente celular de la información• Daño del tejido de la sustancia blanca de apariencia normal• Daño de la sustancia gris• Capacidad de reparación y reorganización tras el daño tisular

Tabla 1: Características idóneas de un biomarcador en RM en esclerosis múltiple. Adaptado de Filippi and Agosta, 2010 y Handbook of Multiple Sclerosis, Stuart Cook 2006.

5.2.1 Técnicas de RM convencional

La RM convencional ha demostrado ser útil para el diagnóstico de la EM en pacientes en los que se sospecha la enfermedad (Polman et al., 2011) y permite alcanzar un diagnóstico más temprano (Montalban et al., 2010; Polman et al., 2011).

Las lesiones de EM se visualizan como áreas de aumento de señal en secuencias potenciadas en T2, densidad protónica o Fluid-Attenuated Inversion Recovery (FLAIR) aunque el incremento de señal no es específico de los cambios patológicos subyacentes en las distintas lesiones (Filippi et al., 2012). Los agujeros negros son aquellas lesiones que se muestran hipointensas en secuencias espin-eco potenciadas en T1. Patológicamente se asocian con áreas donde existe una destrucción tisular severa con pérdida de axones principalmente (van Waesberghe et al., 1999).

La RM convencional es capaz de diferenciar entre lesiones activas y crónicas basándose en la presencia o no de rotura de la BHE. Las lesiones con rotura de la BHE presentan captación de gadolinio que puede persistir entre 2 y 6 semanas. La captación de gadolinio puede tener una morfología nodular o en forma de anillo (Gaitan et al., 2011). Las lesiones captantes en forma de anillo parecen asociarse a un mayor daño tisular (Morgen et al., 2001; Davis et al., 2010) y pertenecen en su mayoría a un patrón patológico de tipo I / II (Lucchinetti et al., 2003). Sin embargo, en la actualidad existen dudas de si estos patrones de captación son consecuencia del tiempo que tarda en adquirirse la imagen de RM tras la administración del contraste o si en realidad representan distinta respuesta inmune o un tipo distinto de lesión (Gaitan et al., 2011). En las fases progresivas de la enfermedad la expansión lenta de las lesiones no suele presentar captación de gadolinio y la inflamación y daño tisular generalmente se dan en ausencia de rotura de la BHE (Filippi et al., 2012).

Algunas lesiones, sobretodo de gran tamaño (lesiones pseudotumorales) (Schwartz et al., 2006; Lucchinetti et al., 2008) presentan un borde hipointenso en secuencias T2 lo cual podría estar traduciendo la presencia de macrófagos activados o radicales libres. Estas lesiones presentan frecuentemente una captación de gadolinio en forma de anillo y podrían corresponder a un sustrato patológico de tipo I / II (Bruck et al., 2001; Lucchinetti et al., 2003). Sin embargo, no se conoce su prevalencia en la población general de EM ni si se asocian con un fenotipo concreto de paciente o a una peor evolución de la discapacidad.

Las nuevas lesiones visibles en secuencias potenciadas en T2 y las lesiones captantes de gadolinio en T1 han sido ampliamente utilizadas como marcadores subrogados de actividad

subclínica inflamatoria para medir el efecto nuevos tratamientos en ensayos clínicos (Goodin, 2006; Barkhof et al., 2012; Cohen et al., 2012). Además, la aparición de nuevas lesiones durante el seguimiento de pacientes que recibían terapia modificadora de la enfermedad se ha asociado con un mayor número de brotes anuales y con un empeoramiento de la función física y cognitiva (Rio et al., 2008; Cadavid et al., 2011; Killestein and Polman, 2011).

La RM convencional también tiene cierta capacidad para dar información pronóstica en etapas tempranas de la enfermedad, a través del número de lesiones en secuencias potenciadas en T2, de su localización y de la presencia de lesiones captantes de gadolinio en secuencias T1 (Fisniku et al., 2008). El número de lesiones cerebrales en T2 y la presencia de lesiones infratentoriales o captantes de gadolinio son los principales factores pronósticos en RM sobre la aparición de un segundo brote tras un SNA (Filippi and Rocca, 2007).

A pesar de estos datos, existe una “paradoja clínico-radiológica” (Rocca et al., 2012). Es decir, la fortaleza de la asociación entre los hallazgos en RM convencional y las manifestaciones clínicas presentes o futuras de la enfermedad es modesta (Filippi and Agosta, 2010; Rocca et al., 2012). Probablemente sea, al menos en parte, el resultado de una baja especificidad para distinguir los distintos fenómenos patológicos subyacentes que se dan en la enfermedad, como el edema, desmielinización, remielinización, gliosis y daño axonal. Otra limitación de la RM convencional es que no ofrece información acerca del daño oculto en la SB (la llamada SBAN) y en la SG (Filippi et al., 2012).

5.2.2 Técnicas de RM no convencional o avanzada

La RM no convencional o avanzada aporta información más allá de las lesiones focales y permite estudiar el tejido que tiene una apariencia normal. Así, es posible obtener datos cuantitativos y patológicamente más específicos a través de estas técnicas (Bakshi et al., 2008; Filippi and Agosta, 2010; Ceccarelli et al., 2012; Filippi et al., 2012). Dichas características dotan a estas técnicas de grandes ventajas para llegar a generar biomarcadores en la EM.

En el artículo de revisión incluido al final de esta introducción se exponen de forma sintética las principales características de las técnicas de RM avanzada más utilizadas en la actualidad, su correlato anatomopatológico y posible utilidad.

Estudio de la atrofia cerebral: En pacientes con EM existe una mayor pérdida de volumen cerebral o atrofia que en personas sanas, en todos los subtipos de EM (Miller et al., 2002; De Stefano et al., 2010), probablemente debido a una pérdida axonal en la SB, y a una pérdida neuronal y glial en la SG junto con disminución de la densidad sináptica (Filippi et al., 2012).

INTRODUCCIÓN

Las lesiones visibles contribuyen al desarrollo de atrofia, sobretodo de la SG (Geurts et al., 2012), aunque también de la SB. En diversos estudios se ha descrito una correlación significativa entre la discapacidad medida por el EDSS o el MSFC y la fracción de parénquima cerebral ("brain parenchymal fraction", BPF) que es el volumen del parénquima cerebral dividido por el volumen de todo el cerebro (Grassiot et al., 2009; Geurts et al., 2012). Asimismo, el cambio en volumen cerebral es capaz de predecir el cambio en las medidas de discapacidad (Frischer et al., 2009; Lukas et al., 2010; Popescu et al., 2013). En general la correlación entre atrofia cerebral global y discapacidad es moderada, sin embargo, los estudios que han evaluado la atrofia a nivel regional han encontrado asociaciones más fuertes con la discapacidad sobretodo en regiones que comprendían funciones motoras (Grassiot et al., 2009) o de la SG (Geurts et al., 2012; Benedict et al., 2013). La discapacidad cognitiva también parece relacionarse con la atrofia cerebral, principalmente de la SG, en todos los subtipos de EM (Grassiot et al., 2009; Calabrese et al., 2010).

Imagen por tensor de difusión: La imagen por tensor de difusión (Diffusion Tensor Imaging, DTI) se basa en el estudio del movimiento de las moléculas de agua en un tejido (Sbardella et al., 2013). Es una técnica sensible y específica para detectar cambios en la integridad microestructural. El movimiento del agua en tres dimensiones puede representarse como un elipsoide, del cual es posible obtener varios índices: la anisotropía fraccional (AF) que refleja la prevalencia de la difusividad en una dirección, la difusividad media (DM) que mide el movimiento global del agua sin direccionalidad, la difusividad radial (DR) y la difusividad axial (DA). Los dos primeros índices son poco específicos y no distinguen entre varios procesos patológicos, como el edema, la inflamación, desmielinización y gliosis (Sbardella et al., 2013), mientras que la DR parece correlacionarse con la integridad de la mielina y la DA con la integridad axonal en modelos animales (Song et al., 2002).

En pacientes con EM existen anomalías en el DTI de la SBAN que traducen un daño microestructural desde fases iniciales de la enfermedad que empeoran a lo largo del tiempo y con el deterioro clínico (Rovaris et al., 2002; Preziosa et al., 2011). Los hallazgos en la SG parecen ser menos consistentes en fases iniciales de la enfermedad. En EMRR se ha detectado un aumento de la DM y disminución de la AF en algunos estudios (Ceccarelli et al., 2007) mientras que otros no han detectado diferencias entre pacientes y controles (Griffin et al., 2001). También las lesiones presentan alteración de los índices de DTI, más marcadas en lesiones captantes de gadolinio y en agujeros negros (Preziosa et al., 2011; Sbardella et al., 2013).

Los estudios de correlación entre índices de DTI y discapacidad han detectado asociaciones entre ambos parámetros (Liu et al., 2012; Onu et al., 2012; Sbardella et al., 2013) y en otros casos no (Griffin et al., 2001). Además las asociaciones han sido débiles-moderadas. Sin embargo, cuando la difusión se analiza a nivel regional, en tractos específicos, se han detectado correlaciones más fuertes. Así, el EDSS se ha correlacionado con cambios en el DTI del tracto córtico espinal y del CC (Wilson et al., 2003; Lin et al., 2005; Kern et al., 2011) y el rendimiento cognitivo con la integridad de algunos tractos concretos (Dineen et al., 2009; Yu et al., 2012).

Espectroscopia: La espectroscopia proporciona información metabólica en vivo permitiendo la cuantificación de diversos metabolitos como el N-acetil aspartato (NAA), mioinositol (mI), creatina (Cr), colina, glutamato y otros (Narayana, 2005; Sajja et al., 2009). El NAA suele estar reducido en el tejido cerebral de pacientes con EM, indicando pérdida o daño axonal (De Stefano et al., 2001; Sastre-Garriga et al., 2005). Asimismo, el mI puede estar incrementado desde fases iniciales de la enfermedad, traduciendo astrogliosis, y se correlaciona con los valores de discapacidad (Chard et al., 2002). Sin embargo, su capacidad de predicción de la discapacidad ha sido muy poco estudiada. Únicamente en un estudio previo, se demostró que aquellos pacientes con SNA que presentaban niveles más bajos de NAA tenían más probabilidades de convertir a EMCD (Wattjes et al., 2008).

Estudio de la mielina a través de la relaxometría del T2: El estudio de la mielina se fundamenta en el tiempo de relajación del T2. La parte inicial de dicho decaimiento parece proceder del agua entre las capas de mielina (Beaulieu et al., 1998). La fracción de agua de la mielina o “Myelin Water Fraction” (MWF) se obtiene dividiendo la señal del agua correspondiente a la mielina entre la señal global del agua. En la SB puede existir una disminución de la MWF que es más pronunciada en las lesiones (Laule et al., 2004; Oh et al., 2007), sin embargo su capacidad de predecir la evolución de la enfermedad no ha sido estudiada. Actualmente se están realizando importantes esfuerzos para solventar algunas dificultades técnicas propias de esta técnica que permitan aumentar su aplicabilidad (Guo et al., 2012; Kitzler et al., 2012).

En definitiva, todas estas técnicas tienen el potencial de generar marcadores en la EM que se asocian y sean capaces de predecir la discapacidad física y cognitiva de una forma más estrecha que las técnicas convencionales, una vez solventadas algunas limitaciones tecnológicas.

Trabajo de revisión

Avances en técnicas de resonancia magnética no convencional en la esclerosis múltiple

Sara Llufriu Duran^{1,2}, Yolanda Blanco Morgado^{1,2}, Iñigo Gabilondo Cuéllar², Eloy Martínez De Las Heras², Francesc Graus Ribas^{1,2}, Albert Saiz Hinarejos^{1,2}

¹Unidad de Neuroinmunología-Esclerosis múltiple. Servicio de Neurología. Hospital Clínic.

Barcelona. ²Institut d'Investigacions Biomèdiques August Pi i Sunyer (IDIBAPS). Barcelona.

Revista Española de Esclerosis Múltiple. Junio de 2011. Número 18. Páginas 10-17.

Artículo de revisión

REVISIÓN

Avances en técnicas de resonancia magnética no convencional en la esclerosis múltiple

SARA LLUFRU DURAN^{1,2}, YOLANDA BLANCO MORGADO^{1,2}, IÑIGO GABILONDO CUÉLLAR², ELOY MARTÍNEZ DE LAS HERAS², FRANCESC GRAUS RIBAS^{1,2}, ALBERT SAIZ HINAREJOS^{1,2}

¹Unidad de Neuroinmunología-Esclerosis múltiple. Servicio de Neurología. Hospital Clínic. Barcelona.

²Institut d'Investigacions Biomèdiques August Pi i Sunyer (IDIBAPS). Barcelona.

RESUMEN. Las técnicas de resonancia magnética (RM) no convencional han revolucionado la investigación en la esclerosis múltiple, debido al gran interés por encontrar parámetros objetivos con especificidad anatomo-patológica, buen correlato clínico y valor pronóstico. Estas técnicas ofrecen una mayor información acerca de la fisiopatología de la enfermedad y se asocian de forma más robusta con datos de discapacidad clínica y cognitiva que las secuencias convencionales. Sin embargo, su adquisición y post-procesado no están exentos de dificultades técnicas. En este trabajo se revisan las aplicaciones de las principales técnicas de RM no convencional y los estudios más destacados publicados hasta la fecha.

Palabras clave: resonancia magnética, esclerosis múltiple, atrofia, transferencia de magnetización, tensor de difusión, espectroscopia, resonancia magnética funcional, relaxometría, resonancia magnética de alto campo.

ABSTRACT. Advanced magnetic resonance imaging (MRI) has been a revolution in multiple sclerosis (MS) research, due to the great interest in finding objective biomarkers with pathology specificity, strong clinical correlation and prognostic value. These techniques offer more information about MS physiopathology and have a better association with clinical and cognitive disability compared to conventional MRI. However, the acquisition and post-processing steps can have technical difficulties. In this paper, the applications and recent research in non conventional MRI techniques are described.

Key words: magnetic resonance imaging, multiple sclerosis, atrophy, magnetization transfer, diffusion tensor imaging, magnetic resonance spectroscopy, functional magnetic resonance imaging, relaxometry, high-field magnetic resonance imaging.

La resonancia magnética (RM) ha supuesto un gran avance en el diagnóstico y monitorización de los pacientes con esclerosis múltiple (EM) en las dos últimas décadas. La presencia de lesiones cerebrales en áreas características, el aumento en su número en secuencias potenciadas en T2 y la aparición de lesiones captantes de gadolinio se consideran los principales criterios para el diagnóstico de la EM en RM^{1,2}. Asimismo, estos parámetros de RM convencional han sido utilizados para evaluar el pronóstico de la enfermedad y la respuesta a los tratamientos³. Sin embargo, estas medidas se asocian sólo parcialmente a la discapacidad clínica del paciente (paradoja clínico-radiológica) y son débiles predictores a largo plazo⁴⁻⁷. La principal limitación de estas técnicas es que traducen de forma incompleta los procesos fisiopatológicos de la enfermedad y que la apariencia de las lesiones no es específica de la patología subyacente. Además, tienen una baja sensibilidad para la detección de la patología de sustancia gris y del daño difuso de la sustancia blanca de apariencia normal^{8,9}.

Dado que existe la necesidad de encontrar buenos biomarcadores en RM con especificidad patológica y que ofrezcan una evaluación global, tanto para el diagnóstico, fenotipo y progresión de la enferme-

dad, las técnicas de RM no convencional o cuantitativa han surgido con fuerza¹⁰. Los biomarcadores ideales de la enfermedad serían aquellas técnicas capaces de evaluar la extensión y naturaleza de las anormalidades de la sustancia blanca, los componentes celulares de la inflamación, la patología de la sustancia gris, así como la eficacia de la reparación y de la reorganización funcional después del daño tisular¹¹.

Las estrategias propuestas para superar las limitaciones de la RM convencional son tres. Primero, desarrollar secuencias avanzadas que sean capaces de detectar la patología invisible a las secuencias estándares. Segundo, implementar mejoras en la maquinaria o “hardware” como el uso de altos campos magnéticos. Tercero, estandarizar técnicas de post-procesado que de forma totalmente automática puedan ser aplicadas en tiempo real para visualizar o cuantificar el daño subyacente en el sistema nervioso central (SNC)⁸.

Algunas de las limitaciones actuales de las técnicas de RM no convencional son el escaso conocimiento de la patología subyacente a los cambios en sus valores, que puede ser variada y concomitante. Además, las mejores estrategias para la adquisición y post-procesado son tema de debate aún en la actua-

lidad. Es por ello que su aplicabilidad está limitada a la investigación.

A continuación describiremos las principales técnicas de resonancia magnética cuantitativa y sus aplicaciones.

□ Mapa de lesiones

Un nuevo enfoque al análisis de las lesiones visibles en RM convencional es a través de su post-procesado para obtener un mapa probabilístico de lesiones (MPL) y con ello información acerca de su distribución regional¹². El análisis del MPL mostró una distribución de lesiones en T2 alrededor del sistema ventricular similar en pacientes con un síndrome clínico aislado (SCA), EM recurrente-remitente (EMRR) y EM secundariamente progresiva (EMSP)¹³. Además, se objetivó que los pacientes con EMSP presentaban lesiones localizadas predominantemente alrededor de los ventrículos y en la fosa posterior, a diferencia de los pacientes con EM primariamente progresiva (EMPP) en los cuales existe una afectación más difusa de regiones corticales y subcorticales¹³. En un estudio en el que se comparaba el MPL en secuencias T1 y T2 entre pacientes con EMRR y EMPP se demostró que la probabilidad máxima de encontrar lesiones en zonas concretas era mayor en EMPP, principalmente en la corona radiata¹⁴.

Otra posibilidad es el análisis seriado para estudiar los cambios de señal relacionados con la evolución de la lesión. Cambios en el patrón de progresión dentro de lesiones individuales pueden indicar un cambio global de la patología del paciente pasando de formas inflamatorias a procesos patológicos más degenerativos¹⁵.

□ Atrofia

Estudios longitudinales han demostrado que la pérdida de volumen cerebral en pacientes con EM (0,5% - 1% al año) es mayor que en sujetos sanos (0,1% - 0,3%)¹⁶. Dicha atrofia se cree que no está únicamente relacionada con las lesiones visibles en T2, sino que también se deriva de cambios en la sustancia blanca y gris de apariencia normal^{17, 18} (Figura 1). La pérdida tisular afecta más a la sustancia gris que blanca en pacientes con EM, y dentro de ésta, las estructuras más afectadas son los ganglios basales y el tálamo¹⁶. Los mejores métodos para la segmentación y la caracterización de la atrofia de la sustancia gris están por establecer, y algunas de sus limitaciones son la clasificación de lesiones como sustancia gris, lo cual requiere corrección manual.

Tanto la pérdida de volumen cerebral global como de sustancia gris se han asociado de forma

importante con la discapacidad¹⁹⁻²². En estudios longitudinales, el volumen cerebral en fases tempranas es un buen predictor de discapacidad tanto para pacientes con formas en brotes como progresivas^{23, 24}. El volumen de la corteza cerebral se asocia de forma significativa con la alteración cognitiva y es el mejor predictor de la alteración de la memoria verbal y de los síntomas neuropsiquiátricos²⁵⁻²⁷. Finalmente, la medida del volumen cerebral puede ser utilizada para evaluar el efecto neuroprotector de las terapias en EM, aunque debe tenerse en cuenta que puede existir una aceleración de la atrofia (pseudoatrofia) en los meses siguientes al inicio de la terapia probablemente por resolución de la inflamación y el edema acompañante²⁸.

□ Transferencia de magnetización

El ratio de transferencia de magnetización (RTM) refleja la capacidad de las macromoléculas de un tejido de intercambiar magnetización con las moléculas de agua circundante²⁹, de forma que una disminución en el RTM indicaría una pérdida de estructura macromolecular, rica en mielina. Anatomopatológicamente, el RTM se asocia con el porcentaje de axones residuales y el grado de desmielinización^{30, 31}. En EM el RTM está disminuido tanto en lesiones como en sustancia blanca de apariencia normal^{32, 33}. Las medidas de RTM se correlacionan de forma moderada a alta con la discapacidad clínica y cognitiva^{34, 35}, y parecen empeorar a lo largo del tiempo en todos los fenotipos de EM^{36, 37}. Su valor pronóstico ha sido evaluado encontrando que la altura del histograma del RTM de la sustancia gris y el porcentaje de cambio del RTM lesional durante el primer año eran predictores independientes del empeoramiento de la discapacidad 8 años después³⁸. Asimismo, es posible seguir la evolución del RTM en las lesiones, monitoreando de esta forma la desmielinización y remielinización *in vivo*³⁹.

□ Tensor de difusión

El movimiento Browniano de traslación de las moléculas en un fluido está influenciado por estructuras celulares como las membranas celulares y los citoesqueletos axonales. El tensor de difusión es una descripción matemática de la magnitud y direcciónalidad (anisotropía) del movimiento de las moléculas de agua en un espacio tridimensional⁴⁰. Del tensor de difusión es posible obtener la difusión media (DM), independiente de la orientación espacial de las estructuras tisulares, y otros índices de la difusión anisotrópica de las moléculas como la anisotropía fraccional (AF), la cual refleja la prevalencia de

REVISIÓN

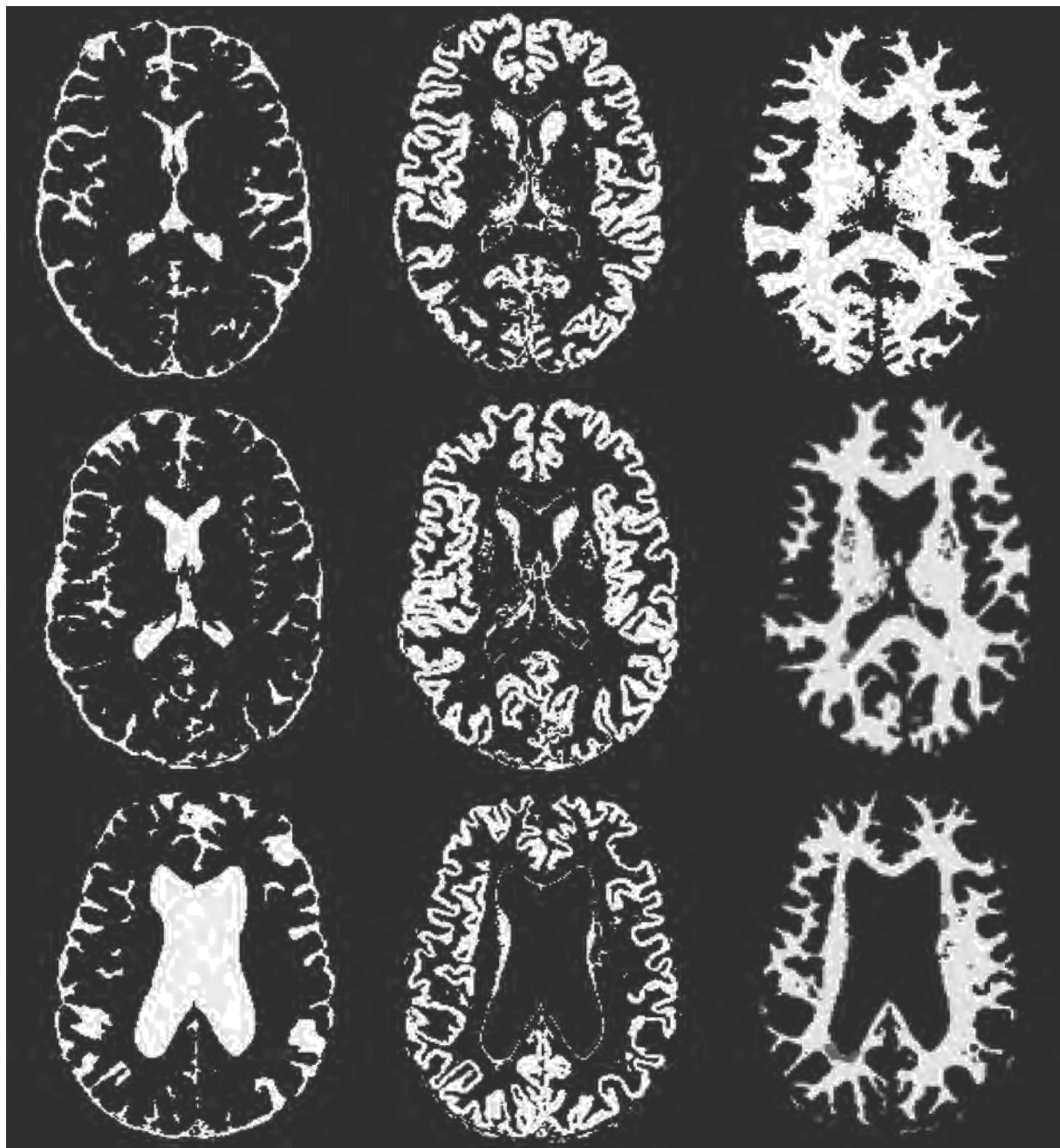


Figura 1 Líquido cefalorraquídeo, sustancia gris y sustancia blanca (junto con mapa de lesiones en color gris) en un control sano (línea superior), en un paciente con EMRR (línea media) y en un paciente con EMSP (línea inferior). Segmentación realizada mediante el programa Sienax (www.fmrib.ox.ac.uk/fsl). Es destacable la atrofia del parénquima cerebral en los pacientes con EM respecto al control sano.

la difusión a lo largo de una dirección del espacio⁴¹ (Figura 2). Los cambios en estos parámetros se corresponden con desmielinización y daño axonal en estudios *post mortem*⁴². En pacientes con EM se han demostrado alteraciones en los patrones de difusión tanto en lesiones focales como en la sustancia blanca y gris de apariencia normal. En el estudio de las lesiones, aquellas consideradas agujeros negros en T1

son las que presentan una mayor alteración de la difusión, mientras que se han obtenido resultados discordantes cuando se comparan lesiones captantes de gadolinio con aquellas no captantes^{43, 44}. También en el parénquima cerebral de apariencia normal es posible detectar anomalías en la difusión⁴⁵, incluso antes del desarrollo de lesiones visibles⁴⁶. Parece ser que el estudio del tensor de difusión es más sensible

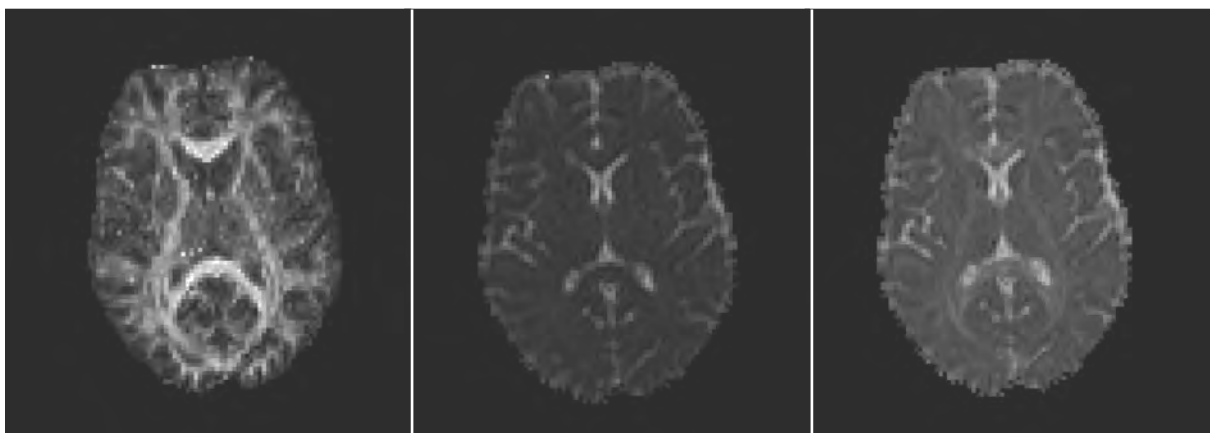


Figura 2 Tensor de difusión. Representación del mapa de anisotropía fraccional, mapa de difusividad axial y mapa de difusividad media.

al acúmulo del daño de sustancia gris que de sustancia blanca de apariencia normal⁴⁷. Existe una buena correlación con los datos clínicos, principalmente la difusión en lesiones visibles en T2⁴⁸ y en sustancia gris⁴⁹⁻⁵¹, lo que ha permitido generar algunas escalas de puntuación en RM que expliquen la varianza de la discapacidad asociada a la EM⁵². Finalmente, ha demostrado un valor predictivo de la discapacidad en una serie de pacientes con EMPP⁵³.

La tractografía es una técnica basada en el movimiento direccional del agua y permite generar una representación virtual, en tres dimensiones, de los tractos de fibras de sustancia blanca⁵⁴. Gracias a ello se abre la posibilidad de estudiar la organización de la sustancia blanca y la conectividad en humanos⁵⁵. Los pacientes con EM que presentan síntomas motores tienen unos índices de difusión anormales en el tracto corticoespinal en comparación con sujetos sanos o con pacientes sin síntomas motores⁵⁶; además, las medidas de difusión de este tracto se correlacionan mejor con datos clínicos que la carga lesional en T2 o los valores de difusión globales del cerebro⁵⁷. Un estudio que combinaba medidas de tractografía

con medidas de conectividad funcional demostró una correlación entre ellas, lo que sugiere que el daño de las fibras de la sustancia blanca puede inducir cambios funcionales adaptativos que limitan sus manifestaciones clínicas⁵⁸.

□ Espectroscopia

La espectroscopia permite medir la señal generada por los protones presentes en moléculas orgánicas de tejidos vivos, a diferencia de otros tipos de técnicas en que la señal proviene de los protones del agua. Entre los principales metabolitos que es posible cuantificar se encuentra el N-acetil-aspartato (NAA) marcador de disfunción o pérdida axonal/neuronal. La colina (Cho) está incrementada cuando existe una destrucción de la mielina, remielinización e inflamación. El aumento de creatina (Cr) está asociado con la densidad celular. El mioinositol (mI) es un marcador de proliferación glial y astrogliosis⁵⁹ (Tabla I). Las lesiones de EM captantes de gadolinio muestran un aumento de la Cr, Cho, mI y glutamato, mientras que el NAA puede ser bajo o levemente disminuido. En

Tabla I**Metabolitos obtenidos mediante espectroscopia**

Metabolitos		Correlato patológico
N acetil aspartato (NAA)	Derivado de la síntesis de aminoácidos. Se sintetiza casi exclusivamente en neuronas.	Disminuido en caso de pérdida o disfunción neuronal o axonal.
Colina (Cho)	Forma parte de los fosfolípidos constituyentes de las membranas celulares.	Elevado en la inflamación, la desmielinización y remielinización.
Creatina (Cr)	Reserva energética de las neuronas y la glía.	Su aumento está relacionado con el aumento de la densidad celular.
Mioinositol (mI)	Molécula similar al azúcar que interviene en la regulación osmótica del tejido cerebral.	Niveles elevados de mI se correlacionan con proliferación glial.
Glutamato (G)	Neurotransmisor excitatorio.	Su aumento se asocia con neurotoxicidad.

REVISIÓN

la sustancia blanca de apariencia normal el patrón es similar, mientras que en las lesiones crónicas el NAA está marcadamente reducido, el mI está incrementado y la concentración de glutamato es normal⁶⁰⁻⁶².

Actualmente se están desarrollando métodos para determinar otros metabolitos relevantes para la EM, como el glutatión⁶³, el ácido gamma amino butírico (GABA), el ácido ascórbico, así como la señal macromolecular de fondo (valina, alanina, leucina, isoleucina, treonina) que contiene elementos que forman parte de la mielina.

□ Resonancia magnética funcional

La RM funcional utiliza un mecanismo de contraste dependiente de la señal BOLD (“blood-oxygenation-level-dependent”), secundaria a las diferencias en la concentración de desoxihemoglobina sanguínea en áreas activadas como consecuencia de variaciones en la actividad neuronal⁶⁴. En los estudios realizados a pacientes con EM evaluando las redes visuales, cognitivas y motoras, se han encontrado alteraciones en el reclutamiento de zonas normalmente implicadas en el desarrollo de una tarea o en la activación de áreas adicionales en comparación con sujetos sanos⁶⁵. Los cambios corticales funcionales varían entre pacientes en diferentes estadios de la enfermedad, después de un brote y en pacientes clínicamente estables^{65, 66}. Parece que al inicio de la enfermedad hay un incremento de la activación de las áreas que están dedicadas normalmente al desempeño de una tarea determinada; en siguientes estadios, se objetiva una activación bilateral de estas regiones concretas, y en fases todavía más avanzadas existe una activación más difusa y que incluye áreas adicionales (aquellas que en sujetos sanos se activan al realizar tareas complejas o nuevas)⁶⁷.

□ Relaxometría. Estudio de la mielina

La fracción de agua de la mielina (“Myelin Water Fraction”, MWF) se obtiene a través de la medición del tiempo de relajación transversal, el cual consta de un componente corto derivado del agua atrapada entre las capas de la mielina⁶⁸ (Figura 3). Dicha medida es específica del contenido de mielina y su integridad⁶⁹. En lesiones de EM existe un 30-50% de disminución de la MWF, mientras que en la sustancia blanca de apariencia normal la disminución es de alrededor del 7-15% en comparación con sujetos sanos^{70, 71}.

Esta técnica, en la actualidad, presenta importantes limitaciones técnicas, como un tiempo largo de adquisición y el estudio únicamente de una pequeña parte del parénquima cerebral. Sin embargo, se están

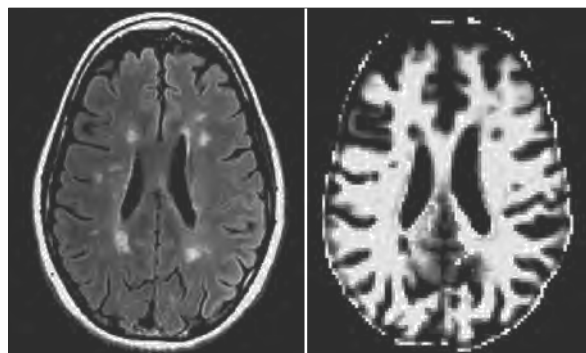


Figura 3 Secuencia FLAIR y secuencia DESPOT (myelin water fraction map). En la secuencia DESPOT es posible observar la disminución o ausencia de mielina en zonas que corresponden a lesiones hiperintensas en FLAIR. Imagen cedida por Roland G. Henry, Center for Functional and Molecular Imaging, Department of Radiology and Biomedical Imaging, UCSF (University of San Francisco, California).

realizando esfuerzos para obtener adquisiciones en tres dimensiones y con una mejor señal/ruido^{72, 73}.

□ Resonancia magnética de alto campo

El uso de altos campos magnéticos (3 Tesla) o muy altos campos (7 Tesla) ofrece la ventaja de mejorar la detección de lesiones tanto en sustancia blanca como en sustancia gris⁷⁴ y una mejor aplicación de técnicas de RM no convencional (espectroscopia, transferencia de magnetización, etc.). La imagen de susceptibilidad de fase que puede obtenerse con RM 7 Tesla permite estudiar la heterogeneidad de las lesiones, dado que el contraste que se obtiene está relacionado con la oxigenación de la sangre, la vasculatura y la actividad macrofágica⁷⁵. Asimismo, la RM de alto campo es más sensible y específica a la detección del hierro, por lo que es una herramienta útil para el estudio de los depósitos de hierro en la sustancia gris y su contribución a la neurodegeneración^{76, 77}.

□ Conclusiones

Aunque la RM convencional ha permitido de forma indudable mejorar nuestra capacidad diagnóstica y de seguimiento de pacientes con EM, está limitada por una baja correlación clínica y poco poder predictivo.

Los nuevos avances en RM magnética no convencional abren un camino para solventar la paradoja clínico-radiológica de las técnicas convencionales. Éstas permiten un estudio más específico de los fenómenos fisiopatológicos subyacentes en la EM de forma cuantitativa y, con ello, más objetiva. Sin embargo, existe un largo camino para que las técnicas de RM no convencional sean perfectas, y es primordial su estandarización y optimización.

BIBLIOGRAFÍA

- 1.- Polman CH, Reingold SC, Edan G, *et al.* Diagnostic criteria for multiple sclerosis: 2005 revisions to the “McDonald Criteria”. *Ann Neurol* 2005; 58: 840-846.
- 2.- McDonald WI, Compston A, Edan G, *et al.* Recommended diagnostic criteria for multiple sclerosis: guidelines from the International Panel on the diagnosis of multiple sclerosis. *Ann Neurol* 2001; 50: 121-127.
- 3.- Lovblad KO, Anzalone N, Dorfler A, *et al.* MR imaging in multiple sclerosis: review and recommendations for current practice. *AJNR Am J Neuroradiol* 2010; 31: 983-989.
- 4.- Barkhof F. The clinico-radiological paradox in multiple sclerosis revisited. *Curr Opin Neurol* 2002; 15: 239-245.
- 5.- Filippi M, Grossman RI. MRI techniques to monitor MS evolution: the present and the future. *Neurology* 2002; 58: 1147-1153.
- 6.- Goodin DS. Magnetic resonance imaging as a surrogate outcome measure of disability in multiple sclerosis: have we been overly harsh in our assessment? *Ann Neurol* 2006; 59: 597-605.
- 7.- Bar-Zohar D, Agosta F, Goldstaub D, Filippi M. Magnetic resonance imaging metrics and their correlation with clinical outcomes in multiple sclerosis: a review of the literature and future perspectives. *Mult Scler* 2008; 14: 719-727.
- 8.- Zivadinov R, Stosic M, Cox JL, *et al.* The place of conventional MRI and newly emerging MRI techniques in monitoring different aspects of treatment outcome. *J Neurol* 2008; 255 Suppl 1: 61-74.
- 9.- Chard D, Miller D. Is multiple sclerosis a generalized disease of the central nervous system? An MRI perspective. *Curr Opin Neurol* 2009; 22: 214-218.
- 10.- Bakshi R, Thompson AJ, Rocca MA, *et al.* MRI in multiple sclerosis: current status and future prospects. *Lancet Neurol* 2008; 7: 615-625.
- 11.- Filippi M, Agosta F. Imaging biomarkers in multiple sclerosis. *J Magn Reson Imaging* 2010; 31: 770-788.
- 12.- Filippi M, Rocca MA. Novel MRI approaches to assess patients with multiple sclerosis. *Curr Opin Neurol* 2010; 23: 212-217.
- 13.- Ceccarelli A, Rocca MA, Pagani E, *et al.* A voxel-based morphometry study of grey matter loss in MS patients with different clinical phenotypes. *Neuroimage* 2008; 42: 315-322.
- 14.- Di Perri C, Battaglini M, Stromillo ML, *et al.* Voxel-based assessment of differences in damage and distribution of white matter lesions between patients with primary progressive and relapsing-remitting multiple sclerosis. *Arch Neurol* 2008; 65: 236-243.
- 15.- Meier DS, Weiner HL, Guttman CR. MR imaging intensity modeling of damage and repair in multiple sclerosis: relationship of short-term lesion recovery to progression and disability. *AJNR Am J Neuroradiol* 2007; 28: 1956-1963.
- 16.- Bermel RA, Bakshi R. The measurement and clinical relevance of brain atrophy in multiple sclerosis. *Lancet Neurol* 2006; 5: 158-170.
- 17.- Jasperse B, Minneboo A, de Groot V, *et al.* Determinants of cerebral atrophy rate at the time of diagnosis of multiple sclerosis. *Arch Neurol* 2007; 64: 190-194.
- 18.- Kalkers NF, Vrenken H, Uitdehaag BM, *et al.* Brain atrophy in multiple sclerosis: impact of lesions and of damage of whole brain tissue. *Mult Scler* 2002; 8: 410-414.
- 19.- Giorgio A, Battaglini M, Smith SM, De Stefano N. Brain atrophy assessment in multiple sclerosis: importance and limitations. *Neuroimaging Clin N Am* 2008; 18: 675-686, xi.
- 20.- Molyneux PD, Kappos L, Polman C, *et al.* The effect of interferon beta-1b treatment on MRI measures of cerebral atrophy in secondary progressive multiple sclerosis. European Study Group on Interferon beta-1b in secondary progressive multiple sclerosis. *Brain* 2000; 123 (Pt 11): 2256-2263.
- 21.- Ingle GT, Stevenson VL, Miller DH, *et al.* Two-year follow-up study of primary and transitional progressive multiple sclerosis. *Mult Scler* 2002; 8: 108-114.
- 22.- Chen JT, Narayanan S, Collins DL, *et al.* Relating neocortical pathology to disability progression in multiple sclerosis using MRI. *Neuroimage* 2004; 23: 1168-1175.
- 23.- Sastre-Garriga J, Ingle GT, Chard DT, *et al.* Grey and white matter volume changes in early primary progressive multiple sclerosis: a longitudinal study. *Brain* 2005; 128: 1454-1460.
- 24.- Fisher E, Rudick RA, Simon JH, *et al.* Eight-year follow-up study of brain atrophy in patients with MS. *Neurology* 2002; 59: 1412-1420.
- 25.- Fisher E, Lee JC, Nakamura K, Rudick RA. Gray matter atrophy in multiple sclerosis: a longitudinal study. *Ann Neurol* 2008; 64: 255-265.
- 26.- Amato MP, Bartolozzi ML, Zipoli V, *et al.* Neocortical volume decrease in relapsing-remitting MS patients with mild cognitive impairment. *Neurology* 2004; 63: 89-93.
- 27.- Sanfilipo MP, Benedict RH, Weinstock-Guttmann B, Bakshi R. Gray and white matter brain atrophy and neuropsychological impairment in multiple sclerosis. *Neurology* 2006; 66: 685-692.

REVISIÓN

- 16
- 28.- Giacomini PS, Arnold DL. Non-conventional MRI techniques for measuring neuroprotection, repair and plasticity in multiple sclerosis. *Curr Opin Neurol* 2008; 21: 272-277.
 - 29.- Wolff SD, Balaban RS. Magnetization transfer imaging: practical aspects and clinical applications. *Radiology* 1994; 192: 593-599.
 - 30.- van Waesberghe JH, Kamphorst W, De Groot CJ, et al. Axonal loss in multiple sclerosis lesions: magnetic resonance imaging insights into substrates of disability. *Ann Neurol* 1999; 46: 747-754.
 - 31.- Schmierer K, Scaravilli F, Altmann DR, et al. Magnetization transfer ratio and myelin in postmortem multiple sclerosis brain. *Ann Neurol* 2004; 56: 407-415.
 - 32.- Ge Y, Grossman RI, Babb JS, et al. Dirty-appearing white matter in multiple sclerosis: volumetric MR. imaging and magnetization transfer ratio histogram analysis. *AJNR Am J Neuroradiol* 2003; 24: 1935-1940.
 - 33.- Phillips MD, Grossman RI, Miki Y, et al. Comparison of T2 lesion volume and magnetization transfer ratio histogram analysis and of atrophy and measures of lesion burden in patients with multiple sclerosis. *AJNR Am J Neuroradiol* 1998; 19: 1055-1060.
 - 34.- van Buchem MA, Grossman RI, Armstrong C, et al. Correlation of volumetric magnetization transfer imaging with clinical data in MS. *Neurology* 1998; 50: 1609-1617.
 - 35.- Rovaris M, Filippi M, Falautano M, et al. Relation between MR abnormalities and patterns of cognitive impairment in multiple sclerosis. *Neurology* 1998; 50: 1601-1608.
 - 36.- Filippi M, Inglese M, Rovaris M, et al. Magnetization transfer imaging to monitor the evolution of MS: a 1-year follow-up study. *Neurology* 2000; 55: 940-946.
 - 37.- Filippi M, Iannucci G, Tortorella C, et al. Comparison of MS clinical phenotypes using conventional and magnetization transfer MRI. *Neurology* 1999; 52: 588-594.
 - 38.- Agosta F, Rovaris M, Pagani E, et al. Magnetization transfer MRI metrics predict the accumulation of disability 8 years later in patients with multiple sclerosis. *Brain* 2006; 129: 2620-2627.
 - 39.- Chen JT, Kuhlmann T, Jansen GH, et al. Voxel-based analysis of the evolution of magnetization transfer ratio to quantify remyelination and demyelination with histopathological validation in a multiple sclerosis lesion. *Neuroimage* 2007; 36: 1152-1158.
 - 40.- Basser PJ. Inferring microstructural features and the physiological state of tissues from diffusion-weighted images. *NMR Biomed* 1995; 8: 333-344.
 - 41.- Rovaris M, Filippi M. Diffusion tensor MRI in multiple sclerosis. *J Neuroimaging* 2007; 17 Suppl 1: 27S-30S.
 - 42.- Mottershead JP, Schmierer K, Clemence M, et al. High field MRI correlates of myelin content and axonal density in multiple sclerosis--a post-mortem study of the spinal cord. *J Neurol* 2003; 250: 1293-1301.
 - 43.- Filippi M, Iannucci G, Cercignani M, et al. A quantitative study of water diffusion in multiple sclerosis lesions and normal-appearing white matter using echo-planar imaging. *Arch Neurol* 2000; 57: 1017-1021.
 - 44.- Filippi M, Cercignani M, Inglese M, et al. Diffusion tensor magnetic resonance imaging in multiple sclerosis. *Neurology* 2001; 56: 304-311.
 - 45.- Rovaris M, Gass A, Bammer R, et al. Diffusion MRI in multiple sclerosis. *Neurology* 2005; 65: 1526-1532.
 - 46.- Rocca MA, Cercignani M, Iannucci G, et al. Weekly diffusion-weighted imaging of normal-appearing white matter in MS. *Neurology* 2000; 55: 882-884.
 - 47.- Oreja-Guevara C, Rovaris M, Iannucci G, et al. Progressive gray matter damage in patients with relapsing-remitting multiple sclerosis: a longitudinal diffusion tensor magnetic resonance imaging study. *Arch Neurol* 2005; 62: 578-584.
 - 48.- Bammer R, Augustin M, Strasser-Fuchs S, et al. Magnetic resonance diffusion tensor imaging for characterizing diffuse and focal white matter abnormalities in multiple sclerosis. *Magn Reson Med* 2000; 44: 583-591.
 - 49.- Bozzali M, Cercignani M, Sormani MP, et al. Quantification of brain gray matter damage in different MS phenotypes by use of diffusion tensor MR imaging. *AJNR Am J Neuroradiol* 2002; 23: 985-988.
 - 50.- Rovaris M, Iannucci G, Falautano M, et al. Cognitive dysfunction in patients with mildly disabling relapsing-remitting multiple sclerosis: an exploratory study with diffusion tensor MR imaging. *J Neurol Sci* 2002; 195: 103-109.
 - 51.- Vrenken H, Pouwels PJ, Geurts JJ, et al. Altered diffusion tensor in multiple sclerosis normal-appearing brain tissue: cortical diffusion changes seem related to clinical deterioration. *J Magn Reson Imaging* 2006; 23: 628-636.
 - 52.- Pulizzi A, Rovaris M, Judica E, et al. Determinants of disability in multiple sclerosis at various disease stages: a multiparametric magnetic resonance study. *Arch Neurol* 2007; 64: 1163-1168.
 - 53.- Rovaris M, Judica E, Gallo A, et al. Grey matter damage predicts the evolution of primary progressive multiple sclerosis at 5 years. *Brain* 2006; 129: 2628-2634.
 - 54.- Ciccarelli O, Catani M, Johansen-Berg H, et al. Diffusion-based tractography in neurological disorders: concepts, applications, and future developments. *Lancet Neurol* 2008; 7: 715-727.

- 55.- Inglese M, Bester M. Diffusion imaging in multiple sclerosis: research and clinical implications. *NMR Biomed* 2010; 23: 865-872.
- 56.- Lin F, Yu C, Jiang T, et al. Diffusion tensor tractography-based group mapping of the pyramidal tract in relapsing-remitting multiple sclerosis patients. *AJNR Am J Neuroradiol* 2007; 28: 278-282.
- 57.- Wilson M, Tench CR, Morgan PS, Blumhardt LD. Pyramidal tract mapping by diffusion tensor magnetic resonance imaging in multiple sclerosis: improving correlations with disability. *J Neurol Neurosurg Psychiatry* 2003; 74: 203-207.
- 58.- Rocca MA, Pagani E, Absinta M, et al. Altered functional and structural connectivities in patients with MS: a 3-T study. *Neurology* 2007; 69: 2136-2145.
- 59.- Narayana PA. Magnetic resonance spectroscopy in the monitoring of multiple sclerosis. *J Neuroimaging* 2005; 15: 46S-57S.
- 60.- Sarchielli P, Presciutti O, Pelliccioli GP, et al. Absolute quantification of brain metabolites by proton magnetic resonance spectroscopy in normal-appearing white matter of multiple sclerosis patients. *Brain* 1999; 122 (Pt 3): 513-521.
- 61.- Srinivasan R, Sailasuta N, Hurd R, et al. Evidence of elevated glutamate in multiple sclerosis using magnetic resonance spectroscopy at 3 T. *Brain* 2005; 128: 1016-1025.
- 62.- Chard DT, Griffin CM, McLean MA, et al. Brain metabolite changes in cortical grey and normal-appearing white matter in clinically early relapsing-remitting multiple sclerosis. *Brain* 2002; 125: 2342-2352.
- 63.- Srinivasan R, Ratiney H, Hammond-Rosenbluth KE, et al. MR spectroscopic imaging of glutathione in the white and gray matter at 7 T with an application to multiple sclerosis. *Magn Reson Imaging* 2010; 28: 163-170.
- 64.- Ogawa S, Lee TM, Kay AR, Tank DW. Brain magnetic resonance imaging with contrast dependent on blood oxygenation. *Proc Natl Acad Sci U S A* 1990; 87: 9868-9872.
- 65.- Rocca MA, Filippi M. Functional MRI in multiple sclerosis. *J Neuroimaging* 2007; 17 Suppl 1: 36S-41S.
- 66.- Rocca MA, Colombo B, Falini A, et al. Cortical adaptation in patients with MS: a cross-sectional functional MRI study of disease phenotypes. *Lancet Neurol* 2005; 4: 618-626.
- 67.- Filippi M, Rocca MA. Functional MR imaging in multiple sclerosis. *Neuroimaging Clin N Am* 2009; 19: 59-70.
- 68.- Beaulieu C, Fenrich FR, Allen PS. Multicomponent water proton transverse relaxation and T2-discriminated water diffusion in myelinated and nonmyelinated nerve. *Magn Reson Imaging* 1998; 16: 1201-1210.
- 69.- Moore GR, Leung E, MacKay AL, et al. A pathology-MRI study of the short-T2 component in formalin-fixed multiple sclerosis brain. *Neurology* 2000; 55: 1506-1510.
- 70.- Oh J, Han ET, Lee MC, et al. Multislice brain myelin water fractions at 3T in multiple sclerosis. *J Neuroimaging* 2007; 17: 156-163.
- 71.- Laule C, Vavasour IM, Moore GR, et al. Water content and myelin water fraction in multiple sclerosis. A T2 relaxation study. *J Neurol* 2004; 251: 284-293.
- 72.- Deoni SC, Peters TM, Rutt BK. High-resolution T1 and T2 mapping of the brain in a clinically acceptable time with DESPOT1 and DESPOT2. *Magn Reson Med* 2005; 53: 237-241.
- 73.- Deoni SC. Transverse relaxation time (T2) mapping in the brain with off-resonance correction using phase-cycled steady-state free precession imaging. *J Magn Reson Imaging* 2009; 30: 411-417.
- 74.- Kangarlu A, Bourekas EC, Ray-Chaudhury A, Ramamohan KW. Cerebral cortical lesions in multiple sclerosis detected by MR imaging at 8 Tesla. *AJNR Am J Neuroradiol* 2007; 28: 262-266.
- 75.- Hammond KE, Lupo JM, Xu D, et al. Development of a robust method for generating 7.0 T multichannel phase images of the brain with application to normal volunteers and patients with neurological diseases. *Neuroimage* 2008; 39: 1682-1692.
- 76.- Stankiewicz J, Panter SS, Neema M, et al. Iron in chronic brain disorders: imaging and neurotherapeutic implications. *Neurotherapeutics* 2007; 4: 371-386.
- 77.- Ge Y, Jensen JH, Lu H, et al. Quantitative assessment of iron accumulation in the deep gray matter of multiple sclerosis by magnetic field correlation imaging. *AJNR Am J Neuroradiol* 2007; 28: 1639-1644.

V. Hipótesis

El conocimiento acerca de los mecanismos involucrados en la discapacidad física y cognitiva en la EM es limitado. Además, existe la necesidad de encontrar buenos marcadores con capacidad para predecir la evolución de la enfermedad y que con ello ayuden en la monitorización y decisión terapéutica. Hay evidencias de que el uso de técnicas de resonancia magnética cerebral o electrofisiológicas puede ayudar a caracterizar mejor la disfunción actual y a predecir su evolución en los pacientes con EM.

Las hipótesis planteadas son:

1. Se ha descrito que las lesiones pseudotumorales en pacientes con esclerosis múltiple presentan un borde hipointenso en secuencias potenciadas en T2 que traduciría la existencia de macrófagos, y captación de gadolinio en forma de anillo. Hipotetizamos que la presencia de lesiones con borde hipointenso en T2 o de lesiones captantes de gadolinio en anillo se asocia a una evolución clínica más severa en la esclerosis múltiple.

2. Los pacientes con esclerosis múltiple presentan alteraciones tanto de la estructura como de la función del cuerpo calloso. Dichas alteraciones pueden estar asociadas con la presencia de discapacidad física y cognitiva a través de un mecanismo de desconexión.

3. La alteración de la integridad de la sustancia blanca y la presencia de lesiones focales no explican completamente la disfunción cognitiva en la esclerosis múltiple. El daño microestructural de la sustancia gris puede contribuir a explicar estos déficits incluso en pacientes en fases iniciales de la enfermedad.

4. El daño axonal, la astrogliosis y la desmielinización, fenómenos que forman parte del sustrato patológico de la enfermedad, se asocian con la progresión de la enfermedad y pueden ser marcadores predictivos de la evolución de la discapacidad en la esclerosis múltiple.

VI. Objetivos

En base a las hipótesis nos planteamos los siguientes objetivos:

1. Conocer la prevalencia de lesiones con borde hipointenso en secuencias potenciadas en T2 y de lesiones captantes de gadolinio en anillo en una cohorte de pacientes seguidos según la práctica clínica habitual, y evaluar la correlación entre ambos patrones radiológicos y su significado clínico.
2. Identificar el daño estructural y microestructural del cuerpo calloso y la disfunción de sus conexiones motoras inhibitorias, y conocer la relación existente entre el daño del cuerpo calloso y la discapacidad física y cognitiva.
3. Identificar aquellas regiones donde la integridad tisular se correlaciona con el rendimiento de funciones cognitivas específicas. Determinar el impacto de la integridad de la sustancia gris y de los tractos de sustancia blanca y las lesiones en la cognición de pacientes poco discapacitados.
4. Determinar la capacidad de los marcadores de daño axonal, astrogliosis y desmielinización en resonancia magnética avanzada de predecir la discapacidad física y la atrofia cerebral a medio plazo.

VII. Resultados

Trabajo número 1

T2 hypointense rims and ring-enhancing lesions in MS

Sara Llufriu¹, Teresa Pujol², Yolanda Blanco¹, Karolina Hankiewicz¹, Mattia Squarcia², Joan Berenguer², Pablo Villoslada³, Francesc Graus¹, Albert Saiz^{1*}

¹ Service of Neurology, Hospital Clinic, Universitat de Barcelona, Spain. ² Service of Radiology, Hospital Clinic, Universitat de Barcelona, Spain. ³ Neurociencias, Institut d'Investigació Biomèdica August Pi i Sunyer (IDIBAPS), Barcelona, Spain.

Multiple Sclerosis Journal. 2010; 16(11): 1317–1325. IF: 4.472

RESULTADOS

En este trabajo se pretendía conocer la prevalencia de lesiones con borde hipointenso en secuencias potenciadas en T2 y de lesiones captantes de gadolinio en anillo en la práctica clínica habitual, la correlación entre ambos patrones radiológicos y su significado clínico.

Para ello, se revisaron de forma retrospectiva todas las RM realizadas a los pacientes de la Unidad de EM del Hospital Clínic de Barcelona entre los años 2000 y 2009. Se analizaron un total de 580 RM pertenecientes a 257 pacientes.

Se identificaron 35 lesiones con borde hipointenso, que correspondían al 9% de los pacientes, y 40 lesiones captantes de gadolinio en anillo, es decir al 12% de los pacientes. De forma infrecuente ambos patrones se presentaron de manera conjunta. Mientras que las lesiones con borde hipointenso no se asociaron a una peor evolución de la enfermedad, la presencia de lesiones captantes de gadolinio en anillo aumentaba el riesgo de alcanzar una discapacidad elevada y los pacientes que las presentaban tardaban menos tiempo en llegar a un EDSS de 4.0 y 6.0.

T2 hypointense rims and ring-enhancing lesions in MS

**Sara Llufriu¹, Teresa Pujol², Yolanda Blanco¹,
Karolina Hankiewicz¹, Mattia Squarcia², Joan Berenguer²,
Pablo Villoslada³, Francesc Graus¹ and Albert Saiz¹**

Multiple Sclerosis

16(11) 1317–1325

© The Author(s) 2010

Reprints and permissions:

sagepub.co.uk/journalsPermissions.nav

DOI: 10.1177/1352458510377905

msj.sagepub.com



Abstract

Background: Hypointense rims peripherally on T2-weighted MRI (rim lesions) have been associated with gadolinium ring-enhancing lesions in multiple sclerosis (MS) in pathological studies. However, little is known about their frequency, we analyzed clinical significance in a cohort of MS sufferers according to routine clinical practice.

Methods: We retrospectively reviewed all available MRI scans performed on our MS patients between 2000 and 2009. A total of 580 MRI scans from 257 patients were analyzed. The presence of rim lesions and ring enhancement was assessed and counted blind. Furthermore, the correlation between both patterns, and with clinical characteristics, was evaluated.

Results: Thirty-five rim lesions were identified and 9% (24/257) of the patients showed at least one of these lesions. Forty ring-enhancing lesions were counted and 12% (29/245) of the patients who had undergone gadolinium MRI presented at least one such lesion. Thirteen lesions co-localized both patterns (40% of the rim lesions and 33% of the ring-enhancing lesions). Rim lesions and ring-enhancing lesions were observed in patients with clinically isolated syndrome (7%, 7%), relapsing-remitting (11%, 15%) and secondary progressive (13%, 9%) but none with primary progressive MS. Presence of ring-enhancing lesions was significantly associated with a shorter time to reach EDSS (Expanded Disability Status Scale) 4.0 and 6.0 (hazard ratio 7.6, 95% confidence interval 2.3–24.6).

Conclusions: Rim lesions and ring-enhancing lesions are present in close to 10% of patients with MS, and frequently both lesions appear independently one to the other. The association of ring enhancement with worst prognosis needs to be confirmed in prospective studies.

Keywords

Multiple sclerosis, magnetic resonance imaging, ring-enhancing lesions, diffusion-weighted imaging, T2 hypointensity

Date received: 25th March 2010; revised: 20th May 2010; 14th June 2010; accepted: 15th June 2010

Introduction

Ring enhancement on MRI images is well recognized as one of the patterns of enhancement in multiple sclerosis (MS). It has been reported to occur in approximately one quarter of all enhancing lesions.^{1–3} However, the presence of an associated hypointense rim peripherally on T2-weighted MRI (rim lesions) has been described in a few case reports and in three particular series.^{4–8} In one study on ring-enhancing lesions of different etiologies, the association of the ring enhancement with hypointense T2 rims was found in 54% (7/13) of the included MS patients.⁶ A pathology study correlating autopsy/biopsy MS subtypes with MRI found hypointense T2 rims in 50% (27/54) of the cases, all with an

immunopathological pattern I/II.⁷ Lastly, rim lesions were detected in 45% (75/168) of patients with biopsy confirmed tumefactive MS.⁸ Despite this, the clinical significance of rim lesions in a cohort of patients with MS, followed according to routine clinical practice, remains unknown.

¹Service of Neurology, Hospital Clinic, Universitat de Barcelona, Spain.

²Service of Radiology, Hospital Clinic, Universitat de Barcelona, Spain.

³Neurociencias, Institut d'Investigació Biomèdica August Pi i Sunyer (IDIBAPS), Barcelona, Spain.

Corresponding author:

Albert Saiz, MD, Service of Neurology, Hospital Clinic, Villarroel 170, 08036 Barcelona, Spain
Email: asaiz@clinic.ub.es

Diffusion-weighted MRI (DWI) is sensitive to the random translational motion of water molecules in tissue and can indeed detect subtle pathological changes not apparent on conventional MRI. The apparent diffusion coefficient (ADC) is usually increased in demyelinating lesions and in normal apparent white matter (NAWM) of MS patients.⁹ However, the relationship between ADC values and enhancement is less well known,^{10,11} and the behavior of rim lesions has not been formally evaluated.

The aim of the present study was to review the brain MRI scans of our MS patients to determine the frequency of rim lesions and ring enhancement, and to analyze the correlation between both patterns and the clinical significance associated with these lesions. In addition, the behavior of these lesions on DWI was also analyzed.

Methods

Patients

We identified 307 consecutive patients from the database at the MS center at the Hospital Clinic of Barcelona with either clinically isolated syndrome or definite MS according to the McDonald criteria,¹² who had had a brain MRI carried out between 2000 and 2009. Patients were included in the database from 2000 and followed every 3–6 months, collecting information about clinical relapses, disability (EDSS [Expanded Disability Status Scale]) and therapies prospectively, as previously reported elsewhere.¹³ The demographics and clinical characteristics of the series (see below for the MRI protocol) are detailed in Table 1, and are similar to those reported in previous studies.^{14,15} There were no significant differences in clinical characteristics or number of MRI scans performed between those patients included and excluded because of the MRI criteria of selection (data not shown). The study was approved by the ethics committee of the Hospital Clinic.

MRI protocol

To guarantee the quality and uniformity of the study, only the MRI scans performed at 1.5 Tesla were included. Thus, 145 MRI scans were excluded, leaving 580 scans from 257 patients for retrospective evaluation. With some exceptions (14 MRI scans did not have post-contrast T1-weighted imaging, and 168 did not have DWI sequences), all MRI scans were performed following the same protocol (Table 2). Three experienced neuroradiologists (TP, MS, and JB) reviewed the MRI scans blinded to the clinical characteristics.

Table 1. Demographic and clinical characteristics of the cohort of MS patients included in the study

	Patients included N = 257
Gender ratio, Female/Male	165/92 = 1.79
Age (y); Mean ± SD	42 ± 12
Median (Range)	41 (17–74)
Type of MS; N (%)	
Clinically isolated syndrome	46 (18%)
Relapsing-remitting	170 (66%)
Secondary progressive	24 (9%)
Primary progressive	17 (7%)
Disease duration (y); Mean ± SD	10.0 ± 7.7
Age of onset (y); Mean ± SD	32.2 ± 10.6
Median (Range)	30 (8–67)
Number of relapses in the first 2 y ^a ; Mean ± SD	2.2 ± 1.4
Number of relapses in the first 5 y ^a ; Mean ± SD	3.7 ± 3.0
Annualized relapse rate ^a ; Mean ± SD	0.7 ± 0.5
EDSS at 5 y from onset; Median (Range)	2.0 (0–7.0)
Time to EDSS 3.0 (y); Mean 95% CI	7.6 (5.9–9.4)
Time to EDSS 4.0 (y); Mean 95% CI	9.7 (7.9–11.5)
Time to EDSS 6.0 (y); Mean 95% CI	12.7 (10.3–14.9)
Time to SP course (y); Mean 95% CI	13.2 (9.6–16.9)

^aOnly relapsing-remitting and secondary progressive patients were considered.

y, years; SD, standard deviation; EDSS, expanded disability status scale; SP, secondary progressive; CI, confidence interval.

Conventional imaging. Prior to blind data collection, the lesions of interest were defined by consensus among the study investigators: rim lesions were defined by the presence of a complete or almost complete border of T2-weighted hypointensity relative to the hyperintensity of the lesion center and surrounding edema (Figure 1) as described previously.⁶ Ring enhancement on post gadolinium T1-weighted images was defined by the presence of a complete circular (closed ring) or incomplete (open ring) border of enhancement (Figure 2). The volume of contrast enhancement was measured by outlining manually the hyperintensity on post gadolinium T1-weighted images and using the MRICro Analyze Viewer program. The presence of rim lesions and ring-enhancing lesions, the number, size and volume of contrast enhancement, the association between them and their evolution were assessed.

Diffusion-weighted MRI. The pattern of DWI was analyzed in the center, the border and the periphery of the rim and the ring-enhancing lesions. In those lesions with an annular morphology (apparent low intensity in the border) in the ADC maps (Figure 3),

Table 2. Summary of the MRI acquisition characteristics used in the study

MRI system	PD / T2-weighted sequence	T1-weighted sequence	T1-weighted sequence	T1-weighted sequence with contrast	DW sequence
	Axial orientation	Axial orientation	Sagittal orientation	Axial orientation	Axial orientation
1.5-T Signa HDxt (General Electrics, Milwaukee, WI, USA)	TES sequence; TR/TE: 3900/ 23/83 ms; Matrix/FOV: 250 mm × 292 mm × 292 mm; × 240 mm; ST: 5 mm; IG: 1 mm	CSE sequence; TR/TE: 500/9 ms; Matrix/FOV: 250 mm × 292 mm × 240 mm; ST: 5 mm; IG: 1 mm	CSE sequence; TR/TE: 500/12 ms; Matrix/FOV: 192 mm × 380 mm × 240 mm; ST: 5 mm; IG: 1.5 mm	CSE sequence; TR/TE: 500/9 ms; Matrix/FOV: 250 mm × 292 mm × 240 mm; ST: 5 mm; IG: 1 mm; Gd IV 0.1 mmol/kg	TR/TE: 7000/89 ms; <i>b</i> : 1000 s/m ² ; Matrix/FOV: 132 mm × 293 mm × 239 mm; ST: 5 mm; IG: 1 mm
1.5-T Magnetom Symphony (Siemens Medical Systems, Germany)	TES sequence; TR/TE: 2980/ 26/106 ms; Matrix/FOV: 256 mm × 192 mm 288 mm × 384 mm × 240 mm ST: 5 mm; IG: 1.5 mm	CSE sequence; TR/TE: 552/17 ms; Matrix/FOV: 192 mm × 256 mm × 240 mm; ST: 5 mm; IG: 1.5 mm	CSE sequence; TR/TE: 400/9 ms; Matrix/ FOV: 192 mm × 256 mm × 240 mm; ST: 5 mm; IG: 1.5 mm	CSE sequence; TR/TE: 552/17 ms; Matrix/FOV: 256 mm × 192 mm × 240 mm; ST: 5 mm; IG: 1.5 mm; Gd IV 0.1 mmol/kg	TR/TE: 3400/94 ms; <i>b</i> : 1000 s/m ² ; Matrix/FOV: 128 mm × 280 mm × 250 mm; ST: 5 mm; IG: 1.5 mm

CSE, conventional spin echo; DW, diffusion weighted; Gd, gadodiamide; IG, interslice gap; IV, intravenous; FOV, field of view; PD, proton density; ST, slice thickness; T, Tesla; TE, echo time; TES, turbo spin echo; TR, repetition time.

a region of interest (ROI) was manually drawn in the three parts of the lesion. A ROI was also drawn in the contralateral matched NAWM. The ADC values were obtained using a Functool 6.3 program with a workstation AW4.4 (2008) General Electric Company.

Statistical analysis

Chi-squared or Fisher exact tests were performed to compare categorical variables. Comparisons between continuous variables were performed using a *t*-test or Wilcoxon's rank test according to the normality of the distributions of the variables. An ANOVA or Kruskal-Wallis test was used for multiple comparisons. Kaplan-Meier analysis was used to estimate cumulative survival probabilities and to build survival plots. The time to reach an EDSS endpoint of 3.0, 4.0 and 6.0 was also analyzed using a Cox proportional hazards regression. All statistical analysis was performed by SPSS 16.0 version. Significant *p*-values were set at the 0.05 level.

Results

Conventional imaging

We identified 35 rim lesions from 9% (24/257) patients. The median number per scan was 1 (range 1–8), and

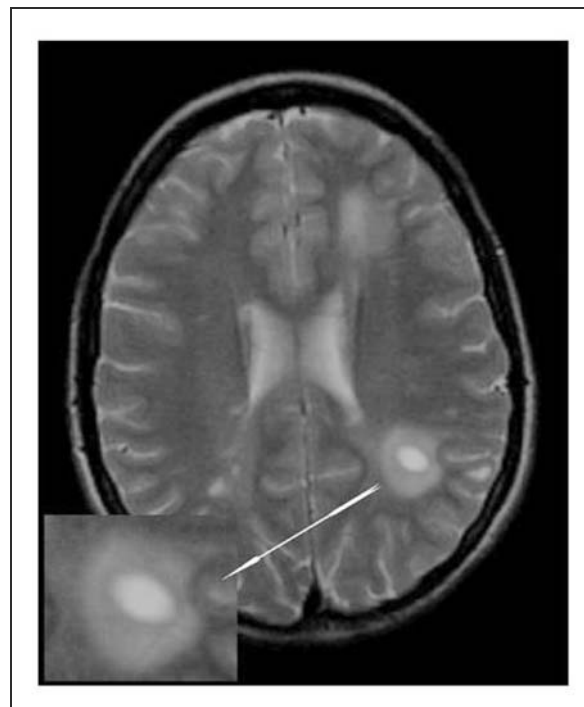


Figure 1. Rim lesions: axial T2-weighted images showing a complete border of hypointensity relative to the hyperintensity of the lesion center and the periphery.

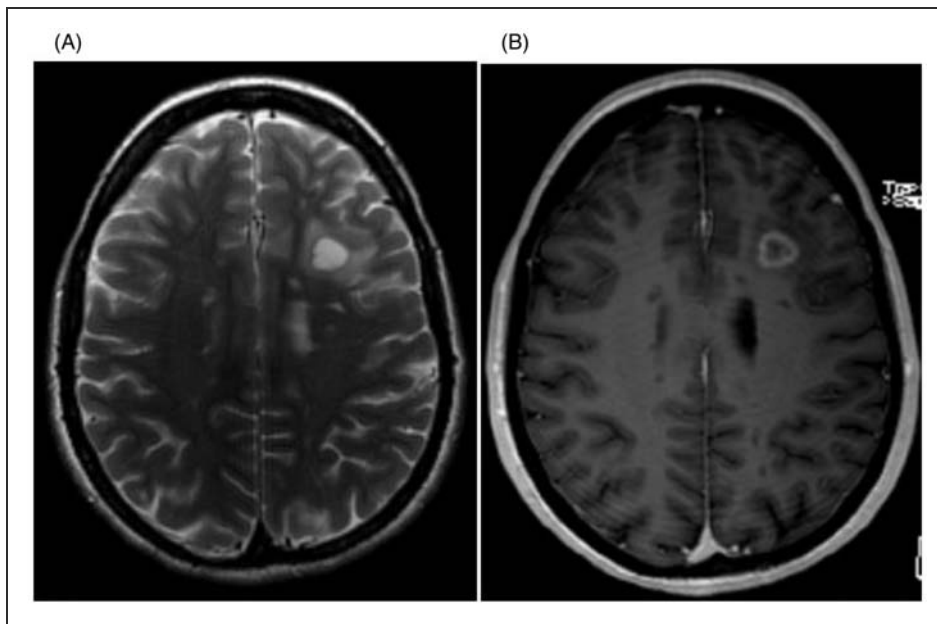


Figure 2. Ring-enhancing lesions: axial T2-weighted image showing a rim lesion (A) and the complete circular border of enhancement (B) on a T1-weighted image after administration of gadolinium-DTPA.

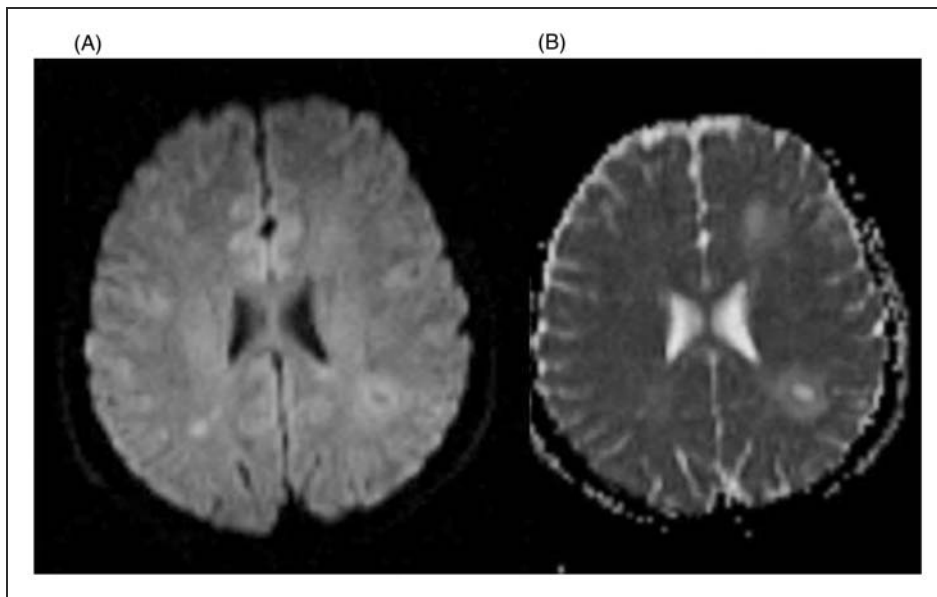


Figure 3. Diffusion-weighted imaging (A) of the rim lesion showed in Figure 1, and the hypointensity of the border in the apparent diffusion coefficient maps (B).

all but 4 lesions had a complete border of hypointensity. The median size of the lesions was 7.7 mm (range 3.4–17.4 mm).

Moreover, we counted 40 ring-enhancing lesions from 12% (29/245) patients. The median number per scan was 1 (range 1–4). The most frequent pattern (60%) was closed ring and 5 patients had both patterns of ring enhancement. The median size of the lesions was 9.8 mm (range 5.6–31.6 mm), and the

median volume of contrast enhancement was 273 mm³ (range 80–6143 mm³).

From the 32 rim lesions with an available post-contrast study, 40% co-localized with ring enhancement and 12.5% with nodular enhancement. Accordingly, 32.5% (13/40) ring-enhancing lesions co-localized with a hypointense rim on T2. Coexistence of rim lesions with and without enhancement was observed in 3 patients.

Fifteen rim lesions had an MRI follow-up (median 12 months, 1–52 months). The hypointense border on T2 persisted in 12% at 3.5 and 13 months, and 88% changed to a homogeneous T2-weighted hyperintensity. The ring enhancement had disappeared in the 19 cases with follow-up MRI (median 12 months, 1–52 months).

Diffusion-weighted MRI. DWI study was available in 44% (12/27) of the isolated ring-enhancing lesions, in 73% (16/22) of the isolated rim lesions and in 69% (9/13) of those with co-localization of both patterns. On DWI, the most frequent pattern was hyperintensity in all the lesion parts except in the center, where hypointensity was the most prevalent pattern in isolated rim lesions and co-localizing lesions.

Mean ADC values were higher in the center, border and periphery compared with the contralateral NAWM. The mean ratio (region analyzed/NAWM) showed the following pattern: increased values in the center > periphery > border of the lesion (Table 3). ADC in the border was significantly lower than in the center for lesions with co-localization ($p=0.004$), and a trend was found in isolated ring-enhancing lesions ($p=0.05$). No significant differences were observed between the three types of lesion. Results of the ADC analysis are summarized in Table 3.

Clinical and MRI relationship

Rim lesions were detected in 7% of the patients with a CIS, in 11% of the relapsing-remitting patients

(RRMS) and in 13% of the secondary progressive (SPMS) patients. Ring-enhancing lesions were found in 7% of the patients with CIS, 15% of the RRMS and 9% of the SPMS patients (Table 4). The 21% (5/24) of patients with rim lesions and 24% (7/29) of patients with ring-enhancing lesions had received corticosteroid treatment within 30 days previous to the MRI where those lesions were present. The frequency of corticosteroid therapy was not significantly different between patients with rim lesions that co-localized with ring enhancement and those who did not have contrast enhancement (23% vs. 22%, $p=1.0$). None of these lesions were found in patients with primary progressive MS (PPMS). There were no significant differences in demographical or clinical characteristics of the patients with rim lesions compared with the rest of the patients (Table 4). However, patients with ring-enhancing lesions had a shorter time to reach an EDSS score of 4.0 (median of 3 years vs. 11 years, $p=0.004$) and an EDSS score of 6.0 (median of 4 years vs. 14 years, $p=0.001$) (Table 4). In a Cox regression model, that included as covariates: MS course; number of relapses in the first 2 years from onset; presence of rim lesions; and presence of ring-enhancing lesions, a significantly higher risk of reaching an EDSS of 4.0 and 6.0 was observed, associated with the presence of ring-enhancing lesions (hazard ratio [HR] 7.6, 95% confidence interval [CI] 2.3 to 24.6, $p=0.001$) and the number of relapses in the first 2 years of disease (HR 1.7, 95% CI 1.3 to 2, $p<0.001$).

Table 3. Apparent diffusion coefficient (ADC) values

		Center		Border		Periphery		NAWM
		ADC ($\times 10^{-3}\text{mm}^2/\text{s}$)	Ratio ^a	ADC ($\times 10^{-3}\text{mm}^2/\text{s}$)	Ratio ^a	ADC ($\times 10^{-3}\text{mm}^2/\text{s}$)	Ratio ^a	ADC ($\times 10^{-3}\text{mm}^2/\text{s}$)
Only Rim hypointensity	Lesion 1	2.54	3.08	1.03	1.24	2.05	2.49	0.83
	Lesion 2	1.75	2.14	0.86	1.05	1.19	1.45	0.82
	Mean \pm SD	2.14 \pm 0.63	2.61 \pm 0.67	0.94 \pm 0.12	1.15 \pm 0.13	1.62 \pm 0.61	1.97 \pm 0.73	0.82 \pm 0.004
Only ring enhancement	Lesion 1	1.39	1.83	1.26	1.66	1.22	1.61	0.76
	Lesion 2	1.46	1.70	0.87	1.01	0.94	1.09	0.86
	Lesion 3	1.16	1.59	0.69	0.95	0.83	1.14	0.73
	Lesion 4	1.86	2.30	0.88	1.08	0.82	1.01	0.81
	Mean \pm SD	1.47 \pm 0.29	1.85 \pm 0.31	0.93 \pm 0.24	1.18 \pm 0.33	0.95 \pm 0.19	1.21 \pm 0.27	0.79 \pm 0.06
Rim hypointensity with ring enhancement	Lesion 1	1.84	2.14	1.25	1.45	1.21	1.41	0.86
	Lesion 2	1.81	2.10	1.26	1.46	1.25	1.45	0.86
	Lesion 3	1.87	2.20	0.94	1.10	1.64	1.93	0.85
	Lesion 4	2.12	2.33	1.31	1.44	1.25	1.37	0.91
	Mean \pm SD	1.91 \pm 0.14	2.19 \pm 0.1	1.19 \pm 0.17	1.36 \pm 0.18	1.34 \pm 0.20	1.54 \pm 0.26	0.87 \pm 0.03

^aRelative to ADC of contralateral normal appearing white matter (NAWM).

Table 4. Demographic and clinical characteristics of the patients according to the presence of rim lesions or ring enhancement

	Rim lesions N=24	No Rim lesions N=233	p	Ring- enhancement N=29	No Ring- enhancement N=216 ^a	p
Gender ratio. Female/Male	1.7	1.87	n.s.	2.2	1.7	n.s.
Age (y); Mean±SD	42±14	42±11	n.s.	40±12	42±11	n.s.
Type of MS; N (%)						
CIS	3 (7%)	43 (93%)	n.s.	3 (7%)	42 (93%)	0.09
RR	18 (11%)	152 (89%)		24 (15%)	138 (85%)	
SP	3 (13%)	21 (87%)		2 (9%)	20 (91%)	
PP	0	17 (100%)		0	16 (100%)	
Duration of disease (y); mean±SD	9.9±7.9	10±7.6	n.s.	9.5±6.6	9.8±7.4	n.s.
Age at onset (y); mean±SD	32.4±11.6	32.2±10.5	n.s.	30±10	33±11	n.s.
Number of relapses ^b first 2 y; mean±SD	1.9±0.9	2.3±1.5	n.s.	2.1±1.4	2.3±1.44	n.s.
Number of relapses ^b first 5 y; mean±SD	3.4±2.4	3.8±3.1	n.s.	3.4±2.0	3.8±3.1	n.s.
Annualized relapse rate ^b ; mean±SD	0.7±0.7	0.7±0.5	n.s.	0.6±0.4	0.7±0.6	n.s.
EDSS at 5 y from onset; median (range)	1.0 (0–6.5)	2.0 (0–6.5)	n.s.	1.6±1.4	2.1±1.4	n.s.
Time to EDSS 3.0 (y); mean 95% CI	8.4 (2.6–14.2)	7.5 (5.7–9.3)	n.s.	3.2(0–6.8)	8.1 (6.2–10.1)	n.s.
Time to EDSS 4.0 (y); mean 95% CI	11.5 (4.5–18.6)	9.5 (7.6–11.3)	n.s.	4.3(1.6–7.1)	10.4 (8.5–12.4)	0.004
Time to EDSS 6.0 (y); mean 95% CI	13 (4.3–21.7)	12.5 (10.1–14.9)	n.s.	4.4(4.4–9.5)	13.4 (11.1–13.8)	0.001

^aTwelve patients were excluded because they did not have post-contrast T1-weighted imaging.

^bOnly relapsing-remitting and secondary progressive patients were considered.

y, years; CIS, clinically isolated syndrome; RR, relapsing-remitting; SP, secondary progressive; PP, primary progressive; SD, standard deviation; CI, confidence interval.

Discussion

The frequency of rim lesions in an unselected MS population, and outside of a pathological series, had not been reported previously. Here we report that 9% of patients with MS have rim lesions on the MRI. This figure is much lower than the 45–50% found in the two available pathological series,^{7,8} although the differences both in techniques and in bias in patient selection for pathological studies do not make a direct comparison possible. It is worth mentioning that only one of the included patients had a lesion that could be considered tumefactive.^{8,16} Regarding MRI studies, a previous study reported rim lesions in 4.5% (6/132) of MS patients,¹⁷ although the definition of a rim lesion (with a central hyperintensity surrounded by a halo of lower intensity) was not identical to our study and previous studies.⁶ The detection of the rim, that might reflect the presence of an iron-rich macrophage layer at the edge of the lesion,^{18,19} containing paramagnetic free radicals,^{3,4} can be masked in conventional T2-weighted

sequences. At 7T the chance of detection of paramagnetic substances increases.²⁰ In that sense a recent report comparing 1.5 T and 7 T MRI found rim lesions at 7 T in 3 of the 12 patients evaluated with T2*-weighted gradient echo (GRE) sequence.²¹ Moreover, a postprocessing technique of GRE (phase imaging) at 7T, which improves the detection of iron, allowed the visualization of a peripheral rim in 8% of lesions that was undetectable with magnitude GRE.²² Taken together, the data in the current and prior studies suggest that rim lesions, are infrequently found in conventional imaging.²³

Additionally, our study shows that the frequency of ring-enhancing lesions at any point in the disease is about 12%. This figure would be in accordance with the fact that, in active MS patients, less than a quarter of the new enhancing lesions have this pattern.^{1,2,3} Classically, lesions with a hypointense rim on T2-weighted imaging have been described in association with gadolinium ring enhancement.^{4,5,7,24} However, we found that they can appear separately, as only

40% of the rim lesions co-localized with the ring enhancement.

Rim lesions were not detected in patients with primary progressive MS, nor were the ring-enhancing lesions. Although the number of patients analyzed was low, these results agree with the low frequency of enhancement reported in primary progressive patients.^{14,25} However, other pathologic processes might contribute because 47% of the rim lesions were not associated with any enhancement. The lower frequency of a hypercellular edge at the lesion border in PPMS compared with SPMS²⁶ could be a part of those differences.

We did not find clinical differences in patients with relapse onset related to the presence of rim lesions. One possible explanation is that these lesions seem to be transient because nearly 90% of the rim lesions disappeared during follow-up. In contrast, the presence of ring-enhancing lesions in the current study was associated with a shorter time to reach a higher disability. Correlations between enhancing lesions, relapses, T2 lesion load and disability measured by the EDSS have been controversial.^{27,28} A recent analysis from the Sylvia Lawry Centre for MS Research, which included 31 RRMS and SPMS trial placebo groups, did not find that baseline enhancing lesions predicted in-trial relapses or disability at trial exit.²⁹ However, in a study with 28 RRMS patients, the percentage of ring-enhancing lesions correlated with EDSS and T2 lesion load, and predicted the occurrence of relapses and worsening of the EDSS after three years.¹ Further reports, which have shown that ring-enhancing lesions evolve most frequently into persistent permanent black holes,³⁰ correlate strongly with increased cerebral atrophy and with a high disease activity.^{3,31} Taken together these data suggest that ring-enhancing and homogeneously enhancing lesions may represent a different pathological process. Correlation studies of MRI findings with lesion pathology have shown that ring-enhancing lesions were associated with massive macrophage infiltration in the zone of myelin destruction at the plaque border,^{4,5,24} and with more destructive damage as measured by magnetization transfer analysis.^{32,33}

In a previous study, rim lesions showed variable signals on DWI, and mostly mixed with regions of bright and dark intensity. However, ADC maps were not evaluated.⁶ We also found variable signals on DWI and lower ADC levels of NAWM compared with the lesions. In addition, in ring-enhancing lesions and in those that co-localized rim hypointensity with ring enhancement, the ADC levels were lower in the border compared with the center. The results are in line with previous studies that found variable ADC values and decreased diffusivity in the edge of the acute lesions compared with the plaque center.³⁴

This probably represents the presence of vasogenic edema in the extracellular space superimposed on a decrease in diffusivity³⁵ caused by cytotoxic edema from the massive cell infiltration,^{4,5,24} or alternatively due to the cell infiltration by itself.

Only one ring-enhancing lesion showed an absolute reduced ADC value in the border, a pattern of restricted diffusion that has been described in isolated reports and in patients with tumefactive demyelinating lesions.^{16,36,37}

This study carries the inherent limitations of any retrospective study. Although patients were followed prospectively, the design of the MRI analysis is retrospective. Therefore, decisions in the number or timing of MRI scans were not controlled. Despite this, the patients we excluded were different neither in terms of clinical characteristics nor the number of MRIs performed. The possible impact of corticosteroid therapy in the observed frequency of ring-enhancing lesions in the whole cohort cannot be answered with this observational study.

In conclusion, the frequencies of rim lesions and ring-enhancing lesions in an unselected cohort of MS patients at some point in the disease are 9% and 12% respectively. Both lesions can be present independently. Ring-enhancing lesions, but not rim lesions, seem to be associated with a worst prognosis. Further prospective studies are needed to confirm the prognostic value of identifying these lesions.

Funding

This work was supported in part by Fondo de Investigaciones Sanitarias (grant number PI060070) and Red Española de Esclerosis Múltiple (grant numbers RD07/0060/0012 and RD07/0060/0001), Instituto de Salud Carlos III (ISCIII), Spain. Sara Llufriu is a recipient of the Contrato Rio Hortega from the ISCIII, Spanish Ministry of Health.

Conflict of interest statement

None declared.

Acknowledgements

We would like to thank Dr Daniel Pelletier for his useful comments on the manuscript.

References

1. Morgen K, Jeffries NO, Stone R, et al. Ring-enhancement in multiple sclerosis: marker of disease severity. *Mult Scler* 2001; 7: 167–171.
2. He J, Grossman RI, Ge Y and Mannon J. Enhancing patterns in multiple sclerosis: Evolution and persistence. *Am J Neuroradiol* 2000; 22: 664–669.

3. Zivadinov R, Gabnato F, Nasuelli D, et al. Short-term brain atrophy changes in relapsing-remitting multiple sclerosis. *J Neurol Sci* 2004; 223: 185–193.
4. Brück W, Neubert K, Berger T and Weber JF. Clinical, radiological, immunological and pathological findings in inflammatory CNS demyelination—possible markers for an antibody-mediated process. *Mult Scler* 2001; 7: 173–177.
5. König FB, Wildemann B, Nessler S, et al. Persistence of immunopathological and radiological traits in multiple sclerosis. *Arch Neurol* 2008; 65: 1527–1532.
6. Schwartz KM, Erickson BJ and Lucchinetti C. Pattern of T2 hypointensity associated with ring-enhancing brain lesions can help to differentiate pathology. *Neuroradiology* 2006; 48: 143–149.
7. Lucchinetti CF, Altintas A, Wegner C, et al. Magnetic Resonance Imaging Correlates of Multiple Sclerosis Pathologic Subtypes. *Ann Neurol* 2003; 54(Suppl 7): S37.
8. Lucchinetti CF, Gavrilova RH, Metz I, et al. Clinical and radiographic spectrum of pathologically confirmed tumefactive multiple sclerosis. *Brain* 2008; 131: 1759–1775.
9. Castriota Scanderbeg A, Sabatini U, Fasano F, et al. Diffusion of water in large demyelinating lesions: a follow-up study. *Neuroradiol* 2002; 44: 764–767.
10. Roychowdhury S, Maldjian JA and Grossman RI. Multiple sclerosis: comparison of trace apparent diffusion coefficients with MR enhancement pattern of lesions. *Am J Neuroradiol* 2000; 21: 869–874.
11. Rovaris M, Gass A, Bammer R, et al. Diffusion MRI in multiple sclerosis. *Neurology* 2005; 65: 1526–1532.
12. McDonald WI, Compston A, Edan G, et al. Recommended diagnostic criteria for multiple sclerosis: guidelines from the International Panel on the diagnosis of multiple sclerosis. *Ann Neurol* 2001; 50: 121–127.
13. Gómez-Choco MJ, Iranzo A, Blanco Y, Graus F, Santamaría J and Saiz A. Prevalence of restless legs syndrome and REM sleep behavior disorder in multiple sclerosis. *Mult Scler* 2007; 13: 805–808.
14. Thompson AJ, Polman CH, Miller DH, et al. Primary progressive multiple sclerosis. *Brain* 1997; 120: 1085–1096.
15. Casado V, Martínez-Yélamos S, Martínez-Yélamos A, et al. Direct and indirect costs of Multiple Sclerosis in Baix Llobregat (Catalonia, Spain), according to disability. *BMC Health Serv Res* 2006; 6: 143.
16. Malhotra HS, Jain KK, Agarwal A, et al. Characterization of tumefactive demyelinating lesions using MR imaging and in-vivo proton MR spectroscopy. *Mult Scler* 2009; 15: 193–203.
17. Yetkin Z and Haughton VM. Atypical demyelinating lesions in patients with multiple sclerosis. *Neuroradiology* 1995; 37: 284–286.
18. LeVine SM. Iron deposits in multiple sclerosis and Alzheimer's disease brains. *Brain Res* 1997; 760: 298–303.
19. Craelius W, Migdal MW, Luessenhop CP, et al. Iron deposits surrounding multiple sclerosis plaques. *Arch Pathol Lab Med* 1982; 106: 397–399.
20. Wattjes MP and Barkhof F. High field MRI in the diagnosis of multiple sclerosis: high field-high yield? *Neuroradiol* 2009; 51: 279–302.
21. Kollia K, Maderwald S, Putzki N, et al. First clinical study on Ultra-High-Field MR imaging in patients with multiple sclerosis: comparison of 1.5 T and 7 T. *Am J Neuroradiol* 2009; 30: 699–702.
22. Hammond KE, Metcalf M, Carvajal L, et al. Quantitative in vivo magnetic resonance imaging of multiple sclerosis at 7 Tesla with sensitivity to iron. *Ann Neurol* 2008; 64: 707–713.
23. Seewann A, Enzinger C, Filippi M, et al. MRI characteristics of atypical idiopathic inflammatory demyelinating lesions of the brain. A review of reported findings. *J Neurol* 2008; 255: 1–10.
24. Brück W, Bitsch A, Kolenda H, Brück Y, Stiefel M and Lassmann H. Inflammatory central nervous system demyelination: correlation of magnetic resonance imaging findings with lesion pathology. *Ann Neurol* 1997; 42: 783–793.
25. Wolinsky JS PROMiSe Trial Study Group. The PROMiSe trial: baseline data review and progress report. *Mult Scler* 2004; 10: S65–S72.
26. Revesz T, Kidd D, Thompson AJ, Barnard RO and McDonald WI. A comparison of the pathology of primary and secondary progressive multiple sclerosis. *Brain* 1994; 117: 759–765.
27. Molyneux PD, Filippi M, Bakhof F, et al. Correlations between monthly enhanced MRI lesion rate and changes in T2 lesion volume in multiple sclerosis. *Ann Neurol* 1998; 43: 332–339.
28. Kappos L, Moeri D, Radue EW, et al. Predictive value of gadolinium-enhanced magnetic resonance imaging for relapse rate and changes in disability or impairment in multiple sclerosis: a meta-analysis. Gadolinium MRI Meta-analysis Group. *Lancet* 1999; 353: 964–969.
29. Daumer M, Neuhaus A, Morrissey S, Hintzen R and Ebers GC. MRI as an outcome in multiple sclerosis clinical trials. *Neurology* 2009; 72: 705–710.
30. Van den Elskamp I, Lembecke J, Dattola V, et al. Persistent T1 hypointensity as an MRI marker for treatment efficacy in multiple sclerosis. *Mult Scler* 2008; 14: 764–769.
31. Leist TP, Gobbi MI, Frank JA and McFarland HF. Enhancing magnetic resonance imaging lesions and cerebral atrophy in patients with relapsing multiple sclerosis. *Arch Neurol* 2001; 58: 57–60.
32. Petrella JR, Grossman RI, McGowan JC, Campbell G and Cohen JA. Multiple sclerosis lesions: relationship between MR enhancement pattern and magnetization transfer effect. *Am J Neuroradiol* 1996; 17: 1041–1049.
33. Rovira A, Alonso J, Cucurella G, et al. Evolution of multiple sclerosis lesions on serial contrast-enhanced T1-weighted and magnetization-transfer MR images. *Am J Neuroradiol* 1999; 20: 1939–1945.
34. Tievsky AL, Ptak T and Farkas J. Investigation of apparent diffusion coefficient and diffusion tensor anisotropy in acute and chronic multiple sclerosis lesions. *Am J Neuroradiol* 1999; 20: 1491–1499.
35. Gass A, Niendorf T and Hirsch JG. Acute and chronic changes of the apparent diffusion coefficient in

- neurological disorders – biophysical mechanisms and possible underlying histopathology. *J Neurol Sci* 2001; 186: S15–S23.
36. Rovira A, Pericot I, Alonso J, Rio J, Grive E and Montalban X. Serial diffusion-weighted MR imaging and proton MR spectroscopy of acute large demyelinating brain lesions: case report. *Am J Neuroradiol* 2002; 23: 989–994.
37. Rosso C, Remy P, Creange A, Brugieres P, Cesaro P and Hosseini H. Diffusion-weighted MR imaging characteristics of an acute stroke-like form of multiple sclerosis. *Am J Neuroradiol* 2006; 27: 1006–1008.

Trabajo número 2

Influence of corpus callosum damage on cognition and physical disability in multiple sclerosis: A multimodal study

Sara Llufriu¹, Yolanda Blanco¹, Eloy Martínez-Heras¹, Jordi Casanova-Mollà², Íñigo Gabilondo¹, María Sepúlveda¹, Carles Falcón^{3,4}, Joan Berenguer⁵, Nuria Bargalló^{3,5}, Pablo Villoslada¹, Francesc Graus¹, Josep Valls-Solé², Albert Saiz^{1*}

¹Center for Neuroimmunology, Service of Neurology, Hospital Clinic and Institut d'Investigacions Biomèdiques August Pi i Sunyer (IDIBAPS), Barcelona, Spain; ²Service of Neurology, Hospital Clinic, Barcelona, Spain; ³Medical Imaging Platform, Institut d'Investigacions Biomèdiques August Pi i Sunyer (IDIBAPS), Barcelona, Spain; ⁴Centros de Investigación Biomédica en Red (CIBER-BBN), Barcelona, Spain; ⁵Service of Radiology and Imaging Diagnostic Center, Hospital Clinic and Institut d'Investigacions Biomèdiques August Pi i Sunyer (IDIBAPS), Barcelona, Spain.

Plos One. 2012 May; 7(5): e37167. IF: 3.730

RESULTADOS

En este artículo se pretendían evaluar las alteraciones en la estructura y función del CC en pacientes con EM y determinar la relación entre dichas alteraciones y la discapacidad física y cognitiva.

Para ello se incluyeron 21 pacientes con EMRR y 13 controles sanos apareados por edad y sexo. El estudio comprendía una evaluación multimodal del CC a través de RM y electrofisiología. A todos los sujetos se les realizó una RM craneal que incluía una secuencia 3D T1-Magnetization Prepared Rapid Acquisition Gradient Echo (MPRAGE) y una secuencia de DTI. Además se les realizó una evaluación electrofisiológica para determinar la duración y latencia del iSP así como el tiempo de conducción central a través del uso de TMS. A los pacientes se les administró la BRB-N, el EDSS y el test MSFC para evaluar su discapacidad cognitiva y física.

Los pacientes presentaron una disminución significativa del volumen del CC y una alteración de su microestructura medida a través de DTI. Además, se objetivó un aumento de la latencia del iSP que podría traducir una alteración de la integridad de las fibras inhibitorias transcallosas entre las cortezas motoras. Las medidas de latencia del iSP se asociaron con el volumen y la integridad microestructural del CC.

La alteración de la microestructura y de la conducción inhibitoria motora del CC se asociaron con una mayor discapacidad cognitiva principalmente en tests que evaluaban la memoria episódica verbal y visual y los tests de rapidez de procesamiento de la información y, en menor medida, con la discapacidad física.

Influence of Corpus Callosum Damage on Cognition and Physical Disability in Multiple Sclerosis: A Multimodal Study

Sara Llufríu¹, Yolanda Blanco¹, Eloy Martínez-Heras¹, Jordi Casanova-Molla², Iñigo Gabilondo¹, María Sepulveda¹, Carles Falcon^{3,4}, Joan Berenguer⁵, Nuria Bargallo^{3,5}, Pablo Villoslada¹, Francesc Graus¹, Josep Valls-Sole², Albert Saiz^{1*}

1 Center for Neuroimmunology, Service of Neurology, Hospital Clinic and Institut d'Investigacions Biomèdiques August Pi i Sunyer (IDIBAPS), Barcelona, Spain, **2** Service of Neurology, Hospital Clinic, Barcelona, Spain, **3** Medical Imaging Platform, Institut d'Investigacions Biomèdiques August Pi i Sunyer (IDIBAPS), Barcelona, Spain, **4** Centros de Investigación Biomédica en Red (CIBER-BBN), Barcelona, Spain, **5** Service of Radiology and Imaging Diagnostic Center, Hospital Clinic and Institut d'Investigacions Biomèdiques August Pi i Sunyer (IDIBAPS), Barcelona, Spain

Abstract

Background: Corpus callosum (CC) is a common target for multiple sclerosis (MS) pathology. We investigated the influence of CC damage on physical disability and cognitive dysfunction using a multimodal approach.

Methods: Twenty-one relapsing-remitting MS patients and 13 healthy controls underwent structural MRI and diffusion tensor of the CC (fractional anisotropy; mean diffusivity, MD; radial diffusivity, RD; axial diffusivity). Interhemispheric transfer of motor inhibition was assessed by recording the ipsilateral silent period (ISP) to transcranial magnetic stimulation. We evaluated cognitive function using the Brief Repeatable Battery and physical disability using the Expanded Disability Status Scale (EDSS) and the MS Functional Composite (MSFC) z-score.

Results: The ISP latency correlated with physical disability scores (r ranged from 0.596 to 0.657, P values from 0.004 to 0.001), and with results of visual memory ($r = -0.645$, $P = 0.002$), processing speed ($r = -0.51$, $P = 0.018$) and executive cognitive domain tests ($r = -0.452$, $P = 0.039$). The area of the rostrum correlated with the EDSS ($r = -0.442$, $P = 0.045$). MD and RD correlated with cognitive performance, mainly with results of visual and verbal memory tests (r ranged from -0.446 to -0.546 , P values from 0.048 to 0.011). The ISP latency correlated with CC area ($r = -0.345$, $P = 0.049$), volume ($r = -0.401$, $P = 0.002$), MD ($r = 0.404$, $P = 0.002$) and RD ($r = 0.415$, $P = 0.016$).

Conclusions: We found evidence for structural and microstructural CC abnormalities associated with impairment of motor callosal inhibitory conduction in MS. CC damage may contribute to cognitive dysfunction and in less extent to physical disability likely through a disconnection mechanism.

Citation: Llufríu S, Blanco Y, Martínez-Heras E, Casanova-Molla J, Gabilondo I, et al. (2012) Influence of Corpus Callosum Damage on Cognition and Physical Disability in Multiple Sclerosis: A Multimodal Study. PLoS ONE 7(5): e37167. doi:10.1371/journal.pone.0037167

Editor: Friedemann Paul, Charité University Medicine Berlin, Germany

Received January 4, 2012; **Accepted** April 16, 2012; **Published** May 14, 2012

Copyright: © 2012 Llufríu et al. This is an open-access article distributed under the terms of the Creative Commons Attribution License, which permits unrestricted use, distribution, and reproduction in any medium, provided the original author and source are credited.

Funding: The work was supported in part by a grant from the Red Española de Esclerosis Múltiple (REEM) RD07/0060/0001, RD07/0060/0012. No additional external funding was received for this study. The funders had no role in study design, data collection and analysis, decision to publish, or preparation of the manuscript.

Competing Interests: Co-author Pablo Villoslada is a PLoS ONE Editorial Board member. This does not alter the authors' adherence to all the PLoS ONE policies on sharing data and materials.

* E-mail: asaiz@clinic.ub.es

Introduction

The corpus callosum (CC) is the major cerebral commissure. It connects homologous regions of both sides of the brain providing interhemispheric communication between cortical and subcortical neurons. It plays an important role in the organization of complex commands involving bilateral tasks with precise timing of information transfer between sides [1]. The CC is a common target in multiple sclerosis (MS) frequently showing focal demyelinating lesions and atrophy since early stages of the disease [2]. Hence it is of interest to study whether CC damage influences cognitive impairment and physical disability in MS, two of the most devastating consequences of the disease.

The association between disability measured by the Expanded Disability Status Scale (EDSS) [3] and CC atrophy remains inconsistent, with some studies showing a positive correlation [2,4], but others reported no significant relationship [5,6]. In contrast to structural magnetic resonance imaging (MRI) techniques, the evaluation of CC by means of diffusion tensor imaging (DTI) seems to correlate better with clinical measures of disability [6,7].

Only few studies have addressed the relationship between CC damage and cognitive impairment in MS. A significant correlation has been reported between CC atrophy and the severity of impairment in the performance of tasks requiring interhemispheric

transfer of information [8] and also between a number of diffusion metrics from tractography maps or DTI voxel-based approaches and the results of a single cognitive test [9,10] or a battery of neuropsychological tests [11,12]. In overall, the revised literature suggests that cognitive impairment in MS could be the consequence of disconnection between cortical and subcortical circuits [13].

The interhemispheric connectivity through the CC can be evaluated by means of transcranial magnetic stimulation techniques (TMS), i.e. interhemispheric inhibition (IHI) and ipsilateral silent period (iSP) [14,15,16]. A recent study found that even with no evidence of macroscopic CC lesions, patients with early relapsing-remitting MS showed abnormally reduced IHI and abnormally reduced fractional anisotropy (FA) from DTI within the motor part of the CC, although the correlation between both measures could not be demonstrated in those patients [17]. However, in healthy controls there was a direct linear correlation between IHI and DTI measures [18] suggesting a close link between microstructure and function.

The iSP reflects the inhibition induced on ipsilateral voluntary activity by focal unilateral TMS [16]. It is thought to be mediated through the CC although other more caudal pathways may also exist [19]. Correlation studies looking at iSP, physical disability and structural CC MRI changes have shown conflicting results [20,21,22]. However, the relationship between iSP and microstructural CC damage or cognition has not been investigated so far. DTI allows the study of microscopic Brownian motion of water molecules hindered by cellular structures, such as cell membranes and axonal cytoskeleton. This property makes the technique sensitive to microstructure integrity disruption, frequent in MS lesions and in normal-appearing white matter (NAWM) [11,23]. White matter damage is reflected by a reduction in FA

and increase in overall diffusion (mean diffusivity, MD), which are non-specific metrics due to the various underlying pathophysiological mechanisms [24]. Other metrics derived from FA are axial diffusivity (AD) and radial diffusivity (RD), which seem to be related to axonal damage and demyelination respectively in animal models [25].

With this background we hypothesized that the cognitive impairment and physical disability in MS could be associated with disconnection between brain areas due to CC damage. To test this hypothesis we used a multimodal approach to investigate CC status by analyzing the structural/microstructural damage of the CC, and the function of motor inhibitory connections through the CC by the iSP in a series of relapsing-remitting MS patients. Then, we analyzed the relationship between the extent of CC damage and cognitive impairment, using a battery of neuropsychological tests, and scores on standard disability scales including the EDSS and the Multiple Sclerosis Functional Composite (MSFC) [26].

Methods

Study subjects

Twenty one consecutive patients with relapsing-remitting MS [27] were prospectively selected from the outpatient MS Clinic of the Hospital Clinic of Barcelona. All patients had to be ambulatory with low to moderate disability (EDSS 0 to 6.0), under stable immunomodulatory treatment and relapse and steroid-free for at least one month prior to the study inclusion. Thirteen age and sex matched healthy individuals were included as controls. The Hospital Clinic Research Ethics Committee approved the study and all participants gave written informed consent.

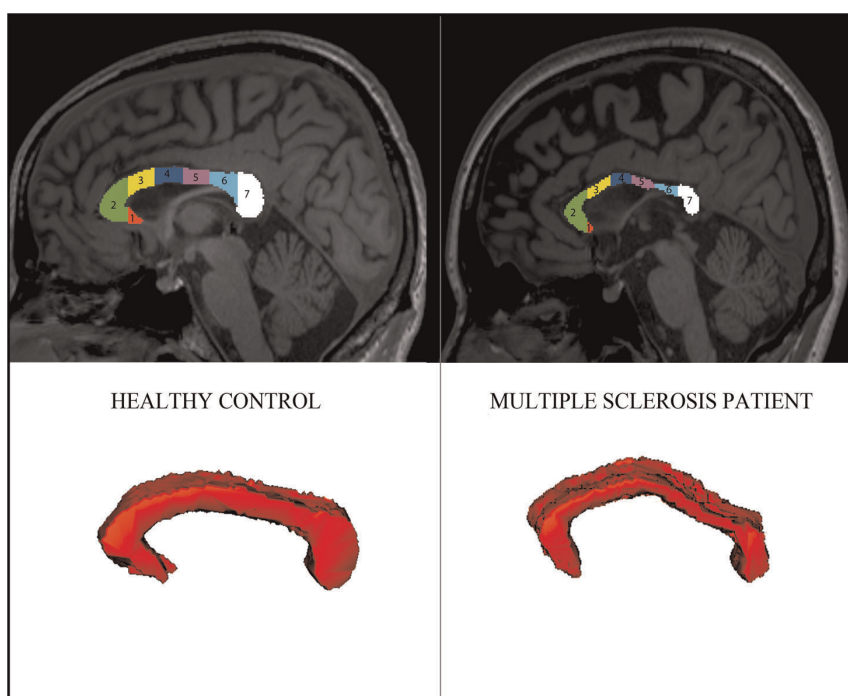


Figure 1. Structural magnetic resonance imaging of the corpus callosum. Area of corpus callosum in midsagittal slice with subdivision in 7 segments, corresponding consecutively to the rostrum, genu, rostral body, anterior midbody, posterior midbody, isthmus, and the splenium (top images) and volume obtained from 11 consecutive central sagittal slices (bottom images). Left images correspond to a healthy control and right images to a multiple sclerosis patient.

doi:10.1371/journal.pone.0037167.g001

Clinical and cognitive evaluation

The disease history was recorded and a complete neurological examination including the EDSS and MSFC z-score punctuation to assess physical disability was obtained. The z-score of the MSFC was calculated by comparison with a standard MS population according to the protocol of the National MS Society [26]. The Brief Repeatable Battery–Neuropsychology test (BRB-N) was used to assess the cognitive status. Neuropsychological test scores were expressed as z-scores for all tests and cognitive domains, derived from normative data obtained from a published Spanish healthy control cohort study and stratified by age and education [28]. Tests included in the BRB-N were: the Selective Reminding Tests (SRT) to assess verbal memory; the 10/36 Spatial Recall Tests (10/36) to assess visual memory; the Symbol Digit Modalities Test (SDMT) to assess attention, visual precision search, processing speed and executive functions; the Paced Auditory Serial Addition Task 3 seconds (PASAT 3) to assess the maintenance of attention, processing speed and working memory; and the World List Generation (WLG) to assess associative verbal fluency. The z-scores from the verbal memory domain, visual memory domain, attentional/executive domain, fluency domain, and the global BRB-N were measured as previously reported [28]. Physical and cognitive scores were not measured in control subjects.

Neurophysiological evaluation

TMS was used to assess motor threshold (passive and active), central motor conduction time and ipsilateral silent period in hand muscles. A Mystro 5Plus EMG was used for recording the responses and triggering the magnetic stimulator. The stimulator was a Novametrix 200 (MagStim, London), equipped with an 8-shaped coil for cortical stimulation and a round coil for cervical foraminal stimulation. Surface recording electrodes were attached over the first dorsal interosseous (FI) muscles of both sides. Resting motor threshold was measured as the minimum stimulus intensity needed to elicit motor evoked potentials (MEPs) of at least 50 µV in 50% of a series of stimuli [29]. The stimulus intensity was changed stepwise in 1% increment or decrement until the threshold was reached. We applied magnetic stimulation to the scalp and to the cervical region. During cortical stimulation, subjects were requested to maintain a slight preactivation of the FI. The latency difference between the MEPs to cortical and cervical stimulation was calculated as the central motor conduction time (CMCT). Then, subjects were asked to keep a steady contraction of about 20% of their maximum voluntary contraction by pressing the index finger against the thumb in both hands. Stimuli of suprathreshold intensity were applied six times in each side. The mean duration and onset latency of the iSP from both hands were manually measured by a technician unaware of clinical and MRI data.

Image acquisition and data postprocessing

All scans were performed on a 3T Siemens Trio MRI scanner (Erlangen, Germany), using a 32 channel head coil for radio frequency transmission and signal reception. The MRI protocol included the following sequences: a) 3D structural T1-weighted MPRAGE (Magnetization Prepared Rapid Acquisition Gradient Echo) sequence: Repetition Time (TR): 2050 ms, Echo Time (TE): 2.4 ms, Inversion recovery time (TI): 1050 ms, Flip angle: 9°, FOV: 220 mm; b) DTI sequence: TR/TE: 7600/89 ms, acquisition matrix 122×122, FOV: 250 mm, 60 contiguous axial slices, diffusion gradients in 30 different directions, b value = 1000 s·mm⁻².

CC area was calculated from the 3D structural T1-weighted midsagittal slice by means of semiautomatic segmentation tool of Analyze software 9.0 (<http://www.analyzedirect.com>; Biomedical Imaging Resource, Mayo Clinic). The midsagittal CC section was then divided in 7 segments with a semiautomated subregional division [30] (Figure 1). A CC mask was drawn in 11 consecutive slices around the midsagittal plane where it could be clearly differentiated from the cingulated gyrus. Moreover, all the CC lesions were manually traced on the MPRAGE sequence to get a lesion load from the CC. The volumetric and DTI analysis of the CC included the visible lesions. The volume of the CC mask was calculated by adding the area of the 11 consecutive slices (area per slice thickness) (Figure 1). The CC area and the volume were then multiplied by a brain scaling factor calculated by SIENAX (FMRIB, Oxford, UK) to normalize for the cranial size.

An experienced neurologist created T1-lesion masks using semi-automated thresholding and manual editing methods directly from the high-resolution T1-MPRAGE images. Subsequent brain segmentation and normalization were performed using SIENAX, which was effectively fully automated once the T1 lesion mask had been used to avoid pixel misclassifications. The following parameters were derived from the segmentation: the normalized brain parenchymal volume (nBPV), normal-appearing white matter volume (nWMV), grey matter volume (nGMV) and whole brain T1-MPRAGE lesion volume (nLV).

FSL (FMRIB, Oxford, UK) tools were used to register DTI to structural images. A linear (FLIRT, solid rigid transformation) and nonlinear (FNIRT) registrations of FA maps to skull removed structural image were performed excluding the CC lesions when estimating the warps. The double registration was done aiming to consider changes in displacement and shape with high accuracy to structural image. The resulting transformation files were applied to index images derived from DTI to coregister them to CC mask. The borders of the CC mask were eroded to avoid that partial volume voxels diminishing mean values of the diffusivity indexes. The mean values of the following parameters were obtained in

Table 1. Results from the cognitive tests and domains included in the Brief Repeatable Battery in patients with multiple sclerosis.

Tests	SRTS	SRTR	SRTD	10/36	10/36D	SDMT	PASAT	WLG
	−0.68 (1.27)	−0.80 (1.21)	−0.03 (1.06)	−0.14 (0.75)	−0.03 (1.15)	0.21 (1.24)	−0.53 (1.16)	−1.13 (0.77)
Cognitive domains	Verbal memory			Visual memory		Attentional/executive		Fluency
	−0.64 (1.14)			−0.09 (0.81)		−0.15 (1.12)		−1.13 (0.77)
Global BRB	−0.50 (0.77)							

Values are mean ± SD z-scores. Abbreviations: SRTS = selective reminding test long term storage; SRTR = selective reminding test long term retrieval; SRTD = selective reminding test delayed recall; 10/36 = spatial recall test; SDMT = symbol digit modalities test; PASAT-3 = paced auditory serial addition task 3 seconds; WLG = world list generation; BRB = Brief Repeatable Battery.

doi:10.1371/journal.pone.0037167.t001

CC: FA, MD, RD (the average of the second and third eigenvalues) and AD (the first eigenvalue) from the CC mask.

Statistical analysis

The statistical analysis was performed using SPSS for Windows (version 17.0). Normality was assessed by the Kolmogorov-Smirnov test; all the variables except for the CC lesion volume had a normal distribution. All values are expressed as mean (SD). The independent-samples Student's *t* test was used to compare demographic, neurophysiologic and MRI metrics between MS and controls. Univariate correlations between clinical, neurophysiological, cognitive and MRI data were examined in patients with the Pearson correlation coefficients. A linear regression model was used to evaluate the effect of disease duration and disability on iSP measures. *P*-values <0.05 were considered to indicate statistical significance.

Results

Clinical and cognitive data

The 21 MS patients had a mean (SD) age of 37.2 (6.9) years, 12 (57%) were female with mean disease duration of 9.5 (5.38) years. Median EDSS score was 2.0 (range 0 to 6.0) and mean MSFC z-score 0.23 (0.59). The 13 healthy controls had a mean age of 35.2 (7.4), similar to the age of the patients (*P*=0.45), and 8 (61.5%) were females. The results of the cognitive tests in the cohort of MS patients are shown in Table 1.

Neurophysiological study

A summary of the data extracted from the TMS study is shown in Table 2. The mean iSP onset latency was significantly longer in MS patients than in controls (*P*=0.001). There was a statistically significant correlation between iSP latency and the EDSS score (*r*=0.657, *P*=0.001), the MSFC z-score (*r*=−0.596, *P*=0.004), and cognitive data, i.e., the 10/36 (*r*=−0.645, *P*=0.002), the SDMT (*r*=−0.51, *P*=0.018) and the executive cognitive domain (*r*=−0.452, *P*=0.039) z-scores. Moreover, the iSP latency correlated with disease duration, but this effect disappeared (*B*=0.170, *P*=0.426) when the EDSS score was added to the model (*B*=0.564, *P*=0.015).

The mean iSP duration was not different between MS patients and controls. We did not find any significant correlation between the duration of the iSP and the physical disability or cognitive dysfunction. The latency of the MEP to cortical stimulation was significantly longer in patients than in controls subjects, resulting in a longer mean CMCT (*P*=0.007). There was no significant correlation between CMCT latency and physical disability (EDSS: *r*=0.248, *P*=0.278; MSFC: *r*=−0.028, *P*=0.905) or cognitive data (data not shown). However, a significant correlation was

Table 2. Results from the ipsilateral silent period and central motor conduction time.

	MS patients	Controls	<i>P</i>
iSP latency	41.25 (4.95)	35.47 (3.62)	0.001
iSP duration	20.06 (4.71)	18.51 (2.67)	0.25
CMCT latency	8.51 (2.60)	6.20 (1.11)	0.007

Values are mean (SD). Results from the electrophysiology study are expressed in milliseconds. Abbreviations: CMCT = central motor conduction time; iSP = ipsilateral silent period; MS = multiple sclerosis.

doi:10.1371/journal.pone.0037167.t002

found between the CMCT and the iSP latency (*r*=0.398, *P*=0.022). Finally, there were no significant differences in resting motor threshold between patients and control subjects (*P*>0.05).

Corpus callosum MRI data

Table 3 summarizes the data concerning MRI findings. There were no significant differences in the area of the CC in the midsagittal slice between MS patients and controls, although the area of segment 1 (rostrum of the CC), but not of the other segments, was smaller in patients (*P*=0.03). The CC volume was smaller in MS patients compared with controls (*P*=0.007). The CC volume correlated with the nLV (*r*=−0.686, *P*=0.001). The area of segment 1 correlated with the EDSS (*r*=−0.442, *P*=0.045) and with the 10/36 delayed (*r*=0.439, *P*=0.047) test. The other CC structural measures did not significantly correlate with physical disability or cognitive data (data not shown).

Compared with controls, MS patients showed lower FA (*P*=0.032) and higher MD (*P*=0.001), AD (*P*=0.022) and RD (*P*=0.003) values. Table 4 shows the results from the DTI analysis.

There was no significant correlation between DTI measures and physical disability (EDDS and MSFC z-score). On the other hand, MD values correlated with the 10/36 delayed test (*r*=−0.546, *P*=0.011), the verbal memory domain (*r*=−0.446, *P*=0.043) and the visual memory domain (*r*=−0.468, *P*=0.033), RD values with some cognitive tests, i.e. the SRT long-term storage (*r*=−0.437, *P*=0.048), the SRT long-term retrieval (*r*=−0.484, *P*=0.026), the 10/36 delayed test (*r*=−0.502, *P*=0.02) and the verbal memory domain (*r*=−0.484, *P*=0.026).

Combination of electrophysiological and MRI data

The iSP latency correlated with the area of the CC (*r*=−0.345, *P*=0.049), with the area of segments 1 (*r*=−0.523, *P*=0.002) and 3 (*r*=−0.359, *P*=0.04) and with the volume of the CC

Table 3. Results from the corpus callosum and the whole brain structural MRI analysis.

	MS patients	Controls	<i>P</i>
Area of CC (midsagittal slice)	6.78 (1.2)	7.11 (0.9)	0.17
Segment 1 area	0.25 (0.1)	0.34 (0.1)	0.03
Segment 2 area	1.55 (0.3)	1.58 (0.3)	0.78
Segment 3 area	0.87(0.2)	0.96 (0.1)	0.20
Segment 4 area	0.84 (0.2)	0.95 (0.09)	0.89
Segment 5 area	0.80 (0.2)	0.78 (0.1)	0.76
Segment 6 area	0.88 (0.2)	0.91 (0.2)	0.68
Segment 7 area	1.60 (0.3)	1.69 (0.3)	0.43
Volume of CC	8.19 (1.65)	9.84 (1.60)	0.007
Volume of CC lesions	0.14 (0.27)	n/a	n/a
nBPV	1,508.8 (72.0)	1,627.3 (81.2)	<0.001
nWMV	725.8 (49.2)	781.7 (32.6)	0.001
nGMV	783 (39.8)	845.6 (57.5)	0.001
nLV	6.99 (8.04)	n/a	n/a

Values are mean (SD). Results from the corpus callosum areas are expressed in cm^2 and volumes in cm^3 . Abbreviations: CC = corpus callosum; n/a = not applicable; nBPV = normalized brain parenchymal volume; nWMV = normalized normal-appearing white matter volume; nGMV = normalized grey matter volume; nLV = normalized whole brain T1-MPRAGE lesion volume; MS = multiple sclerosis.

doi:10.1371/journal.pone.0037167.t003

Table 4. Diffusion-tensor MRI-derived metrics of the corpus callosum.

MS patients	Controls	p
Average FA	0.69 (0.04)	0.72 (0.02)
Average MD	0.97 (0.04)	0.89 (0.03)
Average AD	1.86 (0.09)	1.78 (0.05)
Average RD	0.52 (0.03)	0.44 (0.03)
Values are mean (SD). They refer to metrics of the corpus callosum mask including visible lesions. Average MD, AD and RD are expressed in units of $\text{mm}^2/\text{s} \times 10^{-3}$, FA is a dimensionless index. Abbreviations: AD = axial diffusivity; MD = mean diffusivity; FA = fractional diffusivity; RD = radial diffusivity; MS = multiple sclerosis.		

doi:10.1371/journal.pone.0037167.t004

($r = -0.401$, $P = 0.021$). The iSP onset latency also correlated with whole brain volume metrics, i.e. the nBPV ($r = -0.542$, $P = 0.01$), the nWMV ($r = -0.527$, $P = 0.002$) and the nGMV ($r = -0.439$, $P = 0.011$) but the correlation was not significant with the nLV or the lesion load inside of the CC (data not shown). Finally, the iSP latency also correlated with MD ($r = 0.404$, $P = 0.02$) and RD ($r = 0.415$, $P = 0.016$) values. The CMCT did not show any correlation with structural or DTI measures (data not shown).

Discussion

In this study, we investigated the influence of CC damage on the cognitive dysfunction and physical disability in MS patients, using a multimodal approach. First, we assessed the structural and microstructural characteristics of the CC by MRI and the function of motor inhibitory connections through the CC by the iSP. Then, we examined the relationship between the extent of CC damage and cognitive dysfunction using a battery of neuropsychological tests, and physical disability based on standard disability scales. Our study shows that the microstructural integrity of the CC and the motor callosal conduction are impaired in MS patients and these abnormalities correlate with cognitive dysfunction, mainly verbal and visual memory, information processing speed and executive tasks, and in a lesser extent, with physical disability.

It is well known that stimulation of one hemisphere by TMS inhibits the activity generated in the contralateral hemisphere [14,16]. However, the physiology of this effect is not completely understood. A silent period is produced in the ongoing voluntary activity in both hands to unilateral stimulation. While the contralateral one follows the generation of a MEP and, therefore, it involves post firing of alpha motoneurons, the iSP is never preceded by a MEP and, consequently, it must be considered as the result of suppression of the voluntary corticospinal drive. It is conceivable that the iSP depends on the integrity of transcallosal inhibitory fibers between motor cortices. Increased latency of the iSP in MS patients has been found in some studies [31,32] and prolonged iSP duration in others [20,21,22]. These abnormalities are probably related to demyelination [32]. In the current study the iSP latency was longer in MS patients than in healthy controls, and the same was observed in the 2 patients who did not have evidence of CC lesions (data not shown), revealing motor callosal conduction deficit in MS patients. Although the iSP latency correlated with the duration of the disease, this effect disappeared when the EDSS was added to the statistical model, suggesting that the slowness in the interhemispheric inhibitory command could be a characteristic feature of late disease stages [21] due to the higher physical disability related to those stages.

In agreement with previous studies we found a significant, although moderate, correlation between iSP abnormalities and the CMCT [20]. Although the iSP measures could be in part reflecting the demyelination of the contralateral corticospinal tract, the fact that the iSP but not the CMCT significantly correlated with structural CC damage (atrophy) and with DTI markers of microstructure integrity (MD and RD) would suggest that the CC is a main contributor to this abnormality.

As expected, CC atrophy [6,8] was found in our patients with non-disabling MS [33]. However, differences with respect to healthy subjects were only significant for the area of the rostrum and the volume of the CC. In line with other reports, the overall callosal volume did not correlate with measures of physical disability [6], although a significant but moderate correlation was found with the area of the rostrum, which is composed by axonal fibers that connect ventro-prefrontal cortices of either hemisphere. In the same way, DTI measures of axonal damage and demyelination, reduced FA and increased MD, AD and RD were also found [17,32], even though none of them correlated with the physical disability observed in our patients. Our findings are in line with those found in pathological studies showing a substantial loss of both axonal density and volume in the NAWM of the CC with a trend to higher decrease in the rostrum and midbody [34].

Latency of the iSP significantly correlated with scores on standard disability scales including the EDSS and z-MSFC. This is in agreement with previous studies that showed that the functional impairment of interhemispheric transfer analyzed by neuropsychological testing or IHI correlated with the EDSS [8,22]. Therefore, it is likely that the increased latency of the iSP found in our patients reflects dysfunction of inhibitory fibers connecting the primary motor cortices [35]. In this sense, a previous study found an inverse correlation between iSP duration and the amount of ipsilateral motor cortex activation in functional MRI suggesting that the increased activation represented a consequence of loss of transcallosal inhibitory fibers [32]. This would lead to reduced inhibitory input and, consequently, to impairment of the motor performance [32].

The latency of the iSP significantly correlated with the performance of immediate visual spatial memory, working memory, speed of information processing, attention and executive tasks, while some values from the CC microstructure, MD and RD, correlated with immediate and delayed verbal and visual spatial memory, that is with the profile of neuropsychological dysfunction most frequently reported in MS [13,36,37]. To the best of our knowledge, the relationship between iSP and cognitive performance has not been previously evaluated in MS patients. Interestingly, though, abnormalities in the iSP have been associated with decrease of verbal fluencies, attention functions and MRI atrophy of the CC in patients with corticobasal degeneration [38].

Previous studies in MS have shown significant correlations between cognitive status and CC microstructure. A significant increase in CC MD values was observed in relapsing-remitting MS patients with cognitive impairment [9], even in the benign MS form [12]. Moreover, patterns of tract FA reduction for cognitive tests, including localizations such as the body and splenium of the CC, only partially overlapped with the visible T2 lesions, supporting that NAWM abnormality contributes to cognitive dysfunction [13].

Our study would favor the hypothesis that, in MS, cognitive impairment, and likely also physical disability, are, at least in part, influenced by the CC status and might result from a multiple disconnection syndrome [13,39]. Post-mortem studies have shown strong correlations between regional demyelinating lesion load and

axonal density in the corresponding projection region of the CC in MS patients [40]. In agreement with that, we found a positive correlation between atrophy of the CC and whole brain lesion load. However, the correlation between iSP and atrophy but not with lesion load would suggest that the iSP onset latency reflects abnormalities beyond the visible white matter lesions. In addition, the results of our study add a piece of evidence on the close link between microstructure and function, showing a significant but moderate correlation between the iSP and MD and RD metrics. Nevertheless, the iSP abnormality seems to be able to capture signs of cognitive and physical impairment in MS that could be related to callosal disconnection.

A limitation of our study is the low number of patients included that might have potentially affected the statistical power. However, we studied a relatively homogeneous cohort of relapsing-remitting patients with non-disabling MS as their median EDSS score was 2.0 after mean disease duration longer than 5 years [33]. Moreover, the exploratory nature of this study precluded multiple testing correction analysis. However, the biological plausibility and the consistency of the results in agreement with previous research give further support to the conclusions. Nevertheless, it would be interesting to confirm the results of this study in a larger cohort including multiple testing correction analysis. Finally, we did not perform DTI tractography analysis to further characterize the relationship between the iSP and the topographical distribution of

the CC abnormalities. Although this approach would be interesting to better understand the involved pathophysiology, it is likely that the regional distribution would not reach stronger correlations considering the large variability of both the extent and location of MS lesions.

In conclusion, we found evidence for structural and microstructural abnormalities of the CC that are associated with impairment of motor callosal inhibitory conduction in MS. CC damage is likely to contribute to cognitive dysfunction and in less extent to physical disability through a disconnection mechanism.

Acknowledgments

Sara Llufriu is a multiple sclerosis fellow granted by the Spanish Ministry of Health. The authors would like to thank all the subjects for their participation in the study.

Author Contributions

Conceived and designed the experiments: SL YB JCM JVS AS. Performed the experiments: SL EMH JCM JB NB JVS. Analyzed the data: SL YB EMH JCM CF JVS AS. Contributed reagents/materials/analysis tools: JCM EMH CF JB NB JVS. Wrote the paper: SL YB AS. Interpretation of data: SL YB JVS AS. Revising the article for important intellectual content: SL YB EMH JCM IG MS CF JB NB PV FG JVS AS. Approval of the final version of the manuscript: SL YB EMH JCM IG MS CF JB NB PV FG JVS AS.

References

- Bloom JS, Hynd GW (2005) The role of the corpus callosum in interhemispheric transfer of information: excitation or inhibition? *Neuropsychol Rev* 15: 59–71.
- Audoin B, Ibarrola D, Malikova I, Soulier E, Confort-Gouny S, et al. (2007) Onset and underpinnings of white matter atrophy at the very early stage of multiple sclerosis—a two-year longitudinal MRI/MRSI study of corpus callosum. *Mult Scler* 13: 41–51.
- Kurtzke JF (1983) Rating neurologic impairment in multiple sclerosis: an expanded disability status scale (EDSS). *Neurology* 33: 1444–1452.
- Yaldizli O, Atefy R, Gass A, Sturm D, Glassl S, et al. (2010) Corpus callosum index and long-term disability in multiple sclerosis patients. *J Neurol* 257: 1256–1264.
- Kale N, Agaoglu J, Tanik O (2009) Electrophysiological and clinical correlates of corpus callosum atrophy in patients with multiple sclerosis. *Neurol Res*.
- Ozturk A, Smith SA, Gordon-Lipkin EM, Harrison DM, Shiee N, et al. (2010) MRI of the corpus callosum in multiple sclerosis: association with disability. *Mult Scler* 16: 166–177.
- Sigal T, Shmuel M, Mark D, Gil H, Anat A (2010) Diffusion Tensor Imaging of Corpus Callosum Integrity in Multiple Sclerosis: Correlation with Disease Variables. *J Neuroimaging*.
- Pelletier J, Suchet L, Witjas T, Habib M, Guttmann CR, et al. (2001) A longitudinal study of callosal atrophy and interhemispheric dysfunction in relapsing-remitting multiple sclerosis. *Arch Neurol* 58: 105–111.
- Lin X, Tench CR, Morgan PS, Constantinescu CS (2008) Use of combined conventional and quantitative MRI to quantify pathology related to cognitive impairment in multiple sclerosis. *J Neurol Neurosurg Psychiatry* 79: 437–441.
- Hecke WV, Nagels G, Leemans A, Vandervliet E, Sijbers J, et al. (2010) Correlation of cognitive dysfunction and diffusion tensor MRI measures in patients with mild and moderate multiple sclerosis. *J Magn Reson Imaging* 31: 1492–1498.
- Roosendaal SD, Geurts JJ, Vrenken H, Hulst HE, Cover KS, et al. (2009) Regional DTI differences in multiple sclerosis patients. *Neuroimage* 44: 1397–1403.
- Mesaros S, Rocca MA, Riccitelli G, Pagani E, Rovaris M, et al. (2009) Corpus callosum damage and cognitive dysfunction in benign MS. *Hum Brain Mapp* 30: 2656–2666.
- Dineen RA, Vilisaar J, Hlinka J, Bradshaw CM, Morgan PS, et al. (2009) Disconnection as a mechanism for cognitive dysfunction in multiple sclerosis. *Brain* 132: 239–249.
- Ferber A, Priori A, Rothwell JC, Day BL, Colebatch JG, et al. (1992) Interhemispheric inhibition of the human motor cortex. *J Physiol* 453: 525–546.
- Di Lazzaro V, Oliviero A, Profice P, Insola A, Mazzone P, et al. (1999) Direct demonstration of interhemispheric inhibition of the human motor cortex produced by transcranial magnetic stimulation. *Exp Brain Res* 124: 520–524.
- Giovannelli F, Borgheresi A, Balestrieri F, Zaccara G, Viggiano MP, et al. (2009) Modulation of interhemispheric inhibition by volitional motor activity: an ipsilateral silent period study. *J Physiol* 587: 5393–5410.
- Wahl M, Hubers A, Lauterbach-Soon B, Hattingen E, Jung P, et al. (2011) Motor callosal disconnection in early relapsing-remitting multiple sclerosis. *Hum Brain Mapp* 32: 846–855.
- Wahl M, Lauterbach-Soon B, Hattingen E, Jung P, Singer O, et al. (2007) Human motor corpus callosum: topography, somatotopy, and link between microstructure and function. *J Neurosci* 27: 12132–12138.
- Compta Y, Valls-Sole J, Valdeoriola F, Kumru H, Rumia J (2006) The silent period of the thenar muscles to contralateral and ipsilateral deep brain stimulation. *Clin Neurophysiol* 117: 2512–2520.
- Jung P, Beyerle A, Humpich M, Neumann-Haefelin T, Lanfermann H, et al. (2006) Ipsilateral silent period: a marker of callosal conduction abnormality in early relapsing-remitting multiple sclerosis? *J Neurol Sci* 250: 133–139.
- Schmierer K, Niehaus L, Roricht S, Meyer BU (2000) Conduction deficits of callosal fibres in early multiple sclerosis. *J Neurol Neurosurg Psychiatry* 68: 633–638.
- Schmierer K, Irlbacher K, Gross P, Roricht S, Meyer BU (2002) Correlates of disability in multiple sclerosis detected by transcranial magnetic stimulation. *Neurology* 59: 1218–1224.
- Rovaris M, Filippi M (2007) Diffusion tensor MRI in multiple sclerosis. *J Neuroimaging* 17 Suppl 1: 27S–30S.
- Beaulieu C (2002) The basis of anisotropic water diffusion in the nervous system – a technical review. *NMR Biomed* 15: 435–455.
- Boretius S, Escher A, Dallenga T, Wrzos C, Tammer R, et al. (2011) Assessment of lesion pathology in a new animal model of MS by multiparametric MRI and DTI. *Neuroimage*.
- Rudick R, Antel J, Confavreux C, Cutter G, Ellison G, et al. (1997) Recommendations from the National Multiple Sclerosis Society Clinical Outcomes Assessment Task Force. *Ann Neurol* 42: 379–382.
- Polman CH, Reingold SC, Edan G, Filippi M, Hartung HP, et al. (2005) Diagnostic criteria for multiple sclerosis: 2005 revisions to the “McDonald Criteria”. *Ann Neurol* 58: 840–846.
- Sepulcre J, Vanotti S, Hernandez R, Sandoval G, Caceres F, et al. (2006) Cognitive impairment in patients with multiple sclerosis using the Brief Repeatable Battery-Neuropsychology test. *Mult Scler* 12: 187–195.
- Rossini PM, Pauri F (1999) Central motor conduction time studies. *Electroencephalogr Clin Neurophysiol Suppl* 51: 199–211.
- Witelson SF (1989) Hand and sex differences in the isthmus and genu of the human corpus callosum. A postmortem morphological study. *Brain* 112 (Pt 3): 799–835.
- Hoppner J, Kunesch E, Buchmann J, Hess A, Grossmann A, et al. (1999) Demyelination and axonal degeneration in corpus callosum assessed by analysis of transcallosally mediated inhibition in multiple sclerosis. *Clin Neurophysiol* 110: 748–756.
- Lenzi D, Conte A, Mainiero C, Frasca V, Fubelli F, et al. (2007) Effect of corpus callosum damage on ipsilateral motor activation in patients with multiple sclerosis: a functional and anatomical study. *Hum Brain Mapp* 28: 636–644.

33. Rovaris M, Rocca MA, Barkhof F, Calabrese M, De Stefano N, et al. (2011) Relationship between brain MRI lesion load and short-term disease evolution in non-disabling MS: a large-scale, multicentre study. *Mult Scler* 17: 319–326.
34. Evangelou N, Esiri MM, Smith S, Palace J, Matthews PM (2000) Quantitative pathological evidence for axonal loss in normal appearing white matter in multiple sclerosis. *Ann Neurol* 47: 391–395.
35. Schnitzler A, Kessler KR, Benecke R (1996) Transcallosally mediated inhibition of interneurons within human primary motor cortex. *Exp Brain Res* 112: 381–391.
36. Chiaravalloti ND, DeLuca J (2008) Cognitive impairment in multiple sclerosis. *Lancet Neurol* 7: 1139–1151.
37. Glanz BI, Healy BC, Hviid LE, Chitnis T, Weiner HL (2011) Cognitive deterioration in patients with early multiple sclerosis: a 5-year study. *J Neurol Neurosurg Psychiatry*.
38. Trompetto C, Buccolieri A, Marchese R, Marinelli L, Michelozzi G, et al. (2003) Impairment of transcallosal inhibition in patients with corticobasal degeneration. *Clin Neurophysiol* 114: 2181–2187.
39. Catani M, ffytche DH (2005) The rises and falls of disconnection syndromes. *Brain* 128: 2224–2239.
40. Evangelou N, Konz D, Esiri MM, Smith S, Palace J, et al. (2000) Regional axonal loss in the corpus callosum correlates with cerebral white matter lesion volume and distribution in multiple sclerosis. *Brain* 123 (Pt 9): 1845–1849.

Trabajo número 3

Cognitive functions in multiple sclerosis: Impact of gray matter integrity

Sara Llufriu¹, Eloy Martínez-Heras¹, Juan Fortea², Yolanda Blanco¹, Joan Berenguer³, Íñigo Gabilondo¹, Naroa Ibarretxe-Bilbao⁴, Carles Falcón^{5,6}, María Sepúlveda¹, Nuria Solà-Valls¹, Nuria Bargalló^{3,5}, Francesc Graus¹, Pablo Villoslada¹, Albert Saiz^{1*}

¹Center for Neuroimmunology, Service of Neurology, Hospital Clinic and Institut d'Investigacions Biomèdiques August Pi i Sunyer (IDIBAPS), Barcelona, Spain; ²Memory Unit, Service of Neurology. Hospital de Sant Pau, Barcelona, Spain; ³Service of Radiology and Imaging Diagnostic Center, Hospital Clinic and Institut d'Investigacions Biomèdiques August Pi i Sunyer (IDIBAPS), Barcelona, Spain; ⁴Department of Methods and Experimental Psychology, Faculty of Psychology and Education. University of Deusto, Bilbao, Spain; ⁵Medical Imaging Platform, Institut d'Investigacions Biomèdiques August Pi i Sunyer (IDIBAPS), Barcelona, Spain; ⁶Centros de Investigación Biomédica en Red (CIBER-BBN), Barcelona, Spain.

Multiple Sclerosis Journal. 2013. Sept. [Epub ahead of print]. PMID: 24005025.

IF: 4.472

RESULTADOS

Este trabajo pretendía identificar las regiones cerebrales donde el rendimiento cognitivo se correlaciona con la integridad tisular y determinar el impacto del daño de la sustancia gris, la sustancia blanca y la presencia de lesiones en la disfunción cognitiva.

Se incluyeron 67 pacientes con EMRR y 26 controles sanos. A los pacientes se les realizó un estudio neuropsicológico con la BRB-N. Se utilizaron técnicas no apriorísticas para identificar las regiones de SG o de SBAN donde los valores de DTI en RM se correlacionaban con el rendimiento cognitivo. Además, se identificaron las regiones donde la presencia de lesiones de SB se asociaba con el rendimiento cognitivo. Finalmente, se analizaron de forma conjunta los datos de RM en un modelo de regresión lineal múltiple para conocer cuáles eran los principales determinantes de la cognición.

Los pacientes presentaron una alteración de los índices de DTI en múltiples regiones de SG y SBAN. La alteración de la integridad o la presencia de lesiones en regiones específicas se asociaban con un peor rendimiento cognitivo en funciones concretas. En el modelo de regresión lineal múltiple los elementos que más explicaban la varianza del rendimiento cognitivo eran la integridad de la SBAN junto con la presencia de lesiones, mientras que la integridad de la SG medida a través de DTI sólo añadía un pequeño incremento a dicha varianza.

Cognitive functions in multiple sclerosis: impact of gray matter integrity

Multiple Sclerosis Journal
 0(0) 1–9
 © The Author(s) 2013
 Reprints and permissions:
sagepub.co.uk/journalsPermissions.nav
 DOI: 10.1177/1352458513503722
msj.sagepub.com



**Sara Llufriu¹, Eloy Martínez-Heras¹, Juan Fortea²,
 Yolanda Blanco¹, Joan Berenguer³, Iñigo Gabilondo¹,
 Naroa Ibarretxe-Bilbao⁴, Carles Falcon^{5,6}, María Sepulveda¹,
 Nuria Sola-Valls¹, Nuria Bargallo^{3,5}, Francesc Graus¹,
 Pablo Villoslada¹ and Albert Saiz¹**

Abstract

Objectives: Our aim was to investigate the impact of gray matter (GM) integrity on cognitive performance in multiple sclerosis (MS), and its relationship with white matter (WM) integrity and presence of lesions.

Methods: Sixty-seven patients with MS and 26 healthy controls underwent voxel-based analysis of diffusion tensor images (DTI) in GM and tract-based spatial statistics (TBSS) from WM to identify the regional correlations between cognitive functions and integrity. Lesion probability mapping (LPM) was generated for correlation analysis with cognition. Multiple linear regression analyses were used to identify the imaging measures associated with cognitive scores.

Results: Compared with controls, patients showed abnormal DTI indices in several GM regions and in most WM tracts. Impairment in DTI indices in specific GM regions was associated with worse performance of distinct cognitive functions. Those regions showed anatomical correspondence with cognitively relevant tracts in TBSS and LPM. The combination of regional GM and WM DTI and lesion volume accounted for 36–51% of the variance of memory and attention scores. Regional GM DTI explained less than 5% of that variance.

Conclusion: GM and WM integrity of specific networks influences cognitive performance in MS. However, GM damage assessed by DTI only adds a small increment to the explained variance by WM in predicting cognitive functioning.

Keywords

Multiple sclerosis, cognitive function, MRI, diffusion tensor imaging, voxel-based analysis, tract-based spatial statistics

Date received: 28 May 2013; revised: 23 July 2013; accepted: 11 August 2013

Introduction

Multiple sclerosis (MS) is characterized by inflammatory demyelination and axonal damage responsible for the development of visible lesions and diffuse damage of what appears to be otherwise normal brain tissue.¹

Diffusion tensor imaging (DTI) allows for quantitative measurements of the brain microstructural integrity. In patients with MS, reduced fractional anisotropy (FA) and increased mean diffusivity (MD) indices are usually found in normal-appearing white matter (NAWM) and lesions, reflecting impairment of tissue integrity due to demyelination,² axonal damage or gliosis.³ Axial diffusivity (AD) and radial diffusivity (RD) are other DTI indices which appear to be related to axonal damage and demyelination in animal models, respectively.⁴ The information on gray matter (GM) integrity is more limited, and increases in MD and either decreases or increases in FA have been reported in MS.^{5,6}

Cognitive impairment affects a large proportion of patients^{7,8} and can involve several cognitive domains, including attention, executive functions and long-term

memory.^{7,9} The disconnection between cognitively relevant cortical or subcortical regions seems to contribute to cognitive dysfunction in MS,^{10–12} and there is evidence of GM

¹Center for Neuroimmunology, Service of Neurology, Hospital Clinic and Institut d'Investigacions Biomèdiques August Pi i Sunyer (IDIBAPS), Universitat de Barcelona, Barcelona, Spain.

²Memory Unit, Service of Neurology, Hospital de Sant Pau, Barcelona, Spain.

³Service of Radiology and Diagnostic Imaging Center, Hospital Clinic and Institut d'Investigació Biomèdica August Pi i Sunyer (IDIBAPS), Universitat de Barcelona, Spain.

⁴Department of Methods and Experimental Psychology, Faculty of Psychology and Education, University of Deusto, Bilbao, Spain.

⁵Medical Imaging Platform, Institut d'Investigació Biomèdica August Pi i Sunyer (IDIBAPS), Barcelona, Spain.

⁶CIBER-BBN, Barcelona, Spain.

Corresponding author:

Albert Saiz, Center for Neuroimmunology, Service of Neurology, Hospital Clinic, Villarroel 170, Barcelona, 08036, Spain.
 Email: asaiz@clinic.upc.es

involvement in such effects.^{13,14} However, the influence of GM integrity damage, measured by DTI, on cognitive impairment is not completely known.¹⁵

Non-hypothesis-driven magnetic resonance imaging (MRI) methods allow regional damage to be detected in MS patients and to associate this with cognitive impairment. Tract-based spatial statistics (TBSS) has shown that low FA values in certain WM tracts are associated with worse performance in specific neuropsychological tests.^{10,16,17}

Because WM pathology alone cannot explain cognitive dysfunction in MS,¹⁸ we hypothesize that GM damage assessed by DTI may provide a relevant contribution even in patients in the early phase of the disease. To test this hypothesis, we investigated the impact of regional GM integrity on cognitive performance, and its relationship with WM integrity and presence of lesions using voxel-based analysis (VBA) of GM diffusivity, TBSS of the NAWM and lesion probability mapping (LPM), first to characterize the topographical distribution of GM and WM damage, and then to identify the main imaging measures associated with the specific cognitive domains in patients with mildly disabled relapsing-remitting MS (RRMS).

Methods

Study subjects

For this study, 67 RRMS patients with low-to-moderate disability (Expanded Disability Status Scale¹⁹ (EDSS) 0–5.5) were consecutively selected from the MS Center at the Hospital Clinic of Barcelona. Also included were 26 age and gender-matched healthy controls (HC). The Ethics Committee of the Hospital Clinic approved the study and all the participants provided their informed consent.

Neuropsychological evaluation

The Brief Repeatable Battery⁸ was used to test the following cognitive functions in patients.

Episodic verbal memory was assessed with the selective reminding test (SRT) that comprises several subtests: verbal memory long-term storage (SRT-S), long-term retrieval (SRT-R) and delayed recall (SRT-D) tests. To evaluate immediate working memory we used the immediate recall (SRT-IR) after a single trial in the SRT test (repetition of a 12-item word list).²⁰

Visual memory was measured by the 10/36 Spatial Recall Test (SPART) and 10/36 SPART delayed recall (SPART-D).

Attention was assessed with the Symbol Digit Modalities Test (SDMT) and the Paced Auditory Serial Addition Task-3 seconds (PASAT).

Semantic verbal fluency was assessed with the Word List Generation (WLG).

Test scores were expressed as *z*-scores, derived from normative data obtained from a published HC cohort stratified by age and education.²¹ A test result was considered abnormal if it was over 2.0 SD below the mean test value for the published cohort, and patients were classified as cognitively impaired if they had at least two altered tests.¹² For the SRT-IR test we used the absolute number of correctly repeated words, and the education level was included as a covariate in the analyses performed with this test.

MRI protocol and image analysis

Images were acquired on a 3T Siemens Trio MRI (Erlangen, Germany), using a 32-channel head coil. The protocol included a 3D T1-weighted Magnetization Prepared Rapid Acquisition Gradient Echo (T1-MPRAGE) sequence: repetition time (TR), 2050 ms; echo time (TE), 2.4 ms; inversion recovery time, 1050 ms; 0.9 mm isotropic resolution. DTI sequence: TR/TE, 7600/89 ms; acquisition matrix, 122×122; 2.5 mm isotropic resolution; 1 volume without directional weighting and 30 different gradient directions (1000 s/mm²). For more details on the sequences and processing steps see the Supplementary Materials.

Individual WM lesion masks were generated manually on the T1-MPRAGE sequence in patients using ITK-SNAP.

Voxel-based analysis of GM diffusivity. In patients, the VBA pre-processing protocol was modified using lesion inpainting (LI) in T1-MPRAGE to improve the segmentation and registration processes.²² The default processing parameters from DARTEL toolbox were applied.²³ Then, the diffusion tensor FA, MD, RD and AD maps were normalized to the standard space. A binarized mask of GM was applied to the unmodulated images to exclude non-GM voxels.

Two-sample *t*-tests were used to localize the regions with significant differences in GM DTI indices between patients and controls. Multiple linear regression analyses were performed to identify those areas from the whole brain GM in which the DTI indices correlated with cognitive *z*-scores in patients after adjusting for age, sex and a brain scaling factor. A cluster-defining threshold of *p*=0.001 was used, and clusters were considered significant at *p*<0.05 cluster level family-wise error (FWE) corrected. Then, the DTI indices from those significant regions were obtained.

Tract-based spatial statistics. FMRIB Software Library tools were used to process the diffusion tensor data. Geometric distortions were corrected by a phase-unwrapping method followed by eddy current correction. Reconstruction of the diffusion tensors was performed to obtain FA, MD, RD and AD tensor-derived measures for each voxel. TBSS projected the FA, MD, AD and RD data for each subject on the mean-space tract skeleton.²⁴ To avoid errors in registration processes LI was applied.²⁵

Table 1. Characteristics of the subjects included in the study.

	MS patients (n=67)	Healthy controls (n=26)	p value
Female/Male	43/24	17/9	0.07
Age, years	39.5 (8.8)	36.0 (7.2)	0.56
Educational level, n (%):			
Elementary school	5 (8)	—	—
High school	28 (42)	—	—
Further education or university	31 (46)	—	—
Higher degrees	3 (4)	—	—
Disease duration, years	8.7 (6.8)	—	—
Patients under treatment, n (%)	59 (88)	—	—
Median EDSS score (range)	1.5 (0–5.5)	—	—
Normalized TI-Lesion volume, cm ³	8.8 (9.7)	—	—

EDSS: Expanded Disability Status Scale.

Values are expressed as mean (standard deviation) except for EDSS.

To produce a skeleton of the NAWM we excluded those voxels where at least $\geq 10\%$ of the patients presented a lesion in the lesion maps.

NAWM FA, MD, RD and AD skeletons were compared between MS patients and controls using the *randomize* tool in the FSL library, with 5000 permutations and threshold-free cluster enhancement ($p < 0.05$, corrected for multiple comparisons by controlling for FWE rates),²⁶ while treating age and sex as covariates. We performed similar inter-subject voxel-wise correlations between whole brain skeleton DTI indices and cognitive scores in patients. Finally, we obtained the DTI indices from those significant skeleton regions.

Tractography. Because TBSS applies DTI information from local WM tracts to a skeleton representing the centres of all fibre bundles and does not give the exact information corresponding to the real tract anatomy, we explored the possible anatomical coincidence between regions associated with cognition in VBA of GM and TBSS by tractography on a healthy subject. The DTI sequence parameters were: TR/TE, 16600/110 ms; acquisition matrix, 154×154; 1.5 mm isotropic resolution; 1 volume without directional weighting and 60 different gradient directions (1500 s/mm²). The significant clusters in GM VBA obtained for each cognitive test were used to seed streamlining-based tractography.

Lesion probability mapping. The lesion masks from each patient were normalized to the standard space provided in DARTEL. In the LPM each voxel value can be thought of as an estimate of the probability that the subject has a lesion at that location (Supplementary Figure S-1).²⁷

The relationship between z-scores and the lesion probability at each voxel was modelled as a multiple linear regression, with each cognitive z-score as the dependent variable,²⁸ and age, sex and brain scaling as covariates. Significance was defined in the same way as that

described for the VBA of the GM. Then, the volume of lesions inside the significant clusters was calculated for each patient.

Statistical analysis

Mann–Whitney *U* test was used to compare demographic characteristics between patients and controls. Multiple linear regression (at cluster level) was used to model the relationship between FA values from significant tracts in TBSS, RD values from significant GM regions in VBA and lesion volume from significant clusters in LPM as explanatory variables, and z-score of every test as a response variable. In all models age, disease duration and EDSS were included as covariates. Statistical analyses were performed using SPSS and significance level was set at $p < 0.05$.

Results

Clinical and neuropsychological data

Patients had low disability scores (median EDSS of 1.5, range 0–5.5) (Table 1). At least one abnormal neuropsychological test result was observed in 21 (31.3%) patients. Three (4.5%) patients had two or more abnormal results from the battery and were considered cognitively impaired. Results from the neuropsychological evaluation are shown in Table 2.

DTI comparison between MS patients and controls

In the GM, decreases in the FA, increases in the MD, AD and particularly the RD, were detected in several GM regions in patients with MS as opposed to the HC, including the thalamus, caudate nucleus, hippocampus, cingulum, frontal, temporal and occipital cortex (Figure 1).

In the NAWM, patients showed a widespread decrease in the FA and increase in the MD and RD compared with

Table 2. Results from the neuropsychological evaluation in patients.

Domain	Test	Subscore	Cognitive function	Mean (SD) score	Patients with abnormal subtests n (%)
Verbal memory	SRT	SRT-IR	Verbal memory immediate recall	6.45 (1.87)	–
		SRT-S	Verbal memory long-term storage	-0.09 (1.19)	4 (6)
		SRT-R	Verbal memory long-term retrieval	-0.25 (1.30)	7 (10.4)
		SRT-D	Verbal memory delayed recall	-0.08 (1.17)	8 (11.9)
Visual memory	10/36 SPART	SPART	Visual memory	-0.37 (0.90)	2 (3)
		SPART-D	Visual memory delayed recall	0.04 (1.15)	5 (7.5)
Attention	SDMT		Attention, visual precision search, processing speed and executive functions	0.25 (1.02)	0 (0)
		PASAT	Attention, processing speed and working memory	-0.43 (1.13)	7 (10.4)
Verbal fluency	WLG		Associative verbal fluency	-0.66 (0.96)	5 (7.5)

SRT: Selective Reminding Test; SPART: Spatial Recall Test; SDMT: Symbol Digit Modalities Test; PASAT: Paced Auditory Serial Addition Test; WLG: Word List Generation.

Z-scores were obtained for all tests from comparison with a Spanish healthy population except for immediate recall in which absolute number of correct responses was considered.

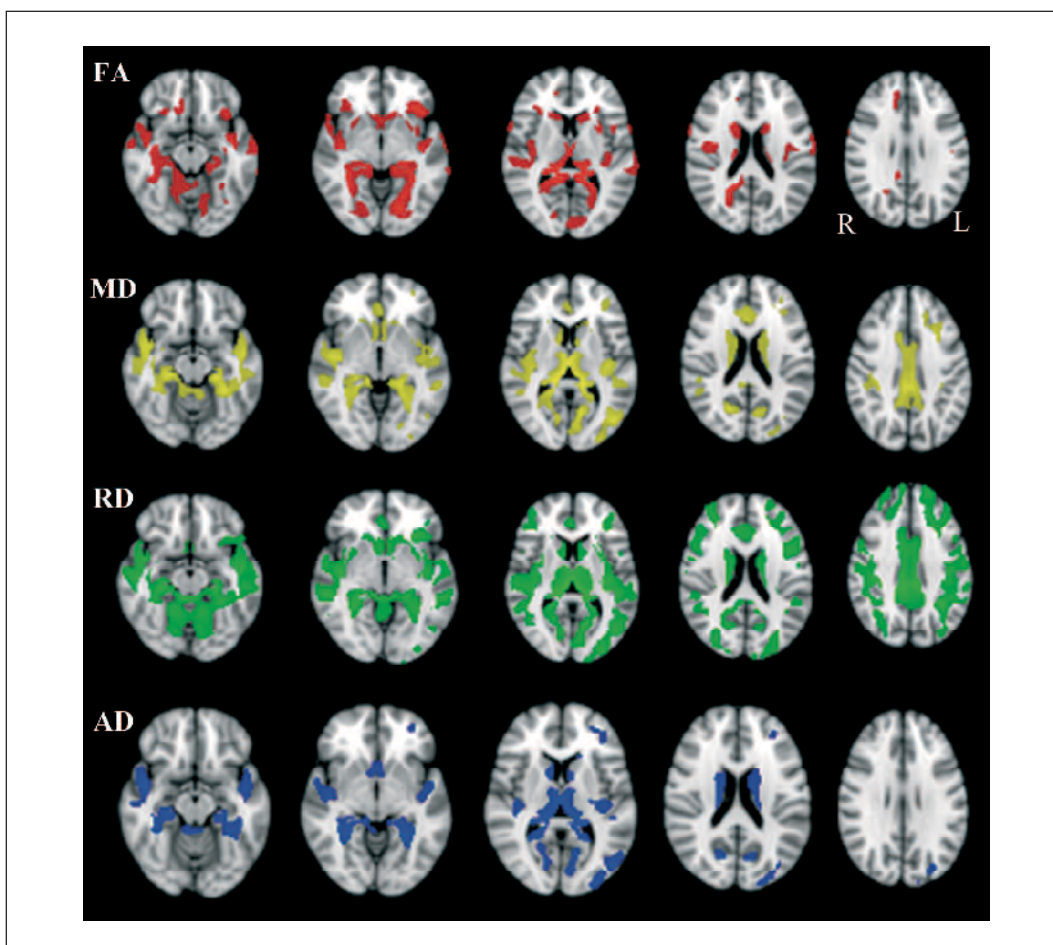


Figure 1. Voxel-based analysis of gray matter diffusivity: regions with decreased gray matter fractional anisotropy (FA) and increased mean diffusivity (MD), radial diffusivity (RD) and axial diffusivity (AD) in patients with MS compared with control subjects ($p < 0.05$, corrected for multiple comparisons).

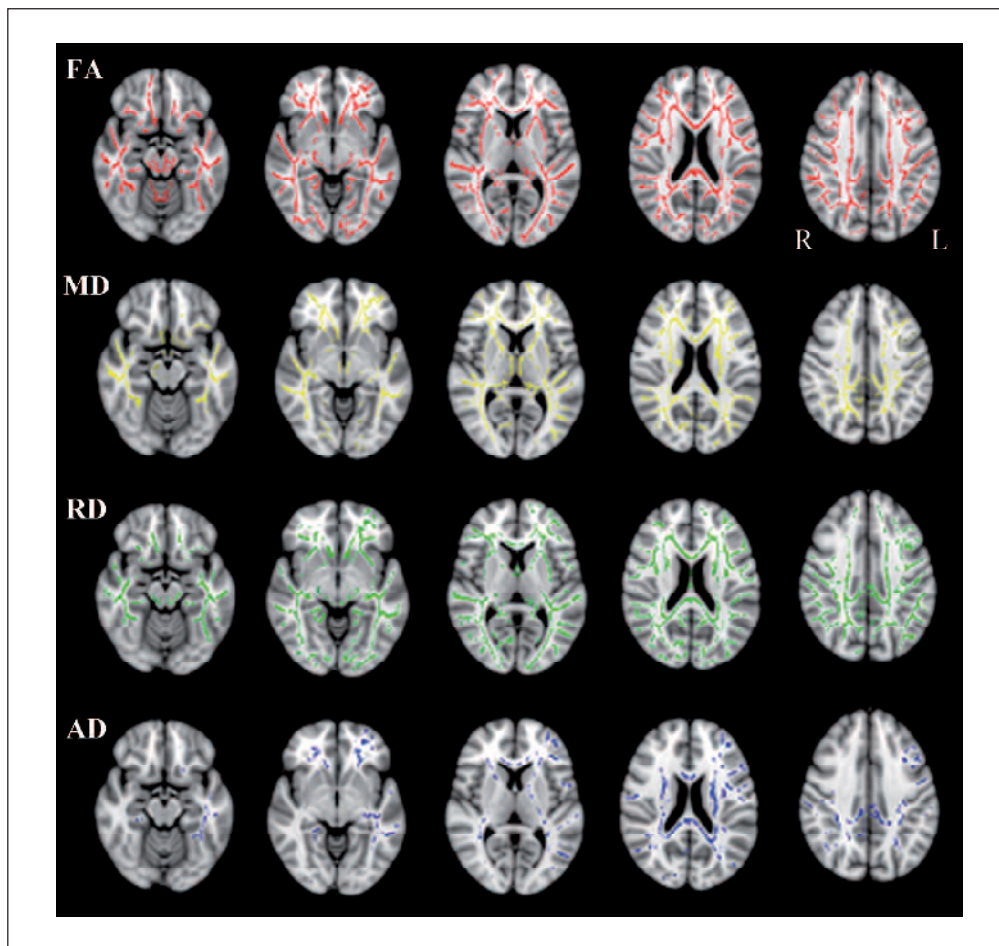


Figure 2. TBSS: skeletal voxels with decreased normal-appearing white matter fractional anisotropy (FA) and increased mean diffusivity (MD), radial diffusivity (RD) and axial diffusivity (AD) in patients with MS compared with control subjects ($p<0.05$, corrected for multiple comparisons).

HC. However, the increases in AD were restricted to a small number of tracts, mainly the corpus callosum (CC), anterior thalamic radiation, corticospinal tract and inferior fronto-occipital fasciculus (Figure 2).

Topographical associations with cognitive functions

Episodic verbal memory. In the GM, the RD was more sensitive than the other indices to detect correlations with verbal memory tests. The different subtests revealed distinct associations with specific GM regions (Figure 3), mainly in the left hemisphere. Thus, decrease in z-scores was associated with increase of RD in the left angular cortex for the SRT-IR z-scores, in the occipital cortex (i.e. angular, calcarine, lingual and fusiform cortex) and medial structures, such as the hippocampus and thalamus for the SRT-S z-scores, in the bilateral cortical (i.e. several regions of the occipital and temporal cortex, insula) and medial structures

(i.e. hippocampus, parahippocampus and thalamus) for the SRT-R z-scores and in the left occipital lobe, hippocampus, thalamus, precuneus and fronto-orbital cortex for the SRT-D z-scores.

The four SRT subtests revealed several WM areas in which cognitive performance was correlated with the TBSS skeleton FA (Figure 3), MD and RD. These results predominated in the left hemisphere, and for all subtests there was significant overlap in the tracts identified, including the CC, cingulum, anterior thalamic radiations, inferior fronto-occipital fasciculus, forceps major, sagittal stratum (including the inferior longitudinal fasciculus (LF)) and the retro Lenticular portion of internal capsule.

Areas of anatomic correspondence between relevant GM regions and skeleton NAWM for memory performance were visually identified (Figure 3) in calcarine and lateral occipital cortex with the left inferior LF. Using tractography from the significant GM clusters, occipital and temporal seeds elicited forceps major tracts and left inferior LF

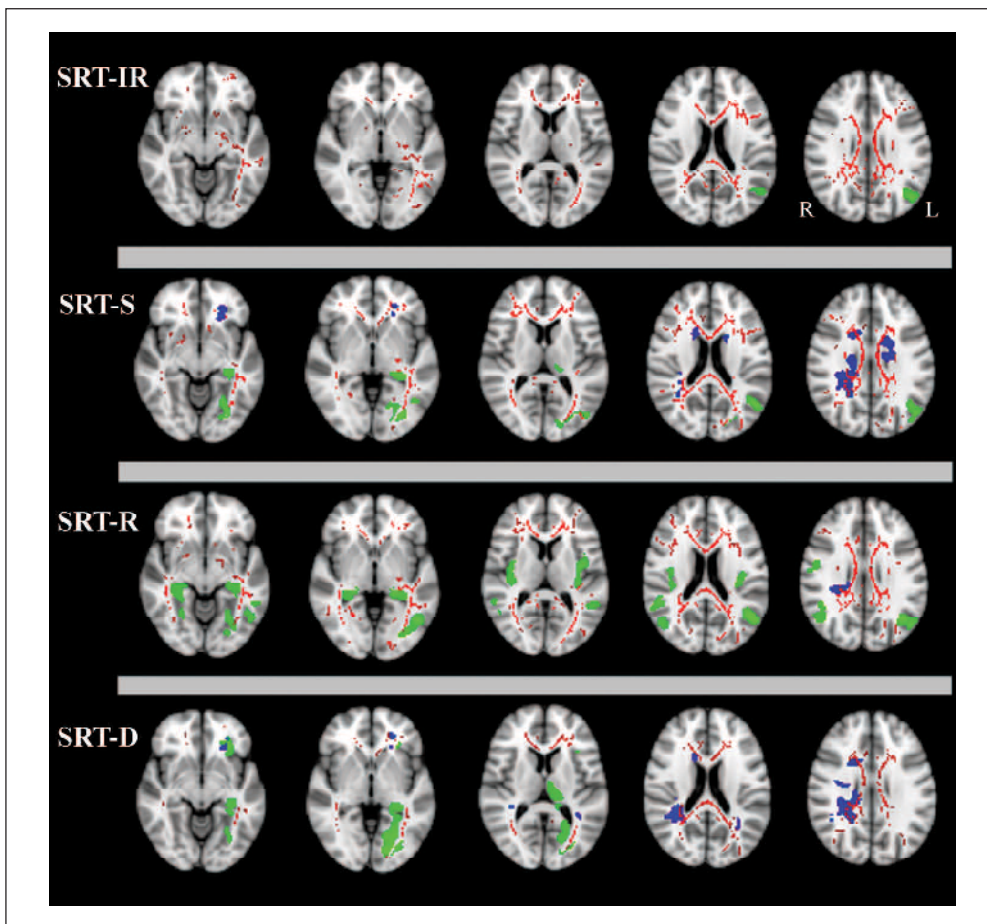


Figure 3. Distribution of significant associations between DTI or lesion probability and the Selective Reminding Tests scores in patients.
 Voxels of GM where increased RD ($p<0.05$ cluster level, corrected) correlated with test z-scores are coloured in green. Voxels from the NAWM skeleton where reduced FA ($p<0.05$, corrected) correlated with cognitive test performance are coloured in red. Voxels where lesions probability correlated ($p<0.05$ cluster level, corrected) with cognitive scores are coloured in blue.

showing an anatomical connection between those GM and WM significant regions (Supplementary Figure S-2 and Table S-1).

Long-term memory tests correlated with probability of lesion in the corona radiata, CC, posterior thalamic radiation extending to superior LF, and the left inferior fronto-occipital fasciculus (Figure 3).

Visual memory. Worse SPART-D but not SPART z-scores were correlated with the decrease of FA (Figure 4) and the increase of RD values in several NAWM tracts, mainly the CC, bilateral anterior and posterior corona radiata, posterior thalamic radiation and cingulum. Lesion probability was correlated with the SPART-D z-scores in the left forceps major (Figure 4), while no significant correlations were detected for the VBA of GM diffusivity.

Attention. In the GM, lower SDMT z-scores were correlated with higher RD in the left occipital cortex, cerebellum and anterior insula (Figure 4). In the NAWM, there was a widespread correlation between the SDMT scores and the FA, MD and RD throughout the skeleton. Through tractography we could generate tracts from left occipital cortex corresponding to the inferior fronto-occipital fasciculus tracts supporting an anatomical connection between those significant regions (Supplementary Figure S-2 and Table S-1). A significant correlation with probability of lesion was detected in the posterior thalamic radiations and left sagittal stratum (Figure 4).

We did not find any significant correlation for PASAT z-score.

Verbal fluency. No significant correlations were found for WLG z-scores in VBA, TBSS and LPM.

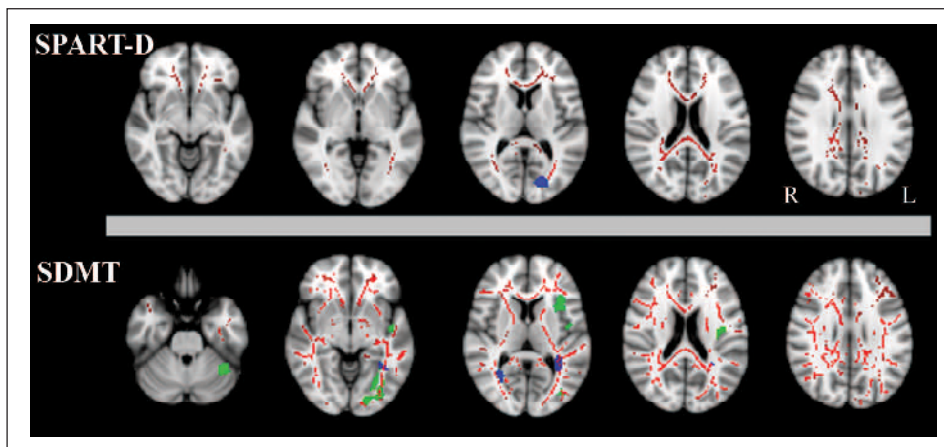


Figure 4. Distribution of significant associations between DTI or lesion probability and cognitive tests (SPART-D and SDMT). Voxels of GM where increased RD ($p<0.05$ cluster level, corrected) correlated with tests are coloured in green. Voxels from the NAWM skeleton where reduced FA ($p<0.05$, corrected) correlated with cognitive test performance are coloured in red. Voxels where lesions probability correlated ($p<0.05$ cluster level, corrected) with cognitive scores are coloured in blue.

Multiple linear regression analyses (cluster level)

The DTI indices selected for the multiple linear regression analyses were RD in GM and FA in NAWM skeleton as they showed the most extensive and consistent associations with cognitive scores in the non-hypothesis-driven techniques. The model that included regional GM RD, NAWM FA, regional lesion volume, and age, disease duration and EDSS as covariates, explained 36–51% of the variance of memory and attention scores (Table 3). GM RD contributed with less than 5% to the explained variance, while FA from the relevant tracts and lesion volume from the significant clusters in LPM were the main elements associated with each z -score. As exploratory measure we analysed the contribution of GM DTI after excluding NAWM FA and regional WM lesions from the model, and we found a significant correlation between GM RD and cognitive z -scores which explained 29–38% of the variance of memory and attention scores (Supplementary Table S-2).

Discussion

Using a combination of non-hypothesis-driven techniques, we identified a wide distribution of tissue integrity impairment throughout the GM and WM in a group of mildly disabled MS patients. Moreover, we defined the regions where integrity of GM and WM tissue are critical for the performance of specific cognitive tasks. Some of those cognitively relevant regions corresponded to GM and their projecting tracts, suggesting that the damage at any point of these networks may influence cognitive performance. Importantly, measures of WM integrity and regional lesions, rather than GM integrity, explained a substantial proportion of the variance in cognitive functions, indicating

that WM damage measured with DTI provides relevant information to monitor cognitive dysfunction in MS.

Our findings confirm the ability of DTI to detect tissue damage in deep and cortical GM as well as in most WM tracts in patients with MS. The presence of extensive micro-structural abnormalities is consistent with the view that MS is an immunological disease with diffuse brain involvement beyond the presence of visible lesions.¹ The most evident differences between patients and controls in GM were seen in the RD measures. Animal models suggest that an increase in RD is associated with demyelination. In the NAWM, the changes associated with a predominant myelin damage were widespread, whereas the increase in AD, that is suggested to reflect axonal injury in animal models,⁴ was limited to a small number of tracts.¹⁶

In addition, we identified several GM regions and WM tracts where changes in tissue integrity or the presence of lesions were associated with a worsening of cognitive performance. Although some of those regions were coincidental for several cognitive tests, most were specific for the domain explored.

In the GM, the regions associated with episodic memory performance in MS patients were mostly coincidental with those networks of structures consistent with current theories regarding the neurobiological basis of memory.²⁹ The associations were predominantly in the left hemisphere, and they evolved from the angular cortex, implicated in the phonological loop in working memory (SRT-IR), towards a predominant medial temporal lobe including the thalamus³⁰ and occipital involvement in the delayed recall. These findings are in agreement with the anatomic substrates that differentially support memory performance in Alzheimer disease.²⁰ Declarative memory performance was associated with the integrity of selected tracts in the WM, including the cingulum, CC, left forceps major and inferior LF, which play

Table 3. Multiple linear regression analyses at cluster level.

	FA in NAWM	RD in GM	Regional lesions	Age	Disease duration	EDSS	R ²	GM contribution ^a
SRT-IR*	B=0.41 p=0.004	B=-0.30 p=0.045	–	B=-0.11 p=0.33	B=0.01 p=0.94	B=0.08 p=0.53	0.41	0.041
SRT-S	B=0.341 p=0.07	B=-0.07 p=0.72	B=-0.28 p=0.04	B=-0.01 p=0.97	B=0.12 p=0.35	B=-0.03 p=0.86	0.39	0.004
SRT-R	B=0.24 p=0.25	B=-0.15 p=0.49	B=-0.22 p=0.18	B=-0.02 p=0.87	B=-0.02 p=0.91	B=-0.07 p=0.62	0.36	0.005
SRT-D	B=0.14 p=0.47	B=-0.09 p=0.63	B=-0.38 p=0.02	B=-0.24 p=0.04	B=0.02 p=0.88	B=-0.07 p=0.64	0.41	0.002
SPART-D	B=0.32 p=0.01	–	B=-0.36 p=0.03	B=-0.18 p=0.11	B=0.11 p=0.39	B=-0.07 p=0.58	0.37	–
SDMT	B=0.26 p=0.08	B=-0.20 p=0.21	B=-0.36 p=0.01	B=0.01 p=0.91	B=0.07 p=0.53	B=-0.07 p=0.51	0.51	0.014

B: standardized beta. SRT-IR: Selective Reminding Test immediate recall; SRT-S: Selective Reminding Test long-term storage; SRT-R: Selective Reminding Test long-term retrieval; SRT-D: Selective Reminding Test long-term delayed recall; SPART-D: Spatial Recall Test delayed; SDMT: Symbol Digit Modalities Test.

DTI values were obtained from the regions that significantly correlated with each cognitive z-scores in TBSS (for NAWM) and in VBA (for GM).

Regional lesions correspond to the volume of lesions in the regions where LPM significantly correlated with each cognitive z-score.

*The analysis for SRT-IR included education as a covariate (B=1.48–0.33 p=0.1–0.7).

^aExplained variance (R^2) from GM RD in the model.

important roles in the maintenance of memory during aging.³¹ Similar results were found in two MS studies using the Rey Auditory Verbal Learning Test.^{10,17} Moreover, our lesion probability results represent additional evidence that declarative verbal memory relies on temporo–thalamo–frontal and temporo–parieto–frontal pathways for storage and retrieval.²⁷

Some of the tracts originating from relevant GM regions were coincidental with the skeleton tracts associated with z-scores. This allowed us to identify important networks for the maintenance of memory functions (i.e. left occipital and temporal lobe regions connecting with forceps major and inferior LF). Altogether, suggesting that microstructural damage or presence of lesions at any point of those networks could be implicated in memory impairment in MS.

Delayed visual memory test scores were correlated with the NAWM DTI indices and with lesion probability in the CC, forceps major and inferior LF, with left predominance, as previously reported using the Benton visual retention test.¹⁰ The similarities observed with episodic verbal memory test results suggest that these WM tracts are essential in maintaining memory functions in MS, independently of the specific modality.

The GM regions associated with SDMT performance were comparable with those areas activated in functional MRI studies.³² However, the association with DTI indices along the skeleton¹⁷ was more widespread compared with memory tests, probably due to the involvement of several cognitive functions and functional traits of this test.³² In contrast to previous studies,^{10,17} we found no correlation between DTI indices and PASAT z-scores³³ or WLG z-scores, a discrepancy that may reflect differences in the clinical characteristics and methods used.

Previous studies pointed out the relevance of WM integrity in MS-associated cognitive impairment.^{10,12,30} Our study reinforces this view and shows that the regional approach we used is sensitive to explain cognitive performance in MS. In addition, we found that the impact of GM damage, as measured with DTI, only adds a small additional variance in cognitive functioning on top of NAWM FA and regional WM lesions in our cohort of mildly disabled RRMS patients. However, GM RD was able to explain 29–38% of the vari-

ance of memory and attention scores when NAWM FA and regional WM lesions were excluded from the analysis. Therefore, our results are not contradictory with the importance of the GM damage in determining disability and cognitive progression in MS, but point out that in the first years of the disease, when the clinical characteristics of RRMS are characterized by relapses due to WM lesions, the influence of GM pathology to cognitive dysfunction might be more limited than that of WM damage.³⁴

The present work has strengths and limitations. It combines the study of DTI measures in both the GM and WM, and incorporates several technical improvements. Although the current study address the impact of GM damage in the cognitive performance of patients with low cognitive disability, it does not answer whether GM DTI measures would be able to differentiate cognitively preserved from cognitively impaired MS patients, and to detect changes over time. Finally, although exclusion criteria to participate were a diagnosis of a psychiatric disorder or a medical illness that could interfere in the neuropsychological evaluation, symptoms of depression, anxiety and fatigue were not formally assessed. Nevertheless, the low percentage of abnormal tests we found suggests a low impact of those symptoms in the cognitive results.

In conclusion, we describe relevant networks where the integrity impairment is associated with a worse performance in specific cognitive functions. WM integrity, rather than GM, seems to be the main contributor to the cognitive performance in mildly disabled RRMS patients. Overall, our results support the view that cognitive impairment in MS is consequence of a disconnection syndrome provoked by damage to multiple tracts, coupled to damage in the GM.

Conflict of interests

The authors declare that there are no conflicts of interest.

Funding

Supported in part by grant from Fondo de Investigaciones Sanitarias (PV, PS09/00259) and Red Española de Esclerosis Múltiple (REEM) Instituto de Salud Carlos III, Spain (RD12/0032/0001 and 0002).

References

1. Filippi M, Rocca MA, Barkhof F, et al. Association between pathological and MRI findings in multiple sclerosis. *Lancet Neurol* 2012; 11: 349–360.
2. Kolasinski J, Stagg CJ, Chance SA, et al. A combined post-mortem magnetic resonance imaging and quantitative histological study of multiple sclerosis pathology. *Brain* 2012; 135: 2938–2951.
3. Schmierer K, Wheeler-Kingshott CA, Boulby PA, et al. Diffusion tensor imaging of post mortem multiple sclerosis brain. *Neuroimage* 2007; 35: 467–477.
4. Song SK, Sun SW, Ju WK, et al. Diffusion tensor imaging detects and differentiates axon and myelin degeneration in mouse optic nerve after retinal ischemia. *Neuroimage* 2003; 20: 1714–1722.
5. Filippi M, Preziosa P, Pagani E, et al. Microstructural magnetic resonance imaging of cortical lesions in multiple sclerosis. *Mult Scler* 2013; 19: 418–426.
6. Griffin CM, Chard DT, Ciccarelli O, et al. Diffusion tensor imaging in early relapsing-remitting multiple sclerosis. *Mult Scler* 2001; 7: 290–297.
7. Chiaravalloti ND and DeLuca J. Cognitive impairment in multiple sclerosis. *Lancet Neurol* 2008; 7: 1139–1151.
8. Rao SM, Leo GJ, Bernardin L, et al. Cognitive dysfunction in multiple sclerosis. I. Frequency, patterns, and prediction. *Neurology* 1991; 41: 685–691.
9. Prakash RS, Snook EM, Lewis JM, et al. Cognitive impairments in relapsing-remitting multiple sclerosis: A meta-analysis. *Mult Scler* 2008; 14: 1250–1261.
10. Dineen RA, Vilisaar J, Hlinka J, et al. Disconnection as a mechanism for cognitive dysfunction in multiple sclerosis. *Brain* 2009; 132: 239–249.
11. Llufriu S, Blanco Y, Martínez-Heras E, et al. Influence of corpus callosum damage on cognition and physical disability in multiple sclerosis: A multimodal study. *PLoS One* 2012; 7: e37167.
12. Hulst HE, Steenwijk MD, Versteeg A, et al. Cognitive impairment in MS: Impact of white matter integrity, gray matter volume, and lesions. *Neurology* 2013; 80: 1025–1032.
13. Morgen K, Sammer G, Courtney SM, et al. Evidence for a direct association between cortical atrophy and cognitive impairment in relapsing-remitting MS. *Neuroimage* 2006; 30: 891–898.
14. Filippi M, Rocca MA, Benedict RH, et al. The contribution of MRI in assessing cognitive impairment in multiple sclerosis. *Neurology* 2010; 75: 2121–2128.
15. Rovaris M, Iannucci G, Falautano M, et al. Cognitive dysfunction in patients with mildly disabling relapsing-remitting multiple sclerosis: An exploratory study with diffusion tensor MR imaging. *J Neurol Sci* 2002; 195: 103–109.
16. Roosendaal SD, Geurts JJ, Vrenken H, et al. Regional DTI differences in multiple sclerosis patients. *Neuroimage* 2009; 44: 1397–1403.
17. Yu HJ, Christodoulou C, Bhise V, et al. Multiple white matter tract abnormalities underlie cognitive impairment in RRMS. *Neuroimage* 2012; 59: 3713–3722.
18. Amato MP, Bartolozzi ML, Zipoli V, et al. Neocortical volume decrease in relapsing-remitting MS patients with mild cognitive impairment. *Neurology* 2004; 63: 89–93.
19. Kurtzke JF. Rating neurologic impairment in multiple sclerosis: An Expanded Disability Status Scale (EDSS). *Neurology* 1983; 33: 1444–1452.
20. Wolk DA and Dickerson BC. Fractionating verbal episodic memory in Alzheimer's disease. *Neuroimage* 2011; 54: 1530–1539.
21. Sepulcre J, Vanotti S, Hernandez R, et al. Cognitive impairment in patients with multiple sclerosis using the Brief Repeatable Battery-Neuropsychology test. *Mult Scler* 2006; 12: 187–195.
22. Ceccarelli A, Jackson JS, Tauhid S, et al. The impact of lesion in-painting and registration methods on voxel-based morphometry in detecting regional cerebral gray matter atrophy in multiple sclerosis. *AJNR Am J Neuroradiol* 2012; 33: 1579–85.
23. Ashburner J. A fast diffeomorphic image registration algorithm. *Neuroimage* 2007; 38: 95–113.
24. Smith SM, Jenkinson M, Johansen-Berg H, et al. Tract-based spatial statistics: Voxewise analysis of multi-subject diffusion data. *Neuroimage* 2006; 31: 1487–1505.
25. Sdika M and Pelletier D. Nonrigid registration of multiple sclerosis brain images using lesion inpainting for morphometry or lesion mapping. *Hum Brain Mapp* 2009; 30: 1060–1067.
26. Smith SM and Nichols TE. Threshold-free cluster enhancement: Addressing problems of smoothing, threshold dependence and localisation in cluster inference. *Neuroimage* 2009; 44: 83–98.
27. Sepulcre J, Masdeu JC, Sastre-Garriga J, et al. Mapping the brain pathways of declarative verbal memory: Evidence from white matter lesions in the living human brain. *Neuroimage* 2008; 42: 1237–1243.
28. Kincses ZT, Ropele S, Jenkinson M, et al. Lesion probability mapping to explain clinical deficits and cognitive performance in multiple sclerosis. *Mult Scler* 2011; 17: 681–689.
29. Squire LR. Memory systems of the brain: A brief history and current perspective. *Neurobiol Learn Mem* 2004; 82: 171–177.
30. Benedict RH, Hulst HE, Bergsland N, et al. Clinical significance of atrophy and white matter mean diffusivity within the thalamus of multiple sclerosis patients. *Mult Scler*. Epub ahead of print 4 March 2013. DOI: 10.1177/1352458513478675.
31. Lockhart SN, Mayda AB, Roach AE, et al. Episodic memory function is associated with multiple measures of white matter integrity in cognitive aging. *Front Hum Neurosci* 2012; 6: 56.
32. Forn C, Belenguer A, Belloch V, et al. Anatomical and functional differences between the Paced Auditory Serial Addition Test and the Symbol Digit Modalities Test. *J Clin Exp Neuropsychol* 2011; 33: 42–50.
33. Kern KC, Sarcona J, Montag M, et al. Corpus callosal diffusivity predicts motor impairment in relapsing-remitting multiple sclerosis: A TBSS and tractography study. *Neuroimage* 2011; 55: 1169–1177.
34. Calabrese M, Romualdi C, Poretti V, et al. The changing clinical course of multiple sclerosis: A matter of grey matter. *Ann Neurol*. Epub ahead of print 12 March 2013. DOI: 10.1002/ana.23882.

ONLINE SUPPLEMENTARY MATERIAL

MRI protocol and image analysis

We identified an artifact in the diffusion-weighted images due to vibration of the MRI platform,¹ which was found in parietal regions and mainly in 6 directions. In order to remove this artifact we discarded the affected directions from all subjects studied.²

The T1-MPRAGE sequence was used by two experienced neurologists to manually generate a lesion mask for each patient using ITK-SNAP.³ The lesion volume measurement revealed a mean intra-observer correlation coefficient of 0.98 ($p < 0.001$, $n = 6$ patients), indicating excellent reliability between the two neurologists.

Voxel-based analysis of gray matter diffusivity

In patients, the VBA pre-processing protocol was modified using lesion inpainting (LI) in T1-MPRAGE to improve the segmentation and registration processes.⁴⁻⁵ Briefly, the *New Segment* tool from SMP8⁶ was applied to the T1-MPRAGE images of each subject to segment the GM and WM. Next, DARTEL⁷ was used to derive a specific template of the entire sample and to normalize the sample to the MNI space. The individual diffusion tensor fractional anisotropy (FA), mean diffusivity (MD), radial diffusivity (RD) and axial diffusivity (AD) maps were aligned rigidly to the T1-MPRAGE images, and subsequently warped to MNI using flow fields generated by DARTEL. The unmodulated DTI images were smoothed using an 8 mm full width at half maximum (FWHM) isotropic Gaussian function before being used as the input for statistical analyses. By applying a binarized mask of GM from the *Anatomical Automatic Labeling* tool,⁸ VBA was performed exclusively using GM indices.

To localize the areas in which there was significant increase or decrease in FA, MD, RD or AD of the GM of patients as opposed to controls, we used a two-sample T-test. Moreover, we performed a multiple linear regression analysis to identify areas in which the MD and RD of the GM was correlated with cognitive scores in patients, adjusting for age, sex and a brain scaling factor. A cluster-defining threshold of $p = 0.001$ (uncorrected) was used and clusters were considered significant at $p < 0.05$ (cluster level family-wise error (FWE) corrected for a whole-brain search).

Tract-based spatial statistics

All tools used to process the diffusion tensor data were from the FMRIB Software Library (FSL, <http://www.fmrib.ox.ac.uk/fsl>). Geometric distortions caused by susceptibility field changes were corrected by applying a phase-unwrapping method followed by eddy current correction. Reconstruction of the diffusion tensors was performed using *FMRIB's Diffusion Toolbox* in order to obtain FA, MD, RD and AD tensor-derived measures for each voxel. Next, the FA maps for

each subject were registered linearly to the corresponding T1-MPRAGE. For patients, an automated method involving lesion inpainting in the T1-MPRAGE sequence was applied to avoid errors in registration.⁹ Afterwards, the T1-MPRAGE images were normalized to the Montreal Neurological Institute (MNI) standard space using affine registration and non-linear registration. Next, the FA data for each subject were aligned in the MNI space applying the corresponding warp fields and the mean FA image was skeletonized¹⁰ using a threshold of 0.2 to exclude non-WM voxels. The individual registration and projection vectors obtained during this process were also applied to the MD, RD and AD data.

To create a mean lesion mask of the patients, individual lesion maps in T1-weighted images were linearly registered and normalized to MNI space through the warping performed during the alignment in TBSS. The lesion maps were averaged to create a lesion probability distribution that showed voxels in which at least 10% of the patients presented a lesion, and they were subtracted from the skeleton to produce a skeleton of the NAWM only.

Whole brain FA, MD, RD and AD skeletons from NAWM were compared between MS participants and controls using the *randomize* tool in the FSL library, with 5,000 permutations and threshold-free cluster enhancement (TFCE, $p < 0.05$, fully corrected for multiple comparisons by controlling for FWE,¹¹ while treating age and sex as covariates. We performed similar inter-subject voxel-wise correlations between skeleton DTI indices and cognitive scores only in patients. The significant regions were located and labeled anatomically to two WM atlases.¹²⁻¹³

Tractography

We used streamline tractography to obtain tracts from the significant clusters in GM VBA for each cognitive test in a healthy control subject. First, the healthy volunteer diffusion tensor image was aligned to the T1-MPRAGE using Boundary-Based Registration (BBR)¹⁴ and local fitting of diffusion tensors was performed. The VBA binary masks were then specified as seeds to perform tensor-based deterministic fiber tracking through MRtrix software package.¹⁵ The elicited tracts were normalized into MNI space and identified anatomically using a tractography atlas.¹³

Lesion Probability Mapping

The lesion masks from each patient were normalized to the standard MNI space images by applying the deformation fields obtained in DARTEL. Individual normalized lesion masks were smoothed with an 8 mm FWHM Gaussian kernel to create a lesion probability map for each patient. In the probability map each voxel value can be thought of as an estimate of the probability that the subject has a lesion at that location (Supplementary Figure S-1).¹⁶ The relationship between disability scores and the lesion probability at each voxel was modeled as a

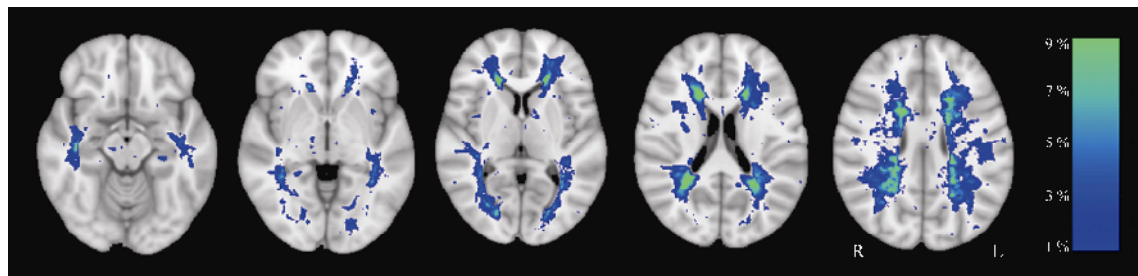
multiple linear regression, with each cognitive score as the dependent variable,¹⁷ and age, sex and brain scaling as covariates. Significance was defined in the same way as that described for the VBA of the gray matter.

References

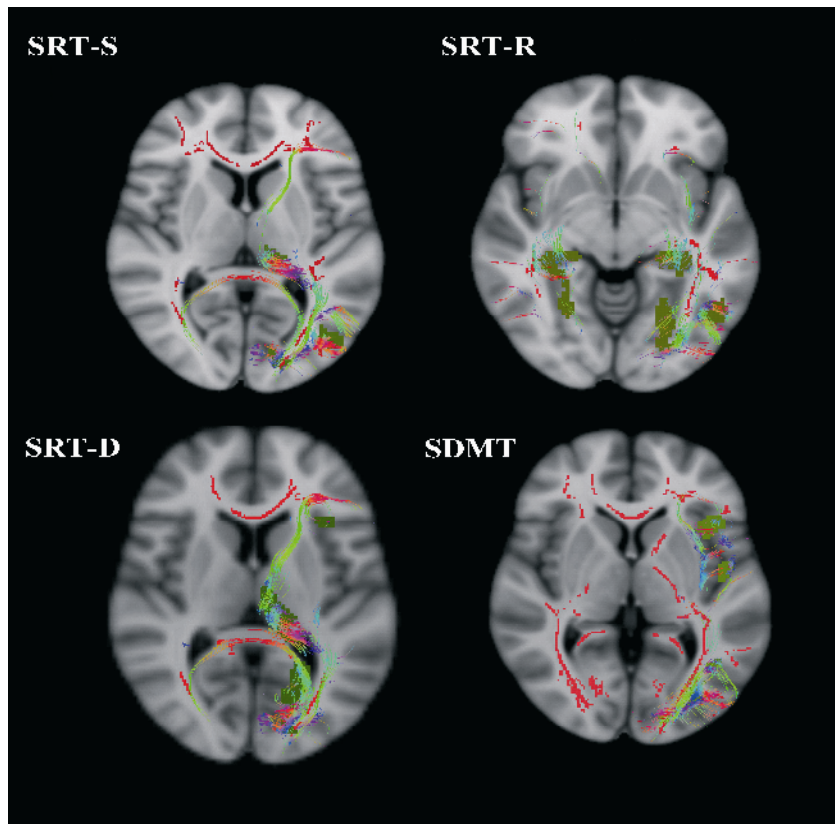
1. Gallichan D, Scholz J, Bartsch A, Behrens TE, Robson MD and Miller KL. Addressing a systematic vibration artifact in diffusion-weighted MRI. *Hum Brain Mapp* 2010; 31: 193-202.
2. Ling J, Merideth F, Caprihan A, Pena A, Teshiba T and Mayer AR. Head injury or head motion? Assessment and quantification of motion artifacts in diffusion tensor imaging studies. *Hum Brain Mapp* 2012; 33: 50-62.
3. Yushkevich PA, Piven J, Hazlett HC, et al. User-guided 3D active contour segmentation of anatomical structures: significantly improved efficiency and reliability. *Neuroimage* 2006; 31: 1116-1128.
4. Ceccarelli A, Jackson JS, Tauhid S, et al. The Impact of Lesion In-Painting and Registration Methods on Voxel-Based Morphometry in Detecting Regional Cerebral Gray Matter Atrophy in Multiple Sclerosis. *AJNR Am J Neuroradiol* 2012.
5. Chard DT, Jackson JS, Miller DH and Wheeler-Kingshott CA. Reducing the impact of white matter lesions on automated measures of brain gray and white matter volumes. *J Magn Reson Imaging* 2010; 32: 223-228.
6. Ashburner J and Friston KJ. Unified segmentation. *Neuroimage* 2005; 26: 839-851.
7. Ashburner J. A fast diffeomorphic image registration algorithm. *Neuroimage* 2007; 38: 95-113.
8. Tzourio-Mazoyer N, Landau B, Papathanassiou D, et al. Automated anatomical labeling of activations in SPM using a macroscopic anatomical parcellation of the MNI MRI single-subject brain. *Neuroimage* 2002; 15: 273-289.
9. Sdika M and Pelletier D. Nonrigid registration of multiple sclerosis brain images using lesion inpainting for morphometry or lesion mapping. *Hum Brain Mapp* 2009; 30: 1060-1067.
10. Smith SM, Jenkinson M, Johansen-Berg H, et al. Tract-based spatial statistics: voxelwise analysis of multi-subject diffusion data. *Neuroimage* 2006; 31: 1487-1505.
11. Smith SM and Nichols TE. Threshold-free cluster enhancement: addressing problems of smoothing, threshold dependence and localisation in cluster inference. *Neuroimage* 2009; 44: 83-98.
12. Mori S, Oishi K, Jiang H, et al. Stereotaxic white matter atlas based on diffusion tensor imaging in an ICBM template. *Neuroimage* 2008; 40: 570-582.
13. Wakana S, Jiang H, Nagae-Poetscher LM, van Zijl PC and Mori S. Fiber tract-based atlas of human white matter anatomy. *Radiology* 2004; 230: 77-87.

14. Greve DN and Fischl B. Accurate and robust brain image alignment using boundary-based registration. *Neuroimage* 2009; 48: 63-72.
15. Smith RE, Tournier JD, Calamante F and Connelly A. Anatomically-constrained tractography: improved diffusion MRI streamlines tractography through effective use of anatomical information. *Neuroimage* 2012; 62: 1924-1938.
16. Sepulcre J, Masdeu JC, Sastre-Garriga J, et al. Mapping the brain pathways of declarative verbal memory: Evidence from white matter lesions in the living human brain. *Neuroimage* 2008; 42: 1237-1243.
17. Kincses ZT, Ropele S, Jenkinson M, et al. Lesion probability mapping to explain clinical deficits and cognitive performance in multiple sclerosis. *Mult Scler* 2011; 17: 681-689.

Supplementary Figure legends



Supplementary Figure-1: Lesion probability map. White matter lesion frequency map resulting from the overlap of the binary masks of the entire sample of patients.



Supplementary Figure-2: Tractography. Regions in GM significantly associated with cognitive scores in VBA (in dark blue) were used as seeds to produce deterministic tractography. In the same image, the significant skeleton tracts from TBSS associated with the cognitive z-scores are shown in red.

Supplementary Table S-1. Results of tractography from significant DTI GM clusters and anatomical correspondence with TBSS significant clusters

	GM cluster	Tract created through tractography	Correspondence with TBSS clusters
SRT-IR	Left angular cortex	Left superior LF	No
SRT-S	Left angular cortex	Left superior LF	No
	Left calcarine cortex	Forceps major and inferior LF	Yes
	Left lingual cortex	Inferior LF	Yes
	Left temporal cortex	Inferior LF	Yes
	Parahippocampus and thalamus	Anterior thalamic radiations	No
SRT-R	Right precentral cortex	None	No
	Left angular cortex	Left superior LF	No
	Left lateral inferior occipital cortex	Left superior LF	Yes
	Left fusiform cortex	Left inferior LF	Yes
	Left inferior temporal gyrus	None	No
	Right lateral occipital cortex	None	No
	Bilateral hippocampus	Anterior thalamic radiations	Yes (left)
	Right and left insula	None	No
SRT-D	Left fronto-orbital cortex	Left inferior fronto-occipital fasciculus	Yes
	Parahippocampus and thalamus	Anterior thalamic radiation	No
	Left precuneus	Forceps major	Yes
	Left calcarine cortex	Left inferior LF	Yes
SDMT	Left anterior insula/operculum	Left inferior fronto-occipital fasciculus	Yes
	Insula	Extreme capsula	No
	Left fusiform cortex	Left inferior LF	Yes
	Lateral occipital cortex	Left inferior fronto-occipital fasciculus and inferior LF	Yes
	Left cerebellum	Tract to middle cerebellar peduncle	No

Supplementary Table S-2. Multiple linear regression analyses at cluster level with GM RD

	RD in GM	Age	Disease duration	EDSS	R ²
SRT-IR	B=-0.58 <i>p</i> <0.001	B=-0.08 <i>p</i> =0.52	B=0.03 <i>p</i> =0.83	B=0.05 <i>p</i> =0.72	0.32
SRT-S	B=-0.59 <i>p</i> <0.001	B=0.03 <i>p</i> =0.80	B=0.07 <i>p</i> =0.61	B=0.05 <i>p</i> =0.72	0.29
SRT-R	B=-0.51 <i>p</i> <0.001	B=0.04 <i>p</i> =0.73	B=-0.05 <i>p</i> =0.69	B=-0.03 <i>p</i> =0.80	0.29
SRT-D	B=-0.44 <i>p</i> =0.001	B=-0.21 <i>p</i> =0.09	B=-0.10 <i>p</i> =0.43	B=0.04 <i>p</i> =0.79	0.31
SDMT	B=-0.64 <i>p</i> <0.001	B=0.11 <i>p</i> =0.33	B=0.06 <i>p</i> =0.96	B=-0.02 <i>p</i> =0.89	0.38

B: standarized beta. SRT-IR: Selective Reminding Test immediate recall; SRT-S: Selective Reminding Test long-term storage; SRT-R: Selective Reminding Test long-term retrieval; SRT-D: Selective Reminding Test long-term delayed recall; SDMT: Symbol Digit Modalities Test.

DTI values were obtained from the GM regions that significantly correlated with each cognitive z-scores in VBA.

Trabajo número 4

MR Spectroscopy Markers of Disease Progression in Multiple Sclerosis

Sara Llufriu^{1,4}, John Kornak³, Helene Ratiney¹, Joonmi Oh², Don Brenneman;¹ Mehul Sampat¹, Stephen L. Hauser¹, Sarah J. Nelson², Radhika Srinivasan², Daniel Pelletier^{1,2,5}.

¹Department of Neurology, University of California San Francisco, San Francisco, US.

²Department of Radiology, University of California San Francisco, San Francisco, US.

³Department of Epidemiology and Biostatistics, University of California San Francisco, San Francisco, US. ⁴Center for Neuroimmunology, Service of Neurology, Hospital Clinic and Institut d'Investigacions Biomèdiques August Pi i Sunyer (IDIBAPS), Barcelona, Spain. ⁵Departments of Neurology and Diagnostic Radiology, Yale University, New Haven, US.

- Artículo en preparación -

RESULTADOS

Este estudio pretendía evaluar la capacidad predictiva de marcadores de desmielinización, astrogliosis y daño axonal obtenidos a través de RM avanzada sobre la atrofia cerebral y la discapacidad a lo largo de 4 años y con ello conocer los eventos patogénicos relacionados con la progresión de la EM.

Se estudiaron dos cohortes de sujetos. En la cohorte preliminar se incluyeron 59 pacientes y 43 controles sanos, y en la confirmatoria se incluyeron 220 pacientes con EM. En ambos grupos se realizó una RM cerebral que incluía espectroscopia para determinar marcadores de astrogliosis (ml) y de daño axonal (NAA) y se estudió la desmielinización a través de la Myelin Water Fraction (MWF). Las medidas a predecir fueron el porcentaje de cambio en el volumen cerebral (“Brain Parenchymal Volume Change” BPVC), el cambio en la discapacidad medida con EDSS y zMSFC y la progresión sostenida de la discapacidad. En la cohorte confirmatoria únicamente se incluyeron datos de espectroscopia como predictores.

En cuanto a resultados, en la cohorte preliminar el incremento de ml y la disminución de NAA en la SBAN y gris se asociaban a un mayor BPVC. De esta forma, surgió la idea de utilizar la ratio ml/NAA en la SBAN como un predictor más. La ratio de ml/NAA en la SBAN fue capaz de predecir la evolución de BPVC, la evolución de zMSFC y la progresión sostenida de zMSFC. El MWF no se asoció a la evolución de la atrofia ni de la discapacidad.

En la cohorte confirmatoria de nuevo la ratio ml/NAA fue capaz de predecir el BPVC y también la evolución de zMSFC y del EDSS así como la progresión sostenida del EDSS.

MR Spectroscopy Markers of Disease Progression in Multiple Sclerosis

Sara Llufriu, M.D.^{1,4} John Kornak, Ph.D.³ Helene Ratiney, PhD.¹ Joonmi Oh, PhD.² Don Brenneman;¹ Mehul Sampat, Ph.D.;¹ Stephen L. Hauser, M.D.;¹ Sarah J. Nelson, Ph.D.;² Daniel Pelletier, M.D.^{1, 2, 5}

¹ Department of Neurology, University of California San Francisco, San Francisco, CA

² Department of Radiology, University of California San Francisco, San Francisco, CA

³ Department of Epidemiology and Biostatistics, University of California San Francisco, San Francisco, CA

⁴ Center for Neuroimmunology, Service of Neurology, Hospital Clinic and Institut d'Investigacions Biomèdiques August Pi i Sunyer (IDIBAPS), Barcelona, Spain

⁵ Departments of Neurology and Diagnostic Radiology, Yale University, New Haven, CT

Corresponding author and proofs:

Daniel Pelletier, M.D.
Department of Neurology
Yale University School of Medicine
15 York Street, LCCI 710A
New Haven, CT 06
Phone (203) 737-5719
Fax (415) 785-7826
e-mail: daniel.pelletier@yale.edu

Author contribution

Dr. Pelletier was involved in the study concept and design, data collection, standardized assessments of subjects, study conduct, data summary and analysis, literature search, and writing of the report.

Dr. Lufriu was involved in the study concept and design, MRI data processing, data summary and analysis, and writing of the report.

Dr. Kornak was involved in the study concept and design, statistical analysis, and writing of the report.

Drs. Srinivasan, Ratiney, Oh, Nelson, Sampat were involved in the study conduct, standardized assessment of MRI/MRS processing, and writing of the report.

Dr. Hauser was involved in the study design and conduct, and data collection.

D. Brenneman was involved in data collection and writing of the report.

Funding

This study was supported by grants from the National Multiple Sclerosis Society (JF 2122-A, preliminary data set), the National Institute of Health (NIH/NINDS R01-NS062885, confirmatory data set), GSK and Biogen-Idec for clinical research data and imaging collection support.

ABSTRACT

Objectives: The aim of this study is to assess the ability of several specific *in vivo* MR markers of CNS injury to predict brain volume loss and clinical disability in multiple sclerosis (MS).

Methods: Baseline N-acetylaspartate (NAA), myo-inositol (ml) in normal-appearing white (NAWM) and grey (NAGM) matter, and Myelin Water Fraction (MWF) in NAWM, markers of axonal damage, astrogliosis and demyelination respectively, were evaluated as predictors in a preliminary dataset (59 MS subjects, 43 healthy controls). Results from potential predictors were subsequently tested for replication in a confirmatory dataset (220 MS subjects). Clinical scores and percentage of brain volume change (PBVC) were obtained annually over 4 years in both datasets. Predictors of outcomes were assessed using linear models, linear mixed-effects models, and logistic regression.

Results: NAA and ml led to statistically significant effects on brain volume in the preliminary dataset, suggesting the consideration of ml/NAA_{NAWM} ratio as a primary predictor. The ratio proved to be a strong predictor of PBVC in both cohorts ([-1.68 annual slope of PBVC per unit of increase in the ratio, p=0.02] and [-1.08 annual slope; p=0.02], respectively). In addition, the ml/NAA_{NAWM} ratio predicted clinical disability (linear Multiple Sclerosis Functional Composite (MSFC) evolution [-0.52 points annually; p<0.001]; MSFC sustained progression [Odds Ratio:2.76 for each increase in one standard deviation in the ratio; p=0.013]) in the preliminary dataset and predicted MSFC evolution [-0.23 points annually; p=0.012], Expanded Disability Status Scale (EDSS) evolution [0.57 points annually; p=0.04], and EDSS sustained progression [Odds Ratio:1.46; p=0.009] in the confirmatory dataset. MWF did not show predictive value in the exploratory dataset and was not evaluated in the confirmatory dataset.

Conclusions: The ml/NAA_{NAWM} ratio has consistent predictive power in the evolution of brain atrophy and neurological disability in MS. The combined presence of astrogliosis and axonal damage in white mater has cardinal importance in disease severity.

Introduction

The mechanisms underlying disease evolution in MS are not fully known. Current predictors based on clinical¹ or conventional (structural) MRI data² are known to relate to long-term disability, but have limited specificity in characterizing and quantifying the heterogeneous pathological features of MS.³ The study of myelin destruction and repair, axonal injury and astrogliosis, major pathological events in MS,^{4,5} by means of non-conventional MRI techniques⁶ could help in achieving that goal.

Magnetic resonance spectroscopic (MRS) has contributed considerably to understanding the pathogenesis and natural history of MS.⁷ Metabolic abnormalities in MS patients are not restricted to lesion sites, but are more diffuse in nature.^{8,9} N-acetylaspartate (NAA) is an amino acid found in the central nervous system. Although the exact physiological function is still unclear, its appearance in neurons and axons and absence from mature glia cells, NAA is used as a marker of neuronal/axonal integrity and function¹⁰. Over the past several years, NAA is found to be depleted in MS patients.^{11,12} Moreover, the loss of NAA could precede brain atrophy¹¹ and moderately correlates with subsequent development of physical disability.¹² Myoinositol (ml) is thought to originate from intracellular astrocyte stores.¹³ ml can be elevated in MS patients,⁹ reflecting astroglial hypertrophy or hyperplasia, even in early stages of the disease¹⁴ and precedes the decrease of NAA and brain volume.¹⁵ Moreover, a relatively new MRI technique allows the estimation of myelin water content derived from the quantification of short T2 relaxometry component.¹⁶ The measure is specific to myelin content and/or its integrity in neurological tissue.¹⁷ The Myelin Water Fraction (MWF) is commonly reduced in MS white matter (NAWM),¹⁸ which may reflect active or chronic demyelination.

The aim of the present study was to conduct a rigorous analysis of spectroscopy and relaxometry markers of axonal integrity, astrogliosis and demyelination *in vivo* with respect to predicting long-term clinical disability and brain volume loss. After performing an initial analysis in a preliminary group of MS patients (preliminary dataset), results were tested for replication in a larger representative MS group (confirmatory dataset).

Material and Methods

Preliminary dataset

Study population: Fifty-nine MS and 43 control subjects were included in a case-control longitudinal study. The MS subjects, fulfilling 2001 McDonald criteria,¹⁹ were prospectively and consecutively selected from clinical patients visiting one of the physician's clinic (DP) at the

University of California, San Francisco (UCSF) Multiple Sclerosis Center (see sponsor in the funding section). At baseline (assessment of predictors) only the use of interferon-B and copolymer-1 disease modifying therapies for MS was allowed. On follow-up visits, the use of natalizumab, rituximab and oral immunosuppressive drugs was permitted. The mean study follow-up time was 3.5 years (SD ±1.2) and eighty percent of the MS subjects (47/59) completed 4 years of the study. All participants gave written and informed consent to enter the study approved by the UCSF Ethics Committee. Demographic and clinical data are available in Table 1.

Predictors: Predictors were derived from a 3-dimensional short-echo proton magnetic resonance spectroscopic imaging (3D-¹HMRSI) sequence and a multi-slice multi-echo T2 relaxometry sequence using a single 3T GE Signa scanner (GE Healthcare, Waukesha, WI, USA) with an eight-channel phased array coil. Spectroscopic signals were acquired from a supratentorial PRESS box covering 4 slices centered on the corpus callosum²⁰ using point-resolved spectroscopy (PRESS) volume selection, with a conventional phase encoding, with TR/TE 1000/40 msec, total acquisition time=15 min. Metabolite contributions within each voxel were estimated by adjusting short echo time signals to a model function created from a prior knowledge basis set of metabolite signals according to the semi-parametric approach developed in HR-QUEST accounting for macromolecular contributions, and for NAA and ml T1 relaxation values estimated at 3T using a similar method described previously.²¹ T1-weighted three-dimensional inversion recovery spoiled gradient-echo (IR-SPGR) images were segmented into GM and WM compartments. The GM and WM maps were re-gridded to spectroscopy resolution and convolved with the point spread function for spectroscopic imaging to yield the percent GM and WM content within each spectroscopic voxel²². For patients, the voxels containing manually segmented lesions on the IR-SPGR sequence were removed from the analysis. Moreover, the spectroscopic voxels were included in the linear fit only if their concentration estimates had estimated Cramer-Rao bounds within threshold values (10% for [NAA], [Cho] and [Cre], 30% for the [ml]). (Appendix e-1).

MWF from NAWM were extracted from a 16-slice T2 prep spiral sequence (TR=2000 ms, *T En* = 7, 17, 28, 38, 49, 60, 70, 92, 124, 177, 220, and 294 msec; in-plane resolution of 2 x 2 mm²; 16 5-mm thick slices; NEX=6) that acquires non-linearly spaced 12-echo datasets as previously reported.²³ Lesion and white matter masks were re-gridded to the lower resolution MWF map derived from the 12-echo data, which was fit to a distribution of T2 values using a nonnegative least square algorithm. MWF maps (defined as ratio between peak area for T2 component < 50 msec and total water) were created to yield the percent content within each voxel. The MWF median value was calculated from the NAWM mask for each patient at baseline and used as a predictor.

Confirmatory dataset

Study Population: An independent group of MS subjects from the UCSF MS Center were prospectively recruited from a large genotype-phenotype separately funded research project (see funding section), and used here to confirm the results obtained in the preliminary study. All participants gave written and informed consent to enter the study. A total of 220 MS subjects meeting the 2005 revised McDonald criteria²⁴ were included with a mean follow-up time of 3.6 years ($SD \pm 0.9$). As described in the preliminary study, the use of MS therapies was permitted. Eighty nine percent of the subjects (193/220) completed 3 years and 68% (150/220) completed four years of follow up. Demographic and clinical data are provided in Table 1.

Predictors: Four predictors from the preliminary dataset analysis were retained (MWF was not used). NAA and ml from NAWM and NAGM were derived from a 2-dimentional TE-Averaged spectroscopic imaging technique (TE-Averaged-CSI)²⁵ using the same 3T GE scanner and phased-array coil used for the preliminary dataset. The spatial data were acquired with a nominal in plane spatial resolution of 1.2x1.0 cm with a volume selection box placed in the supratentorial brain, covering a single 1.5cm-thick slice, just above the corpus callosum body (TR = 1sec, 64 echo time steps starting at TE = 35 msec with an echo time increment of 2.5 msec, total acquisition time= 21 minutes) to encompass as much cortical grey matter possible. The resulting 8-coil combination data were TE-averaged. Then NAA and ml values were quantified using the LCmodel in millimoles/L (mM) and corrected for T1 and T2 metabolite relaxation times measured from cortical grey matter and white matter.²¹ After obtaining the percent GM and WM content within each voxel the same way as for the preliminary dataset, pure GM and WM metabolite concentrations were extrapolated²⁵ by modeling the metabolite concentrations as a linear function of WM content. The same estimated Cramer Rao lower bound threshold as for the preliminary dataset was used.

Study outcome measures (preliminary and confirmatory datasets)

All outcome metrics were collected similarly for both datasets. Brain atrophy progression for each pair of scans (baseline-year1, year1-year2, year2-year3, etc.) over the observation period was measured by estimated brain volume changes using SIENA (Structural Image Evaluation using Normalization of Atrophy. Image Analysis Group, Oxford, UK). Clinical outcomes were measured longitudinally using the Expanded Disability Status Scale (EDSS) and the Multiple Sclerosis Functional Composite (MSFC) scores over the observation period.

Brain volume changes: Structural MR images for both studies were acquired on the same 3T GE scanner prior to the spectroscopy sessions. The main MRI outcome was the slope in the

percent brain volume change (PBVC) over the study period based on annual brain images acquired using a 3D high-resolution IR-SPGR (TR/TE/TI = 7/2/400 msec, 15° flip angle, matrix: 256 x 256 x 180, FOV: 240 x 240 x 180 mm³, IS: 180 1-mm).

Clinical measures: Annual neurological evaluations included standardized MS clinical metrics (EDSS and MSFC). All examiners were blinded to radiological predictors and outcomes. Subjects with a baseline EDSS of 5.5 or less were defined to have a sustained progression in their EDSS if an overall increase of ≥1.0 points was observed for at least two consecutive measures (sustained EDSS progression for 12 months); for patients with a baseline EDSS of 6.0 or more, progression was defined as an increase of ≥0.5 points over 2 consecutive measures. Three formally trained research coordinators at the UCSF MS Center administered the MSFC. MSFC standardized scores (z-scores) were derived by the methods previously described by the National MS Society's Clinical Assessment Task Force²⁶ and calculated from a reference population published previously.²⁷ Sustained progression in zMSFC was defined as having a Z score that worsened ≥20% from baseline value over two consecutive time points. The main clinical outcomes of the study were the longitudinal change in EDSS and zMSFC scores along with the binary summary outcomes of sustained EDSS or MSFC progression over 12 months.

Imaging covariates: Experienced neurologists created T1-lesion masks using semi-automated thresholding and manual editing methods directly from the high-resolution IR-SPGR images. Subsequent brain segmentation and normalization were performed using SIENAX (Image Analysis Group, Oxford, UK), which was effectively fully automated once the T1 lesion mask had been used to avoid pixel misclassifications. The final normalized brain parenchymal volume (nBPV) and normalized lesion volume (nLesVol) metrics derived from SIENAX were used as covariates in statistical modeling.

Statistical Analysis

All statistical analyses were performed using R (<http://www.r-project.org/>). Cross-sectional comparisons of metabolites (NAA, mI) and MWF between MS subjects and controls were performed using Wilcoxon Rank Sum tests. Linear mixed-effects models were used to longitudinally model all outcomes (disability scores (EDSS, MSFC), and brain volume changes). The linear mixed effects models were fitted using restricted maximum likelihood (R NLME package lme function, Pinheiro and Bates²⁸ with disability score, or brain volume change at each time point as the dependent variable. Additional covariates considered included time from baseline exam, baseline imaging variables (nLesVol, nBPV), and baseline disease duration. All baseline covariates were included with corresponding interactions with time. Random effects for

both intercept and slope were included in the model to accommodate between subject variability in the outcome and its rate of change.

All fitted linear mixed effects models used an unstructured covariance matrix for the random effects with independent and identical distributed normal errors, except for the SIENA volumetric change outcome for which we adopted a model²⁹ accommodating the inherent correlation between subsequent pairs of change scores. This change model implements random intercept and slope, but with fixed part of the intercept set at zero (in the smaller original dataset a random intercept and slope was not estimable in which case we used a random intercept only). In contrast to the specification in the paper²⁹, we only modeled PBVC measurements between subsequent pairs of time points (baseline-year1, year1-year2, year2-year3, year3-year4) to create a slope for each patient rather than changes between all time point pairs. We did this to account for the non-additivity of percent changes (albeit close to additive for small percent changes) while still working on a scale of percent change.

Mixed-effects models were initially fit with single predictors (each outcome versus each predictor). Subsequently, models with multiple predictors were fitted to determine independent additive value of predictors, e.g., combinations of multiple metabolites in NAWM, NAGM and MWF_{NAWM}. Finally, additional covariates: disease duration, treatment status (ever or never on therapy for the duration of the observation period), nLesVol, and nBPV were added to each of the final statistical models to determine whether the effects of primary predictors remained consistent after accounting for these additional covariates. Results are given in terms of estimated annualized changes along with 95% confidence interval (CI) and associates p-values. Many of the mixed-effects models were checked for assumptions of normality (via qq-plots) and they appeared reasonable with no extreme outliers (including metabolite ratios).

Logistic regression analysis allowing for over-dispersion was used to determine the influence of metabolite levels on the risk of EDSS and zMSFC sustained progression. Results are given in terms of estimated odds-ratios along with 95% CI and associated *P*-values.

All results are reported based on a significance level of $\alpha=0.05$. Although we examine many differences and issues, we report nominal p-values, without adjustment for multiple testing. (Appendix e-1).

Results

Preliminary study

Predictors: All metabolites and MWF measures are reflected in Table 2. Statistically significant differences were found between MS subjects and healthy controls for all predictors except for NAA concentration levels in NAGM. It is notable that the ml/NAA ratio in NAWM (ml/NAA_{NAWM}) provided the largest percent difference (31%; $p < 0.001$).

Prediction of brain atrophy evolution: Results of longitudinal mixed-effects models predicting brain volume change are shown in Table 3. Overall, the mean PBVC from baseline to year 4 was -1.63% (SD ±1.1%). In the single predictor analyses we did not find any statistically significant associations between metabolite levels or MWF and PBVC evolution (Table 3). However, in a multiple predictor analysis that included ml, NAA and their interaction as predictors, there was a statistically significant positive interaction between ml and NAA in NAWM, indicating that NAA levels may modify the influence of ml on volume loss [+0.02 annual slope of PBVC for each simultaneous unit increase in both NAA and ml; 95% CI: 0.006 to 0.03; $p = 0.003$]. A similar interaction pattern was also observed in NAGM where a statistically significant interaction revealed that NAA_{NAGM} could reduce the influence of ml on brain tissue loss [0.008 annual slope; 95% CI: 0.003 to 0.014; $P = 0.003$]. These statistical significant interactions between ml and NAA along with biological plausibility (increased gliosis, reduced axonal integrity) prompted consideration of ml/NAA as a predictor. Higher baseline ml/NAA_{NAWM} predicted increased longitudinal brain volume loss. Specifically, for each unit of increase in ml/NAA_{NAWM} ratio, we estimated a corresponding annual slope of PBVC of -1.68; 95% CI:-3.05 to -0.30; $p = 0.017$ (Table 3).

Prediction of change in disability: The median EDSS increase over the course of the study was only 0.5 point, with individual patient changes ranging from -1.5 to 4.5. Forty eight percent (24/50) of the patients presented EDSS sustained progression (12-month sustained) and 20% (10/49) of the patients showed zMSFC progression. No predictors were found to have a statistically significant influence on EDSS evolution. However, ml [-0.043 zMSFC point annually for each increase in one mM; 95% CI: -0.08 to -0.009; $p = 0.015$] and ml/NAA ratio [-0.522 zMSFC point annually; 95% CI: -0.82 to -0.23; $p < 0.001$] in NAWM were statistically significant predictors of longitudinal zMSFC decline (Table 3).

Moreover, the ml/NAA_{NAWM} was a significant predictor of zMSFC sustained progression over 12 months: estimated Odds Ratio (OR) per standard deviation increase in the ratio= 2.76; 95% CI: 1.32 to 6.47; $p = 0.013$, but not of EDSS sustained progression [OR= 1.04; 95% CI: 0.60 to 1.79; $p = 0.87$].

When the additional covariates (disease duration, nBPV, nLesVol, treatment status) were added into the models, the pattern of results was unchanged.

MWF did not show any predictive value on the evolution of brain atrophy or disability.

Confirmatory study

Predictors: Predictors used in the confirmatory study are summarized in Table 4. Our main goal in this part of the study was to prioritize the assessment of ml/NAA_{NAWM}. However, as the confirmatory dataset had a larger number of patients, results with absolute metabolites were also analyzed but presented in the supplementary material (Appendix e-1). MWF as a predictor was not acquired as part of this study.

Prediction of brain atrophy evolution: The overall mean PBVC from baseline to year 4 was -2.02% (SD ± 1.15). Similar to the preliminary study, higher ml/NAA_{NAWM} ratio predicted larger brain parenchyma volume loss [-1.08 annual slope; 95% CI: -1.95 to -0.20]; $p = 0.02$] (Table 3 and Figure 1).

Prediction of change in disability: The median EDSS change was 0.0 point, ranging from -3.0 to 3.0, at the end of the study. For each unit increase of ml/NAA_{NAWM} ratio there was an estimated corresponding annual mean EDSS increase [0.57 point annually; 95% CI: 0.015 to 1.13; $p = 0.04$] over the subsequent 4 years (Figure 1). Longitudinal changes in zMSFC were also predicted by baseline ml/NAA_{NAWM} [-0.23 point annually; 95% CI: -0.41 to -0.05; $p = 0.012$] (Figure 1).

Twenty seven percent (55/204) of patients experienced 12-month sustained EDSS progression, and 16% (31/191) zMSFC sustained progression. 12-month sustained EDSS progression was significantly predicted by ml/NAA_{NAWM} ratio (OR per standard deviation increase in the ratio of 1.46; 95% CI: 1.10 to 1.94; $p = 0.009$), but not by ml/NAA_{NAGM} [OR=0.25; 95% CI: -0.64 to 0.15; $P = 0.22$]. However, contrarily to the preliminary dataset, we did not observe a significant effect of the ml/NAA_{NAWM} on the 12-month zMSFC sustained progression [OR=1.19; 95% CI: 0.84 to 1.66; $p = 0.32$].

Similarly to the preliminary dataset, when the additional covariates (disease duration, nBPV, nLesVol, treatment status) were added into the models, the pattern of results was unchanged.

Discussion

The main focus of our study was to investigate longitudinally the predictive value of pathologically specific MR metrics on MS disease progression and to replicate our findings using independent datasets. Our observations provide evidence that the relationship between axonal damage and astrogliosis from MS white matter areas is a key element in the development of clinical disability and brain volume loss in MS. More specifically, we report that ml/NAA_{NAWM} metabolite ratio is a predictor of MS progression.

MS subjects were first recruited in a preliminary study. PBVC from SIENA³⁰ served in this long-term study as the MRI correlate of brain tissue loss. Our multiple predictor analyses included baseline ml and NAA from both MS white and grey matter areas. The interaction between NAA and ml showed a statistically significant effect on PBVC. This statistical interaction between ml and NAA in opposite directions (reduced NAA, increased ml) along with biological plausibility (reduced axonal integrity, increased gliosis) immediately prompted consideration of ml/NAA as a predictor. Indeed, higher baseline ml/NAA_{NAWM} was a statistically significant predictor of increased longitudinal brain volume loss, MSFC evolution and sustained MSFC progression (Odds Ratio = 2.76), but not sustained EDSS progression. MWF, a marker of myelin integrity, was not a statistically significant predictor in any statistical models we performed. The lack of sensitivity and robustness (despite good quality fits of all compartment peaks in the cases used, data not shown) of our technique used in detecting myelin injury could explain these findings, or alternatively, it could support the notion that permanent disability in MS may be driven by axonal rather than myelin damage.³¹⁻³²

A large confirmatory study using an independent MS group of subjects and a different metabolite quantification method was conducted in order to replicate the results from the preliminary study. Notably, ml/NAA_{NAWM} ratio was again able to statistically significantly predict brain volume loss, zMSFC, and EDSS change over time and 12-month sustained EDSS progression, overall confirming the main findings of the preliminary results.

Previous smaller studies had found that ml correlated cross-sectionally with clinical disability^{33,34} and that low levels of NAA and high ml in NAWM of clinically isolated syndrome subjects were predictors of conversion to clinically definite MS.³⁵ Higher ml/NAA ratio levels in MS patients are likely to reflect the combination of astrogliosis and axonal damage. From both datasets, ml levels (mainly from NAWM) consistently predicted brain volume changes and disability. Although causality was not determined in this study, the results could highlight the importance of reactive astrocytes in MS, potentially having a deleterious action on disability and brain atrophy when astrogliosis increases. However, its deleterious effect can be influenced by axonal status. This reinforces the theory of the dual roll of astrocytes in MS: on one side they may contribute to degeneration and demyelination, by promoting inflammation, damage of oligodendrocytes and axons, and glial scarring, but on the other side they may create a permissive environment for remyelination, by their action on oligodendrocyte precursor migration, oligodendrocyte proliferation, and differentiation.^{36,37} Nonetheless, both *in vivo* metabolite levels taken together seem to be important to predict the outcomes of interest.

Overall, the predictive power of the metabolites in grey matter was less pronounced than metabolites estimated from white matter areas. However, the importance of grey matter

pathology in MS is not questioned by these findings. Estimating metabolites *in vivo* is challenging in the cortical grey matter, especially when using a 2D spectroscopy single-slice technique, like the one used in the confirmatory study. Some of the differences we found in metabolite levels could come from the different techniques used in each dataset (for example, mean NAA in NAGM was numerical lower than in NAWM in the confirmatory dataset, although the difference was not significant). Additionally, issues related to partial voluming may be at play, this being particularly important for cortical grey matter due to its “ribbon-like” morphological nature. Nonetheless, this does not invalidate the robust predictive value of ml/NAA ratio derived from white matter.

Our study has limitations. We did not evaluate the longitudinal variations of our metabolites and of myelin water fraction. We were therefore unable to characterize the longitudinal progression of all predictors considered in the study; obtaining such data would address a different question but could provide additional insight into this progressive disease. Nonetheless, a cross-sectional ('baseline') predictor derived from a single scan offers to clinicians a practical and convenient tool for patient monitoring. However, the low number of progressive MS patients (SP and PP MS) included in the study precluded drawing inferences in these patient groups. Additionally, all spectroscopy scans were acquired on a single 3T GE platform and subjects were recruited from a single site. Although generalization of the findings and potential population biases could represent limitations, a single site study design has the advantage of minimizing scanner and site heterogeneity, especially in estimating metabolite concentration levels (mM), and of increasing sensitivity to detect disease patterns. Importantly, the effect sizes of the changes in PBVC and disability measures predicted by the ratio were overall low, preventing the application of this measure at this point for prediction at the individual level. We rather think our results inform about the pathological substrates of disease evolution.

A practical result of this experiment is that a metabolite ratio came up as our most robust predictor. A major advantage for the use of metabolite ratios over individual metabolite concentrations in clinical settings is that they are relatively easy to measure and can be readily obtained from most clinical MRI facilities.³⁸ Of note however, we think that the biological interpretation of ml/NAA is different than NAA/Cr ratio, another metabolite ratio that has been used in MS research for over two decades. ml/NAA ratio rather reflects two known pathological processes of CNS injury instead of using Creatine as a “normal” reference. As such, its validation in other neurodegenerative disorders may also prove to be promising.³⁹

In summary, we conclude from this work that ml/NAA_{NAWM} ratio in multiple sclerosis is a robust predictor of brain volume loss and clinical disability over time. Our work demonstrated that the

combination of astrogliosis and axonal damage has cardinal importance in the evolution of multiple sclerosis. Further studies should evaluate its potential in clinical settings.

Acknowledgements

The authors would like to thank all the physicians at the UCSF MS Center for referring subjects to the study and all the subjects for their participation.

Abbreviations

CI, confidence interval; CIS, clinically isolated syndrome; EDSS, Expanded Disability Status Scale; ml, myo-inositol; MR, magnetic resonance; MS, multiple sclerosis; MSFC, Multiple Sclerosis Functional Composite; NAGM, normal-appearing grey matter; NAWM, normal-appearing white matter; MWF, Myelin Water Fraction; NAA, N-acetylaspartate; PBVC, percentage of brain volume change; RRMS, relapsing remitting multiple sclerosis; SD, standard deviation; SPMS, secondary progressive multiple sclerosis.

References

1. Degenhardt A, Ramagopalan SV, Scalfari A, Ebers GC. Clinical prognostic factors in multiple sclerosis: a natural history review. *Nat Rev Neurol* 2009;5:672-682.
2. Arnold DL, Matthews PM. MRI in the diagnosis and management of multiple sclerosis. *Neurology* 2002;58:S23-31.
3. Filippi M, Agosta F. Imaging biomarkers in multiple sclerosis. *J Magn Reson Imaging* 2010;31:770-788.
4. Lassmann H, Bruck W, Lucchinetti CF. The immunopathology of multiple sclerosis: an overview. *Brain Pathol* 2007;17:210-218.
5. Frohman EM, Racke MK, Raine CS. Multiple sclerosis--the plaque and its pathogenesis. *N Engl J Med* 2006;354:942-955.
6. Bakshi R, Thompson AJ, Rocca MA, et al. MRI in multiple sclerosis: current status and future prospects. *Lancet Neurol* 2008;7:615-625.
7. Arnold DL, Wolinsky JS, Matthews PM, Falini A. The use of magnetic resonance spectroscopy in the evaluation of the natural history of multiple sclerosis. *J Neurol Neurosurg Psychiatry* 1998;64 Suppl 1:S94-101.
8. Sarchielli P, Presciutti O, Pelliccioli GP, et al. Absolute quantification of brain metabolites by proton magnetic resonance spectroscopy in normal-appearing white matter of multiple sclerosis patients. *Brain* 1999;122 (Pt 3):513-521.
9. Srinivasan R, Sailasuta N, Hurd R, Nelson S, Pelletier D. Evidence of elevated glutamate in multiple sclerosis using magnetic resonance spectroscopy at 3 T. *Brain* 2005;128:1016-1025.
10. Bitsch A, Bruhn H, Vougioukas V, et al. Inflammatory CNS demyelination: histopathologic correlation with in vivo quantitative proton MR spectroscopy. *AJNR Am J Neuroradiol* 1999;20:1619-1627.
11. Ge Y, Gonon O, Inglese M, Babb JS, Markowitz CE, Grossman RI. Neuronal cell injury precedes brain atrophy in multiple sclerosis. *Neurology* 2004;62:624-627.
12. Ge Y, Grossman RI, Udupa JK, et al. Brain atrophy in relapsing-remitting multiple sclerosis and secondary progressive multiple sclerosis: longitudinal quantitative analysis. *Radiology* 2000;214:665-670.
13. Fisher SK, Novak JE, Agranoff BW. Inositol and higher inositol phosphates in neural tissues: homeostasis, metabolism and functional significance. *J Neurochem* 2002;82:736-754.
14. Fernando KT, McLean MA, Chard DT, et al. Elevated white matter myo-inositol in clinically isolated syndromes suggestive of multiple sclerosis. *Brain* 2004;127:1361-1369.
15. Kirov, II, Patil V, Babb JS, Rusinek H, Herbert J, Gonon O. MR spectroscopy indicates diffuse multiple sclerosis activity during remission. *J Neurol Neurosurg Psychiatry* 2009;80:1330-1336.

16. Moore GR, Leung E, MacKay AL, et al. A pathology-MRI study of the short-T2 component in formalin-fixed multiple sclerosis brain. *Neurology* 2000;55:1506-1510.
17. Laule C, Kozlowski P, Leung E, Li DK, Mackay AL, Moore GR. Myelin water imaging of multiple sclerosis at 7 T: correlations with histopathology. *Neuroimage* 2008;40:1575-1580.
18. Oh J, Han ET, Lee MC, Nelson SJ, Pelletier D. Multislice brain myelin water fractions at 3T in multiple sclerosis. *J Neuroimaging* 2007;17:156-163.
19. McDonald WI, Compston A, Edan G, et al. Recommended diagnostic criteria for multiple sclerosis: guidelines from the International Panel on the diagnosis of multiple sclerosis. *Ann Neurol* 2001;50:121-127.
20. Pelletier D, Nelson SJ, Grenier D, Lu Y, Genain C, Goodkin DE. 3-D echo planar (1)HMRS imaging in MS: metabolite comparison from supratentorial vs. central brain. *Magnetic resonance imaging* 2002;20:599-606.
21. Ratiney H, Noworolski SM, Sdika M, et al. Estimation of metabolite T1 relaxation times using tissue specific analysis, signal averaging and bootstrapping from magnetic resonance spectroscopic imaging data. *MAGMA* 2007;20:143-155.
22. Zhang Y, Brady M, Smith S. Segmentation of brain MR images through a hidden Markov random field model and the expectation-maximization algorithm. *IEEE Trans Med Imaging* 2001;20:45-57.
23. Oh J, Han ET, Pelletier D, Nelson SJ. Measurement of in vivo multi-component T2 relaxation times for brain tissue using multi-slice T2 prep at 1.5 and 3 T. *Magnetic resonance imaging* 2006;24:33-43.
24. Polman CH, Reingold SC, Edan G, et al. Diagnostic criteria for multiple sclerosis: 2005 revisions to the "McDonald Criteria". *Ann Neurol* 2005;58:840-846.
25. Srinivasan R, Cunningham C, Chen A, et al. TE-averaged two-dimensional proton spectroscopic imaging of glutamate at 3 T. *Neuroimage* 2006;30:1171-1178.
26. Rudick R, Antel J, Confavreux C, et al. Recommendations from the National Multiple Sclerosis Society Clinical Outcomes Assessment Task Force. *Ann Neurol* 1997;42:379-382.
27. Okuda DT, Srinivasan R, Oksenberg JR, et al. Genotype-Phenotype correlations in multiple sclerosis: HLA genes influence disease severity inferred by 1HMR spectroscopy and MRI measures. *Brain* 2009;132:250-259.
28. Pinheiro JC, Bates DM. Mixed-effects models in S and S-PLUS. New York: Springer, 2000.
29. Frost C, Kenward MG, Fox NC. The analysis of repeated 'direct' measures of change illustrated with an application in longitudinal imaging. *Statistics in medicine* 2004;23:3275-3286.
30. Pelletier D, Garrison K, Henry R. Measurement of whole-brain atrophy in multiple sclerosis. *J Neuroimaging* 2004;14:11S-19S.
31. Leray E, Yaouanq J, Le Page E, et al. Evidence for a two-stage disability progression in multiple sclerosis. *Brain* 2010;133:1900-1913.

32. Bjartmar C, Kidd G, Mork S, Rudick R, Trapp BD. Neurological disability correlates with spinal cord axonal loss and reduced N-acetyl aspartate in chronic multiple sclerosis patients. *Ann Neurol* 2000;48:893-901.
33. Chard DT, Griffin CM, McLean MA, et al. Brain metabolite changes in cortical grey and normal-appearing white matter in clinically early relapsing-remitting multiple sclerosis. *Brain* 2002;125:2342-2352.
34. Sastre-Garriga J, Ingle GT, Chard DT, et al. Metabolite changes in normal-appearing gray and white matter are linked with disability in early primary progressive multiple sclerosis. *Arch Neurol* 2005;62:569-573.
35. Wattjes MP, Harzheim M, Lutterbey GG, et al. Prognostic value of high-field proton magnetic resonance spectroscopy in patients presenting with clinically isolated syndromes suggestive of multiple sclerosis. *Neuroradiology* 2008;50:123-129.
36. Williams A, Piaton G, Lubetzki C. Astrocytes--friends or foes in multiple sclerosis? *Glia* 2007;55:1300-1312.
37. Nair A, Frederick TJ, Miller SD. Astrocytes in multiple sclerosis: a product of their environment. *Cell Mol Life Sci* 2008;65:2702-2720.
38. De Stefano N, Filippi M, Miller D, et al. Guidelines for using proton MR spectroscopy in multicenter clinical MS studies. *Neurology* 2007;69:1942-1952.
39. Schott JM, Frost C, MacManus DG, Ibrahim F, Waldman AD, Fox NC. Short echo time proton magnetic resonance spectroscopy in Alzheimer's disease: a longitudinal multiple time point study. *Brain* 2010;133:3315-3322.

Figure legend

Figure 1. Association of brain atrophy and clinical measures evolution with ml/NAA_{NAWM} ratio levels. The annualized change in the PBVC (A) and zMSFC (C) decreased with the increase in the mean ml/NAA while the change in EDSS (B) increased with the increase in the ml/NAA levels. “BLUP” refers to best linear unbiased predictors of the rates of change extracted from the linear mixed effects model.

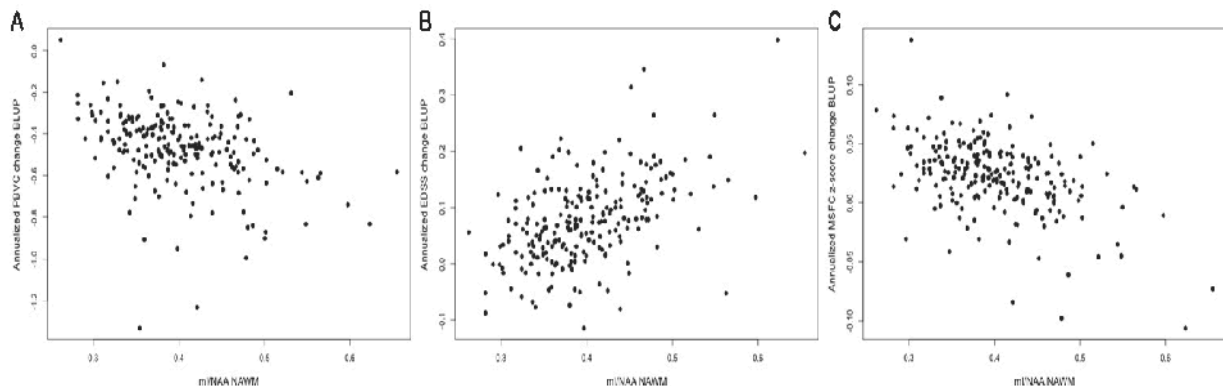


Table 1: Subjects baseline demographic and clinical characteristics from the preliminary and the confirmatory studies.

Variable	Preliminary dataset			Confirmatory dataset			
	MS subjects (n = 59)	Controls (n = 43)	All subjects (n = 220)	MS (n= 33)	CIS (n= 33)	RRMS (n = 164)	SPMS (n= 17)
Female sex — no. (%)	42 (71.2)	27 (62.8)	156 (70.9)	20 (60.6)	122 (74.4)	11 (64.7)	3 (50)
Age — yr	43.2 ± 9.4	38.9 ± 10.1	42.4 ± 9.5	40.7 ± 9.6	41.8 ± 9.2	40.6 ± 9.2	46.3 ± 10.5
Disease duration — yr	10.3 ± 9.7	n/a	9.7 ± 8.2	3.5 ± 3.2	10.2 ± 8.0	18.2 ± 8.7	8.1 ± 4.9
Subjects on DMT— no. (%)	29 (49)	n/a	146 (66.4)	12 (36.4)	118 (72.0)	13 (76.5)	3 (50.0)
EDSS — points, (Range)	Median 1.5 (0-4.5)	n/a	2.0 (0 – 7.0)	1.5 (0 – 4.0)	2.0 (0 – 6.0)	5.5 (2.5 – 7.0)	4.0 (3.0 – 5.5)
MSFC—z score	0.19 ± 0.5	n/a	0.12 ± 0.67	0.43 ± 0.5	0.17 ± 0.53	-0.86 ± 1.2	-0.71 ± 1.02

* Continuous variables are given as mean ± standard deviation (SD), categorical variables as N (%). Abbreviations: DMT = disease modifying therapy; EDSS = Expanded Disability Status Scale; MSFC = Multiple Sclerosis Functional Composite; CIS = clinically isolated syndrome; RRMS = relapsing remitting MS; SPMS = secondary progressive MS; PPMS = primary progressive MS; n/a = not applicable.

Table 2: Summary of imaging parameters used as predictors in the preliminary study

Predictor	MS Subjects Mean \pm SD (n = 59)	Controls* Mean \pm SD (n = 43)	Percent difference MS vs. Ctrl	P Value
NAA _{NAWM} — mM	7.72 \pm 1.42	8.43 \pm 1.19	↓ 8.4 %	0.013
NAA _{NAGM} — mM	9.44 \pm 2.0	9.18 \pm 1.54	↑ 2.8 %	0.49
ml _{NAWM} — mM	2.57 \pm 0.52	2.22 \pm 0.45	↑ 15.8 %	0.001
ml _{NAGM} — mM	4.03 \pm 0.95	3.39 \pm 0.78	↑ 18.9 %	0.001
ml/NAA _{NAWM} — ratio	0.34 \pm 0.04	0.26 \pm 0.06	↑ 30.8 %	<0.001
ml/NAA _{NAGM} — ratio	0.44 \pm 0.1	0.37 \pm 0.08	↑ 18.9 %	0.004
MWF — %	10.52 \pm 1.12	11.18 \pm 0.92	↓ 5.9 %	0.041

*For healthy control subjects, metabolite concentrations are extracted from white matter and grey matter regions. Abbreviations: SD = standard deviation; mM = millimoles per liter; NAA = *N*-acetyl-aspartate; ml = myo-inositol; NAGM = MS normal-appearing grey matter; NAWM = MS normal-appearing white matter; MWF = myelin water fraction. P values are derived from Wilcoxon Rank Sum test.

Table 3: Effect of imaging parameters tested as predictors (in single predictor models) on longitudinal outcomes (annual slopes) from the preliminary and confirmatory studies.

Predictors	PBVC preliminary	(%/y)	PBV C confirmatory	(%/y)	EDSS preliminary	(pts/y)	EDSS confirmatory	(pts/y)	zMSFC preliminary	(pts/y)	zMSFC confirmatory	(pts/y)
NAA _{NAWM}	0.03 (-0.03, 0.09), P=0.34	0.02 (-0.02, -0.06), P=0.35	-0.007 (-0.06, 0.05), P=0.81	-0.008 (-0.04, 0.02), P=0.56	-0.008 (-0.04, 0.02), P=0.56	-0.008 (-0.04, 0.02), P=0.56	-0.0004 (-0.014, 0.014), P=0.95	-0.0004 (-0.014, 0.014), P=0.95	-0.004 (-0.01, 0.004), P=0.32	-0.004 (-0.01, 0.004), P=0.32	-0.004 (-0.01, 0.004), P=0.32	
NAA _{NAGM}	0.03 (-0.02, 0.08), P=0.19	0.02 (-0.02, 0.05), P=0.34	-0.01 (-0.06, 0.03), P=0.58	-0.002 (-0.02, 0.02), P=0.89	-0.002 (-0.02, 0.02), P=0.89	-0.002 (-0.02, 0.02), P=0.89	-0.007 (-0.02, 0.005), P=0.24	-0.007 (-0.02, 0.005), P=0.24	-0.003 (-0.01, 0.004), P=0.40	-0.003 (-0.01, 0.004), P=0.40	-0.003 (-0.01, 0.004), P=0.40	
mI _{NAWM}	-0.1 (-0.14 , 0.03), P=0.22	-0.06 (-0.14, 0.02), P=0.16	0.008 (-0.14, 0.15), P=0.91	0.04 (-0.01, 0.09), P=0.14	0.04 (-0.01, 0.09), P=0.14	0.04 (-0.01, 0.09), P=0.14	-0.04 (-0.08, - 0.009), P=0.015	-0.04 (-0.08, - 0.009), P=0.015	-0.03 (-0.042, - 0.009), P=0.002	-0.03 (-0.042, - 0.009), P=0.002	-0.03 (-0.042, - 0.009), P=0.002	
mI _{NAGM}	-0.004 (-0.09, 0.09), P=0.94	0.02 (-0.03, 0.08), P=0.45	-0.02 (-0.11, 0.07), P=0.70	-0.015 (-0.05, 0.02), P=0.40	-0.015 (-0.05, 0.02), P=0.40	-0.015 (-0.05, 0.02), P=0.40	-0.02 (-0.04, 0.004), P=0.11	-0.02 (-0.04, 0.004), P=0.11	0.0006 (-0.01, 0.01), P=0.92	0.0006 (-0.01, 0.01), P=0.92	0.0006 (-0.01, 0.01), P=0.92	
mI/NAA _{NAWM} ratio	-1.68 (-3.05, -0.30), P=0.02	-1.08 (-1.95, -0.20), P= 0.02	0.29 (-0.93, 1.52), P=0.64	0.57 (0.015, 1.13), P=0.04	0.57 (0.015, 1.13), P=0.04	0.57 (0.015, 1.13), P=0.04	-0.52 (-0.82, -0.23), P=<0.001	-0.52 (-0.82, -0.23), P=<0.001	-0.23 (-0.41, -0.05), P=0.01	-0.23 (-0.41, -0.05), P=0.01	-0.23 (-0.41, -0.05), P=0.01	
mI/NAA _{NAGM} ratio	-0.78 (-1.69, 0.14), P=0.09	-0.13 (-0.75, 0.49), P=0.69	-0.02 (-0.81, 0.78), P=0.97	-0.25 (-0.64, 0.15), P=0.22	-0.25 (-0.64, 0.15), P=0.22	-0.25 (-0.64, 0.15), P=0.22	-0.06 (-0.27, 0.14), P=0.55	-0.06 (-0.27, 0.14), P=0.55	0.07 (-0.06, 0.20), P=0.29	0.07 (-0.06, 0.20), P=0.29	0.07 (-0.06, 0.20), P=0.29	
MWF _{NAWM}	-0.03 (-0.1, 0.03), P=0.33	n/a	-0.02 (-0.1, 0.05), P=0.48	n/a	0.003 (-0.02, 0.02), P=0.78	0.003 (-0.02, 0.02), P=0.78	n/a	n/a	n/a	n/a	n/a	

* Mean and 95% confidence intervals of longitudinal effect of metabolite predictors on longitudinal change in PBVC, EDSS and zMSFC expressed in annual slope per year are shown, based on single predictor models analysis (longitudinal mixed-effects models). Abbreviations:

PBVC = percentage of brain volume change; ml = myo-inositol; MWF = Myelin Water Fraction; NAA = *N*-acetyl aspartate; NAGM = MS normal-appearing grey matter; NAWM = MS normal-appearing white matter; EDSS = Expanded Disability Status Scale; MSFC = Multiple Sclerosis Functional Composite; n/a = not applicable. PBVC results are described in terms of annualized percent (%) change, whereas EDSS and zMSFC are given as annualized change in points (pts) score. Results are given for both preliminary and confirmatory studies using estimates from linear mixed effects models. Cells with statistically significant results at $\alpha = 0.05$ are highlighted in bold.

Table 4: Summary of imaging parameters tested as predictors in the confirmatory study. All MS subjects and MS subtypes are included

Abbreviations: SD = standard deviation; mM = millimoles per liter; NAA = *N*-acetyl-aspartate; ml

Predictors	All MS Mean \pm SD (n = 220)	CIS Mean \pm SD (n = 33)	RRMS Mean \pm SD (n = 164)	SPMS Mean \pm SD (n = 17)	PPMS Mean \pm SD (n = 6)
NAA _{NAWM} — mM	9.8 \pm 1.34	10.1 \pm 1.22	9.84 \pm 1.36	9.42 \pm 1.24	9.03 \pm 1.44
NAA _{NAGM} — mM	8.76 \pm 1.6	8.93 \pm 1.46	8.79 \pm 1.66	8.07 \pm 1.30	8.53 \pm 1.93
ml _{NAWM} — mM	3.92 \pm 0.69	3.93 \pm 0.59	3.90 \pm 0.72	3.93 \pm 0.64	3.92 \pm 0.69
ml _{NAGM} — mM	4.74 \pm 1.05	4.99 \pm 1.45	4.70 \pm 0.99	4.52 \pm 0.72	5.00 \pm 0.99
ml/NAA _{NAWM} — ratio	0.40 \pm 0.07	0.39 \pm 0.06	0.40 \pm 0.06	0.42 \pm 0.07	0.47 \pm 0.1
ml/NAA _{NAGM} — ratio	0.54 \pm 0.09	0.56 \pm 0.12	0.54 \pm 0.08	0.57 \pm 0.11	0.60 \pm 0.08

= myoinositol; NAGM = normal-appearing grey matter; NAWM = normal-appearing white matter; CIS = clinically isolated syndrome; RRMS = relapsing remitting MS; SPMS = secondary progressive MS; PPMS = primary progressive MS.

Appendix e-1

Material and Methods

Preliminary dataset

Spectroscopy predictors: The acquisitions had a phase-encoding matrix of 12x12x8 with an FOV of 120x120x80 mm resulting in a nominal voxel size of 1cm³. Chemical shift misregistration was reduced by prescribing a PRESS box larger than the region of interest (ROI, overpress) by a factor of 1.2 using 4 saturation bands to suppress signals arising from beyond the ROI. Metabolite contributions within each voxel were estimated by adjusting short echo time signals to a model function created from a prior knowledge basis set of metabolite signals according to the semi-parametric approach developed in HR-QUEST accounting for macromolecular contributions, and for NAA and ml T1 relaxation values estimated at 3T (T1 NAA_[WM]=1.37s and T1 NAA_[GM]=1.36s in healthy controls; T1 NAA_[WM]=1.31s and T1 NAA_[GM]=1.44s in MS subjects; T1 ml_[WM]=1.09s and T1 ml_[GM]=1.28s in healthy controls; T1 ml_[WM]=0.98s and T1 ml_[GM]=1.16s in MS subjects) using a similar method described previously.¹ Non-brain regions were removed from the anatomical images using a semi-automated brain extraction tool (FSL, www.fmrib.ox.ac.uk/fsl). T1-weighted three-dimensional inversion recovery spoiled gradient-echo (IR-SPGR) images were segmented into GM and WM compartments using a hidden Markov random field model with expectation maximization. The GM and WM maps were re-gridded to spectroscopy resolution and convolved with the point spread function for spectroscopic imaging to yield the percent GM and WM content within each spectroscopic voxel.² Manual lesion segmentation was performed on from 3D T1-weighted gradient-echo images. For patients, the voxels containing the manually segmented lesions were removed from the analysis. Moreover, the spectroscopic voxels were included in the linear fit only if their concentration estimates had estimated Cramer-Rao bounds within threshold values (10% for [NAA], [Cho] and [Cre], 30% for the [ml]).

Statistical Analysis

Mixed-effects models were initially fit with single predictors (each outcome versus each predictor). Subsequently, models with multiple predictors were fitted to determine independent additive value of predictors, e.g., combinations of multiple metabolites in NAWM, NAGM and MW_{NAWM}. Postulated models were based on clinical relevance and once the model was fitted, variables with no clinical or/and statistical significance were dropped. Clinical relevance was primarily based on biological plausibility and was used to define subsets of variables to consider as predictors (e.g. all GM metabolite predictors).

Many of the mixed-effects models were checked for assumptions of normality (via qq-plots) and they appeared reasonable with no extreme outliers. There were too many models examined to check the assumptions for every one of them. However, because many of the outcomes considered were inter-related, the checks performed on a subset of models provide some insurance against distributional violations in the remaining models.

Although we examine many differences and issues, we report nominal p-values, without adjustment for multiple testing. Adjustment would require that each result detract from the others, but there are clear biological relationships among many of the variables that we examine leading to correlated tests (in contrast to the assumed independence of tests in conventional multiple testing procedures), and these permit coherent sets of findings to reinforce each other rather than detract from one another. Thus, multiple comparison adjustment would do exactly the wrong thing in this situation³⁻⁴. We therefore rely on scientific judgment and study design rather than formal adjustment methods to indicate where caution is warranted despite findings with $P < 0.05$. Finally, because we are validating all results on an independent dataset the potential for false positive results is greatly diminished.

Results

Individual metabolites as predictors of brain volume and clinical outcomes from the confirmatory dataset (n=220)

Using single predictor analyses, we did not observe a statistically significant influence of ml or NAA on brain volume loss (Table 3). However, there were additive longitudinal effects of ml and NAA in NAWM on PBVC over the course of the study [-0.1 annual slope; 95% CI: -0.19 to -0.008; $p = 0.03$ and 0.05%; 95% CI: -0.001 to 0.096; $p = 0.06$ respectively], but not in NAGM as we had observed in the preliminary dataset. Longitudinal changes in MSFC were predicted by ml levels in NAWM [-0.03 point annually; 95% CI: -0.042 to -0.009; $p = 0.002$]. When combined additively in a multiple predictor analysis, NAA [-0.31; 95% CI: -0.59 to -0.04; $p = 0.03$] and ml [0.62; 95% CI: 0.11 to 1.15; $p = 0.02$] from NAWM predicted sustained EDSS progression.

References

1. Ratiney H, Noworolski SM, Sdika M, et al. Estimation of metabolite T1 relaxation times using tissue specific analysis, signal averaging and bootstrapping from magnetic resonance spectroscopic imaging data. MAGMA 2007;20:143-155.

-
-
-
2. Zhang Y, Brady M, Smith S. Segmentation of brain MR images through a hidden Markov random field model and the expectation-maximization algorithm. *IEEE Trans Med Imaging* 2001;20:45-57.
3. Bacchetti P. Peer review of statistics in medical research: the other problem. *BMJ* 2002;324:1271-1273.
4. Perneger TV. What's wrong with Bonferroni adjustments. *BMJ* 1998;316:1236-1238.

Table e-1: Comparison of clinical and spectroscopy data from both datasets

	Preliminary dataset Mean \pm SD (n = 59)	Confirmatory dataset Mean \pm SD (n = 220)	P Value
Age — y	43.2 \pm 9.5	42.4 \pm 9.5	0.61
Disease duration — y	10.4 \pm 9.6	9.3 \pm 9.3	0.97
EDSS — points	1.5 \pm 1.2	2.2 \pm 1.5	0.006
MSFC — z-score	0.1 \pm 0.5	0.1 \pm 0.7	0.65
NAA _{NAWM} — mM	7.7 \pm 1.4	9.8 \pm 1.3	<0.001
NAA _{NAGM} — mM	9.4 \pm 2.0	8.7 \pm 1.6	0.01
ml _{NAWM} — mM	2.6 \pm 0.5	3.9 \pm 0.7	<0.001
ml _{NAGM} — mM	4.0 \pm 1.0	4.7 \pm 1.1	<0.001
ml/NAA _{NAWM} — ratio	0.34 \pm 0.06	0.40 \pm 0.07	<0.001
ml/NAA _{NAGM} — ratio	0.44 \pm 0.11	0.54 \pm 0.09	<0.001

Abbreviations: SD = standard deviation; mM = millimoles per liter; NAA = *N*-acetyl-aspartate; ml = myoinositol; NAGM = normal-appearing grey matter; NAWM = normal-appearing white matter.
P values are derived from Wilcoxon Rank Sum test.

VIII. Discusión



La EM es una enfermedad extremadamente heterogénea tanto en su forma de presentación como en su evolución o respuesta terapéutica. Mientras algunos pacientes van a presentar una discapacidad leve a lo largo de décadas, otros presentan una evolución tórpida acumulando una gran discapacidad con alteraciones motoras, sensitivas, del equilibrio y cognitivas, en un plazo corto de tiempo. Los eventos fisiopatológicos subyacentes responsables de la discapacidad son poco conocidos aunque se postula que depende de un equilibrio entre daño y reparación y que probablemente la discapacidad persistente o mantenida esté en relación con un daño de predominio axonal (Bjartmar *et al.*, 2000; Tallantyre *et al.*, 2010). Dada la heterogeneidad de la enfermedad, son muchos los estudios que han buscado factores predictivos determinantes de una u otra evolución, con la finalidad de poder seleccionar aquellos pacientes que se pueden beneficiar, por ejemplo, de tratamientos más agresivos pero que llevan más efectos adversos, y no someter al mismo riesgo a todos los pacientes. Sin embargo, las variables clínicas identificadas en estudios de historia natural de la enfermedad han mostrado que tienen una utilidad muy limitada, y de ahí la búsqueda y desarrollo de biomarcadores que nos permitan predecir de forma más fiable, el pronóstico o la respuesta terapéutica.

En este sentido, la neuroimagen ha supuesto un gran avance por su contribución tanto al diagnóstico como a la evaluación del pronóstico de la enfermedad. Sin embargo, la identificación y cuantificación de las lesiones cerebrales por sí misma sólo se asocia de forma parcial con la discapacidad clínica del paciente. Por ello, el objetivo de esta tesis ha sido el de caracterizar mejor a través de marcadores de neuroimagen y electrofisiológicos las alteraciones asociadas a la presencia de discapacidad física y/o cognitiva, y su contribución en predecir la evolución de la enfermedad.

La neuroimagen permite detectar de forma incruenta las lesiones presentes en la SB de los pacientes. Algunos patrones de lesiones en RM pueden sugerir un sustrato patológico concreto, y así se ha descrito la existencia de lesiones con un borde hipointenso visible en secuencias T2 causado por el acúmulo de sustancias paramagnéticas como los macrófagos cargados de hierro o radicales libres y que podrían pertenecer al patrón I/II en anatomía patológica (Lucchinetti *et al.*, 2000; Lucchinetti *et al.*, 2003; Schwartz *et al.*, 2006). Estas lesiones suelen presentar de forma mayoritaria una captación de gadolinio en anillo (Bruck *et al.*, 2001; Abou Zeid *et al.*, 2012), y se han descrito principalmente en series de pacientes de EM con lesiones pseudotumorales (Bruck *et al.*, 2001; Schwartz *et al.*, 2006; Lucchinetti *et al.*, 2008). Sin embargo, su prevalencia y significado clínico en pacientes con EM seguidos de

DISCUSIÓN

forma rutinaria en la práctica clínica no era bien conocida, y este fue el objetivo del primer trabajo de esta tesis.

Así, en el **primer trabajo** evaluamos de forma retrospectiva 580 RM pertenecientes a 257 pacientes con EM seguidos en la Unidad de EM del Hospital Clínic según la práctica clínica habitual. En el estudio identificamos que las lesiones con borde hipointenso en T2 y las lesiones captantes de gadolinio en forma de anillo estaban presentes en el 9% y 12% de los pacientes con EM, respectivamente, y que con frecuencia estos dos patrones aparecían de forma independiente. Por tanto, la frecuencia de las lesiones con borde hipointenso en T2 en una población general de EM era mucho menor a la descrita en series de pacientes con lesiones pseudotumorales de EM en las que se detectaban hasta en el 30-53% de los pacientes (Lucchinetti *et al.*, 2008; Abou Zeid *et al.*, 2012). Otro hecho diferencial fue la menor asociación a captación de gadolinio en anillo, pues sólo el 40% de las lesiones con borde hipointenso en T2 presentaban este patrón de captación, y el que un 12.5% de estas lesiones presentaran una captación homogénea de gadolinio. De forma interesante, un 47.5% de las lesiones no presentaba captación de gadolinio, lo que indicaría que este borde hipointenso persiste en fases más crónicas de la lesión cuando ya no es evidente la rotura de la BHE. En este sentido, un estudio piloto reciente que utilizó la imagen de susceptibilidad magnética, que es más sensible en la detección de sustancias paramagnéticas o acúmulo de hierro, identificó lesiones con un borde hipointenso en imagen de fase que persistía tras un seguimiento de 31 meses (Bian *et al.*, 2013). Este dato iría a favor de que el borde hipointenso puede permanecer en una fase crónica de la lesión traduciendo la persistencia de macrófagos cargados de hierro. Aunque en nuestro trabajo algunas lesiones mostraban el borde hipointenso a los 3.5 o 13 meses de seguimiento, no nos fue posible concluir sobre este aspecto por la limitación en el bajo número de casos con seguimiento a largo plazo, dada la naturaleza retrospectiva del estudio.

Las lesiones captantes de gadolinio en anillo, con o sin borde hipointenso en T2 se identificaron en el 12% de los pacientes de la presente cohorte. Si bien estudios previos asociaban la captación en forma de anillo a una mayor destrucción tisular que aquellas lesiones que tenían una captación homogénea de contraste (Morgen *et al.*, 2001), estudios más recientes indican que ambos patrones de captación podrían representar un estadio distinto de un proceso patogénico común más que un tipo distinto de lesión (Davis *et al.*, 2010; Gaitan *et al.*, 2011). Es posible que este patrón de captación esté reflejando una inflamación masiva y desmielinización perilesional, lo cual explicaría que pueda detectarse una alteración de la

difusión de las moléculas de agua en el borde (Abou Zeid *et al.*, 2012) similar a lo que detectamos en una de las lesiones descritas en nuestro trabajo.

En los pacientes con EMPP no identificamos ni lesiones con borde hipointenso en T2 ni captantes de gadolinio en anillo. Aunque el número de pacientes con esta forma de EM era bajo en nuestro estudio, este dato iría a favor de que en este tipo de pacientes la inflamación focal está menos presente que la inflamación difusa o neurodegeneración (Filippi *et al.*, 2012).

Al analizar el significado clínico de la presencia de estas lesiones, observamos que las lesiones con borde hipointenso en T2 no parecían asociarse a una evolución clínica distinta. Sin embargo, la presencia de lesiones con captación de gadolinio en anillo se asociaba a un peor pronóstico. Así los pacientes con lesiones captantes en anillo alcanzaron una discapacidad elevada en menos tiempo, requiriendo el uso de un apoyo (EDSS de 6.0 puntos) en una media de 4.4 años respecto a 13.4 años en aquellos pacientes sin este tipo de lesiones. Estos datos concuerdan con trabajos previos que han asociado estas lesiones con la discapacidad presente y futura y la aparición de nuevos brotes (Morgen *et al.*, 2001). Por tanto, las lesiones captantes de gadolinio en anillo pueden estar caracterizando un subtipo agresivo de enfermedad y su detección puede ser de utilidad para identificar aquellos pacientes con más riesgo de progresión de la discapacidad a corto plazo.

Aunque las técnicas de RM convencionales utilizadas en el primer trabajo permitan identificar lesiones de la SB, la información que aportan acerca de la naturaleza de estas lesiones y del daño en el tejido cerebral de apariencia normal es muy limitada. Sin embargo, las técnicas de RM avanzada, son capaces de aportar información sobre la SBAN y la SG (Bakshi *et al.*, 2008; Ceccarelli *et al.*, 2012) parecen correlacionar mejor con la discapacidad. Además permiten realizar diferentes abordajes capaces de extraer una información más precisa de la relación existente entre las alteraciones en la neuroimagen y la discapacidad (Ceccarelli *et al.*, 2012). Por ejemplo, el uso de medidas compuestas de RM combinando distintos tipos de información (ej. presencia de lesiones y daño microestructural) o el abordaje regional que permita relacionar regiones o tractos específicos con funciones concretas. A través del uso de estos métodos, estudios previos han sugerido que la afectación de la SB, tanto por la presencia de lesiones macroscópicas como por un daño microestructural, puede producir una desconexión entre estructuras cerebrales corticales y subcorticales que explicarían, en parte, la discapacidad física y cognitiva en los pacientes (Dineen *et al.*, 2009; Filippi and Agosta, 2010; Ceccarelli *et al.*, 2012). La utilización de estas aproximaciones a través de RM avanzada fue la base para profundizar en estos aspectos en la presente tesis.

Así, en el **segundo trabajo**, se eligió una estructura específica, el cuerpo caloso (CC) que es la mayor comisura cerebral y diana frecuente de lesiones, para determinar la relación entre el daño de esta estructura y la discapacidad física y cognitiva en la EM. En el estudio se incluyeron 21 paciente, todos ellos con una forma remitente-recidivante de la enfermedad, y con una discapacidad leve-moderada, intentando asegurar una muestra que fuera lo más homogénea posible. Como era de esperar, observamos alteraciones estructurales (disminución de volumen) y microestructurales (alteración de los valores de DTI) en el CC de los pacientes. Una atrofia del CC que podría explicarse por la presencia de lesiones (Barkhof *et al.*, 1998), pero también por un daño directo de la integridad microestructural o secundario a una degeneración Walleriana (Evangelou *et al.*, 2000), lo cual estaría en concordancia con la correlación encontrada entre volumen del CC y el volumen de lesiones en la SB. Además, identificamos una alteración en la conducción interhemisférica inhibitoria que conecta las cortezas cerebrales motoras de ambos hemisferios a través del estudio del iSP (Hoppner *et al.*, 1999; Lenzi *et al.*, 2007) y que estas alteraciones correlacionaban con los datos de atrofia y daño microestructural evaluado a través del DTI, pero no con el volumen lesional. Vale la pena remarcar que los pacientes que no presentaban lesiones focales en el CC, también presentaban una alteración del iSP, todo ello indicando que se requiere un daño más extenso que el producido por las lesiones focales para que se produzca una alteración de la conducción interhemisférica.

La observación en nuestro estudio de que el daño estructural /microestructural del CC se asocia a discapacidad física y, sobretodo, cognitiva, refuerza el papel relevante de esta estructura en la EM, tal como habían puesto de manifiesto otros estudios utilizando diferentes técnicas y aproximaciones (Pelletier *et al.*, 2001; Lin *et al.*, 2008; Mesaros *et al.*, 2009; Kale *et al.*, 2010; Ozturk *et al.*, 2010; Yaldizli *et al.*, 2010; Sigal *et al.*, 2012). De hecho, demostramos por primera vez que la integridad de la conducción interhemisférica inhibitoria del CC está asociada al rendimiento cognitivo en tests de memoria visual y de funciones ejecutivas y, por tanto, que la integridad del CC tanto en términos de estructura como de función, es importante para el mantenimiento de las funciones cognitivas.

En definitiva, los datos obtenidos en este estudio a través de la utilización de técnicas de RM no convencional y electrofisiología apoyan la hipótesis de que en la EM existe una desconexión de áreas cerebrales por afectación de tractos de la SB (Catani and ffytche, 2005; Dineen *et al.*, 2009) responsables, en parte, de la disfunción física y sobretodo de la cognitiva.

Sin embargo, el daño de la SB por sí sólo no puede explicar de forma completa los déficits neurológicos y, en especial, la disfunción cognitiva de los pacientes con EM. En los últimos años numerosos trabajos han destacado la importancia del daño de la SG en el proceso patológico de la enfermedad ya desde fases tempranas de la enfermedad (Geurts *et al.*, 2012; Horakova *et al.*, 2012). Este avance ha sido posible gracias a las nuevas técnicas de RM que han mejorado la sensibilidad para detectar la afectación de la SG (Pirko *et al.*, 2007) y han puesto de manifiesto su posible asociación con la discapacidad física y cognitiva (Dalton *et al.*, 2004; Fisher *et al.*, 2008; Fisniku *et al.*, 2008; Calabrese *et al.*, 2010).

Dado que el daño microestructural de la SG podría contribuir a explicar los déficits cognitivos el **tercer trabajo** de esta tesis tuvo el objetivo de determinar el impacto del daño de la SG, evaluado a través del DTI, en la alteración cognitiva en pacientes con EM en fases tempranas de la enfermedad, y su relación con el daño microestructural de la SBAN y la presencia de lesiones. Para ello utilizamos métodos no-apriorísticos, primero para caracterizar la distribución topográfica del daño de SG y SB, y posteriormente para identificar las principales medidas de neuroimagen que se correlacionan con el rendimiento de funciones cognitivas específicas.

En el presente trabajo los pacientes incluidos tenían una forma remitente-recidivante de EM y presentaban una discapacidad física y cognitiva baja (31,3% de los pacientes presentan al menos un test neuropsicológico anormal, pero sólo un 4.5% tenían 2 o más tests alterados y se podían considerar cognitivamente afectos). A pesar de la baja discapacidad, los pacientes presentaban alteraciones de la integridad microestructural en múltiples regiones de la SG (Ceccarelli *et al.*, 2008) y en la mayoría de tractos de la SBAN (Yu *et al.*, 2012). Las medidas de DTI más ampliamente alteradas eran las que reflejaban un daño predominantemente por desmielinización (Song *et al.*, 2003; Song *et al.*, 2005), mientras que el daño axonal medido con la difusividad axial estaba presente en regiones más circunscritas de la SG y en algunos tractos de SG. Además, el daño microestructural se extendía más allá de las lesiones visibles a través de la RM convencional. Estos datos están en consonancia con estudios patológicos que demuestran que la EM es una enfermedad que afecta de forma difusa al SNC, y que estas alteraciones ya están presentes en fases tempranas de la enfermedad (Filippi *et al.*, 2012).

A pesar de la constatación de que existe una alteración difusa de la microestructura, observamos que las regiones cerebrales donde la integridad microestructural se asociaba con el rendimiento cognitivo eran distintas en función del dominio cognitivo evaluado. Así, la integridad de la SG en regiones específicas se asociaba con el rendimiento en tests cognitivos concretos, como por ejemplo el giro angular, tálamo o estructuras mediales temporales con la

memoria episódica verbal. Resultados que concuerdan con las teorías actuales de las bases neurobiológicas de las funciones cognitivas (Squire, 2004; Forn *et al.*, 2011; Wolk and Dickerson, 2011). Además, en los tests de memoria episódica verbal las asociaciones topográficas cambiaban según el subtest utilizado. Esto coincide con trabajos que defienden que una correcta memoria episódica implica sustratos anatómicos distintos según el estadio del procesamiento de la información (Wolk and Dickerson, 2011). Asimismo, también el daño microestructural en algunos tractos o la presencia de lesiones en localizaciones concretas se asoció con el rendimiento cognitivo, similar a estudios previos (Dineen *et al.*, 2009; Sepulcre *et al.*, 2009; Yu *et al.*, 2012). Algunos de estos tractos coincidían anatómicamente con las regiones de SG relevantes en la misma función cognitiva, lo cual refuerza los resultados obtenidos con las distintas técnicas. Además permitió definir algunas redes relacionadas con la memoria o con las funciones ejecutivas que comprendían regiones corticales occipitales y temporales izquierdas con el fascículo longitudinal inferior o el fascículo fronto-occipital. Finalmente, la alteración de la integridad del CC en los pacientes y su asociación con la memoria episódica verbal, visual y con funciones ejecutivas coincide con los resultados encontrados en el trabajo número dos de esta tesis.

Para evaluar el impacto de la alteración de la SG y SB en el rendimiento cognitivo, realizamos un análisis de regresión lineal múltiple con los valores de integridad microestructural en la SG, en la SBAN y el volumen de las lesiones. Estos valores provenían de las regiones obtenidas del análisis de correlación entre integridad tisular o lesiones y rendimiento cognitivo. El modelo explicaba el 36-51% de la varianza en los tests de memoria y atención. Sin embargo, la integridad de la SG sólo aportaba algo menos de un 5% a la varianza en los tests cognitivos. Por tanto, nuestro estudio ponía de manifiesto que en pacientes en fase precoz de la enfermedad y con baja discapacidad cognitiva, los principales elementos asociados a la cognición son la integridad de la SBAN y la presencia de lesiones de SB.

Este hallazgo no contradice la importancia del papel de la SG en la discapacidad, tal como han defendido múltiples trabajos sobretodo basados en la atrofia (Geurts *et al.*, 2012; Horakova *et al.*, 2012), pues cuando el análisis lo limitamos a la SG, pudimos observar que la integridad de la SG explicaba el 29-38% de la varianza de los test cognitivos. Por tanto, nuestro trabajo apunta a que en las fases iniciales de la enfermedad cuando la enfermedad se caracteriza por brotes secundarios a lesiones focales de SB la influencia de la patología de SG sobre la cognición podría ser más limitada que la ocasionada por el daño de la SB.

En definitiva, estos hallazgos junto con los del trabajo número dos van a favor de que existe un mecanismo de desconexión múltiple, por afectación de un gran número de tractos, junto con un daño de SG, que están causando la disfunción cognitiva en los pacientes con EM. Además, demuestra que el uso del DTI como marcador de la integridad microestructural del tejido cerebral es útil para conocer los efectos de la enfermedad sobre el SNC y sus consecuencias clínicas.

La RM avanzada también nos permite estudiar los mecanismos de destrucción y reparación, analizar el daño axonal y la astrogliosis, patología que forma parte de los principales eventos de la EM (Filippi *et al.*, 2012). Así, podemos medir metabolitos como el NAA y el ml, que son marcadores de integridad axonal y astrogliosis, respectivamente, mediante espectroscopia. Además, el MWF obtenido a través del estudio de la relaxometría en T2 puede informar sobre la integridad de la mielina (Oh *et al.*, 2007; Laule *et al.*, 2008) probablemente de una forma más específica que otras técnicas como el DTI o la transferencia de magnetización pero con mayores limitaciones técnicas (Bakshi *et al.*, 2008). Trabajos previos han encontrado correlaciones entre el NAA (De Stefano *et al.*, 1998; Fu *et al.*, 1998; Sarchielli *et al.*, 1999; De Stefano *et al.*, 2001; Ruiz-Pena *et al.*, 2004; Sastre-Garriga *et al.*, 2005) o ml (Chard *et al.*, 2002) y la presencia de atrofia cerebral o discapacidad en estudios transversales en general limitados por un pequeño tamaño muestral. Sin embargo, la capacidad de predecir la evolución de la enfermedad de estos marcadores es poco conocida (Wattjes *et al.*, 2008; Sbardella *et al.*, 2011).

Por ello, en el **trabajo número cuatro** de esta tesis, se quisieron identificar qué eventos patológicos preceden a la progresión de la enfermedad a medio plazo y evaluar su capacidad de predicción de la progresión de la discapacidad y de la atrofia cerebral. Para ello utilizamos el NAA y el ml como marcadores de daño axonal y astrogliosis, respectivamente, cuantificados en la SBAN y en la SG y el MWF en la SBAN como marcador de desmielinización, y se analizó su utilidad en un grupo preliminar de pacientes y controles. Observamos que el ml y NAA en la SBAN parecían tener un efecto sobre la atrofia y que el NAA era capaz de modular la influencia de ml sobre dicha atrofia. De ello surgió la idea de utilizar una ratio combinando ambos metabolitos, la ratio de ml/NAA. Dicha ratio medida en SBAN fue capaz de predecir la evolución de la atrofia cerebral a lo largo de 4 años y la evolución de la discapacidad. Sin embargo las medidas de los metabolitos en SG y el MWF no se asociaron con la evolución de la enfermedad.

Para confirmar los hallazgos se realizó el mismo análisis con el ratio de ml/NAA en un grupo distinto de pacientes con un mayor número de casos (220) incluyendo diferentes

DISCUSIÓN

fenotipos de pacientes. En este estudio confirmatorio el incremento de la ratio de mI/NAA en la SBAN también fue capaz de predecir el aumento de la discapacidad y la atrofia en los siguientes 4 años.

Estos resultados ponen de manifiesto que existe una importante relación entre la progresión de la enfermedad y la presencia de daño axonal y astrogliosis en la SB. Además apoyarían que los astrocitos puedan ejercer un efecto deletéreo a través de la promoción de la inflamación y desmielinización así como la formación de una cicatriz glial que dificulte la remielinización y el crecimiento axonal (Moore *et al.*, 2011; Cambron *et al.*, 2012). Un efecto, no obstante, que puede ser más complejo, pues también se sabe que la acción de los astrocitos sobre la migración, proliferación y diferenciación de los oligodendrocitos (Williams *et al.*, 2007; Nair *et al.*, 2008) puede ayudar a crear un ambiente permisivo para la remielinización. En cualquier caso, nuestro estudio refuerza la idea de trabajos previos de que los cambios en marcadores de astrogliosis preceden al daño axonal y al desarrollo de atrofia (Kirov *et al.*, 2009).

Además de informar sobre los eventos subyacentes al futuro desarrollo de discapacidad y pérdida de volumen cerebral, la importancia de este trabajo radica en que identifica un nuevo marcador, la ratio de mI/NAA en la SBAN, capaz de predecir la evolución de la enfermedad a medio plazo. Es importante tener en cuenta que una de las ventajas que ofrece este marcador, en comparación con la obtención de valores absolutos de metabolitos, es que es más fácilmente medible lo que puede facilitar su aplicación en estudios más amplios en que se involucren distintos centros (Narayana, 2005; De Stefano *et al.*, 2007). Por el contrario, la potencia del efecto predictor es baja, lo cual puede limitar su uso como biomarcador predictivo a nivel individual.

A pesar de que el MWF no fuera capaz de predecir la evolución de la enfermedad, esto no invalida la importancia de la desmielinización en la evolución de la discapacidad y la atrofia. Es probable que este hecho se haya visto influenciado por las limitaciones técnicas de la secuencia utilizada para la adquisición del MWF. El uso de mejoras técnicas que aumenten la sensibilidad a los cambios en la mielina (Guo *et al.*, 2012; Kitzler *et al.*, 2012) puede ayudar a confirmar la importancia de este evento en la progresión de la enfermedad en futuros estudios. Algo parecido ocurre con los marcadores de espectroscopia en la SG, donde la propia naturaleza de esta región (bajo grosor cortical y posible efecto de volumen parcial) puede hacer menos fiable la cuantificación de los metabolitos.

En definitiva, los estudios incluidos en esta tesis han servido para profundizar en el conocimiento de la fisiopatología de los condicionantes de la discapacidad, y en el avance en la búsqueda de marcadores útiles para evaluar y predecir la discapacidad en la esclerosis múltiple. Así, hemos evidenciado que la inflamación evaluada a través de la presencia de lesiones captantes de gadolinio en anillo puede ser un indicador de peor pronóstico. Además, el daño microestructural de la sustancia gris y blanca medible a través de DTI, se asocia a discapacidad física y, en especial, a disfunción cognitiva, y que existe un mecanismo de desconexión entre estructuras corticales y subcorticales debido no sólo a la presencia de lesiones sino también a un daño difuso que participa en el desarrollo de las alteraciones neurológicas. Por último, el daño axonal y la astrogliosis en la sustancia blanca de apariencia normal son elementos que participan en la progresión de la enfermedad, y que su medida a través de la ratio de ml/NAA es capaz de predecir la evolución de la discapacidad y la atrofia a lo largo de los siguientes 4 años.



IX. Conclusiones



1. Las lesiones con un borde hipointenso en secuencias potenciadas en T2 y las lesiones captantes de gadolinio en anillo se presentan en un pequeño porcentaje de pacientes con EM (9 y 12% respectivamente), y ambos patrones pueden aparecer de forma independiente. Mientras que las lesiones con borde hipointenso no se asocian a una peor evolución clínica, las lesiones captantes de gadolinio en anillo incrementan el riesgo de progresión de la discapacidad, y por tanto se asocian a un peor pronóstico.
2. El cuerpo calloso de los pacientes con EM presenta alteraciones tanto en su estructura/microestructura como en su función inhibitoria de la conducción entre ambas cortezas motoras. Dichas alteraciones se asocian con la discapacidad física y sobretodo con un peor rendimiento en tests de memoria y funciones ejecutivas.
3. Desde fases tempranas de la EM existe una alteración extensa de la microestructura del tejido cerebral. La integridad de la sustancia gris y de la sustancia blanca de apariencia normal y la presencia de lesiones en regiones específicas se asocian con el rendimiento de funciones cognitivas concretas. La alteración en la integridad de la sustancia blanca y la presencia de lesiones visibles, más que la alteración de la integridad de la sustancia gris, parecen ser los principales contribuyentes a la disfunción cognitiva en pacientes en la fase precoz de la enfermedad.
4. El daño axonal junto con la astrogliosis en la sustancia blanca de apariencia normal son eventos importantes en el desarrollo de la discapacidad y la atrofia cerebral. La ratio de mI/NAA obtenido a través de espectroscopia es capaz de predecir la evolución de la discapacidad y de la atrofia cerebral a medio plazo.



X. Bibliografía



Abou Zeid N, Pirko I, Erickson B, et al. Diffusion-weighted imaging characteristics of biopsy-proven demyelinating brain lesions. *Neurology* 2012; 78: 1655-62.

Awad A, Hemmer B, Hartung HP, Kieseier B, Bennett JL, Stuve O. Analyses of cerebrospinal fluid in the diagnosis and monitoring of multiple sclerosis. *J Neuroimmunol* 2010; 219: 1-7.

Bakshi R, Thompson AJ, Rocca MA, et al. MRI in multiple sclerosis: current status and future prospects. *Lancet Neurol* 2008; 7: 615-25.

Barkhof F, Simon JH, Fazekas F, et al. MRI monitoring of immunomodulation in relapse-onset multiple sclerosis trials. *Nat Rev Neurol* 2012; 8: 13-21.

Barkhof FJ, Elton M, Lindeboom J, et al. Functional correlates of callosal atrophy in relapsing-remitting multiple sclerosis patients. A preliminary MRI study. *J Neurol* 1998; 245: 153-8.

Beaulieu C, Fenrich FR, Allen PS. Multicomponent water proton transverse relaxation and T2-discriminated water diffusion in myelinated and nonmyelinated nerve. *Magn Reson Imaging* 1998; 16: 1201-10.

Bejarano B, Bianco M, Gonzalez-Moron D, et al. Computational classifiers for predicting the short-term course of Multiple sclerosis. *BMC Neurol* 2011; 11: 67.

Benedict RH, Bruce JM, Dwyer MG, et al. Neocortical atrophy, third ventricular width, and cognitive dysfunction in multiple sclerosis. *Arch Neurol* 2006; 63: 1301-6.

Benedict RH, Cookfair D, Gavett R, et al. Validity of the minimal assessment of cognitive function in multiple sclerosis (MACFIMS). *J Int Neuropsychol Soc* 2006; 12: 549-58.

Benedict RH, Hulst HE, Bergsland N, et al. Clinical significance of atrophy and white matter mean diffusivity within the thalamus of multiple sclerosis patients. *Mult Scler* 2013.

Benedict RH, Zivadinov R. Risk factors for and management of cognitive dysfunction in multiple sclerosis. *Nat Rev Neurol* 2011; 7: 332-42.

Bian W, Harter K, Hammond-Rosenbluth KE, et al. A serial in vivo 7T magnetic resonance phase imaging study of white matter lesions in multiple sclerosis. *Mult Scler* 2013; 19: 69-75.

Bielekova B, Martin R. Development of biomarkers in multiple sclerosis. *Brain* 2004; 127: 1463-78.

BIBLIOGRAFÍA

Bjartmar C, Kidd G, Mork S, Rudick R, Trapp BD. Neurological disability correlates with spinal cord axonal loss and reduced N-acetyl aspartate in chronic multiple sclerosis patients. *Ann Neurol* 2000; 48: 893-901.

Bosca I, Villar LM, Coret F, et al. Response to interferon in multiple sclerosis is related to lipid-specific oligoclonal IgM bands. *Mult Scler* 2010; 16: 810-5.

Bruck W, Neubert K, Berger T, Weber JR. Clinical, radiological, immunological and pathological findings in inflammatory CNS demyelination--possible markers for an antibody-mediated process. *Mult Scler* 2001; 7: 173-7.

Cadavid D, Kim S, Peng B, et al. Clinical consequences of MRI activity in treated multiple sclerosis. *Mult Scler* 2011; 17: 1113-21.

Calabrese M, Agosta F, Rinaldi F, et al. Cortical lesions and atrophy associated with cognitive impairment in relapsing-remitting multiple sclerosis. *Arch Neurol* 2009; 66: 1144-50.

Calabrese M, Filippi M, Gallo P. Cortical lesions in multiple sclerosis. *Nat Rev Neurol* 2010; 6: 438-44.

Calabrese M, Poretti V, Favaretto A, et al. Cortical lesion load associates with progression of disability in multiple sclerosis. *Brain* 2012; 135: 2952-61.

Calabrese M, Rinaldi F, Mattisi I, et al. Widespread cortical thinning characterizes patients with MS with mild cognitive impairment. *Neurology* 2010; 74: 321-8.

Calabrese P. Neuropsychology of multiple sclerosis--an overview. *J Neurol* 2006; 253 Suppl 1: I10-5.

Cambron M, D'Haeseleer M, Laureys G, Clinckers R, Debruyne J, De Keyser J. White-matter astrocytes, axonal energy metabolism, and axonal degeneration in multiple sclerosis. *J Cereb Blood Flow Metab* 2012; 32: 413-24.

Camp SJ, Stevenson VL, Thompson AJ, et al. A longitudinal study of cognition in primary progressive multiple sclerosis. *Brain* 2005; 128: 2891-8.

Catani M, ffytche DH. The rises and falls of disconnection syndromes. *Brain* 2005; 128: 2224-39.

Ceccarelli A, Bakshi R, Neema M. MRI in multiple sclerosis: a review of the current literature. *Curr Opin Neurol* 2012; 25: 402-9.

Ceccarelli A, Rocca MA, Falini A, et al. Normal-appearing white and grey matter damage in MS. A volumetric and diffusion tensor MRI study at 3.0 Tesla. *J Neurol* 2007; 254: 513-8.

Ceccarelli A, Rocca MA, Pagani E, et al. The topographical distribution of tissue injury in benign MS: a 3T multiparametric MRI study. *Neuroimage* 2008; 39: 1499-509.

Cohen JA, Reingold SC, Polman CH, Wolinsky JS. Disability outcome measures in multiple sclerosis clinical trials: current status and future prospects. *Lancet Neurol* 2012; 11: 467-76.

Comabella M, Fernandez M, Martin R, et al. Cerebrospinal fluid chitinase 3-like 1 levels are associated with conversion to multiple sclerosis. *Brain* 2010; 133: 1082-93.

Comabella M, Racke MK. New technologies for biomarker discovery in multiple sclerosis. *J Neuroimmunol* 2012; 248: 1.

Comi G, Filippi M. Clinical trials in multiple sclerosis: methodological issues. *Curr Opin Neurol* 2005; 18: 245-52.

Compston A, Coles A. Multiple sclerosis. *Lancet* 2008; 372: 1502-17.

Confavreux C, Vukusic S. Natural history of multiple sclerosis: a unifying concept. *Brain* 2006; 129: 606-16.

Cook SD. Handbook of multiple sclerosis. 4th ed. New York ; London: Taylor & Francis; 2006.

Chard DT, Griffin CM, McLean MA, et al. Brain metabolite changes in cortical grey and normal-appearing white matter in clinically early relapsing-remitting multiple sclerosis. *Brain* 2002; 125: 2342-52.

Chiaravalloti ND, DeLuca J. Cognitive impairment in multiple sclerosis. *Lancet Neurol* 2008; 7: 1139-51.

Dalton CM, Chard DT, Davies GR, et al. Early development of multiple sclerosis is associated with progressive grey matter atrophy in patients presenting with clinically isolated syndromes. *Brain* 2004; 127: 1101-7.

Davis M, Auh S, Riva M, et al. Ring and nodular multiple sclerosis lesions: a retrospective natural history study. *Neurology* 2010; 74: 851-6.

BIBLIOGRAFÍA

De Stefano N, Filippi M, Miller D, et al. Guidelines for using proton MR spectroscopy in multicenter clinical MS studies. *Neurology* 2007; 69: 1942-52.

De Stefano N, Giorgio A, Battaglini M, et al. Assessing brain atrophy rates in a large population of untreated multiple sclerosis subtypes. *Neurology* 2010; 74: 1868-76.

De Stefano N, Matthews PM, Fu L, et al. Axonal damage correlates with disability in patients with relapsing-remitting multiple sclerosis. Results of a longitudinal magnetic resonance spectroscopy study. *Brain* 1998; 121 (Pt 8): 1469-77.

De Stefano N, Narayanan S, Francis GS, et al. Evidence of axonal damage in the early stages of multiple sclerosis and its relevance to disability. *Arch Neurol* 2001; 58: 65-70.

Degenhardt A, Ramagopalan SV, Scalfari A, Ebers GC. Clinical prognostic factors in multiple sclerosis: a natural history review. *Nat Rev Neurol* 2009; 5: 672-82.

Dineen RA, Vilisaar J, Hlinka J, et al. Disconnection as a mechanism for cognitive dysfunction in multiple sclerosis. *Brain* 2009; 132: 239-49.

Dobson R, Ramagopalan S, Davis A, Giovannoni G. Cerebrospinal fluid oligoclonal bands in multiple sclerosis and clinically isolated syndromes: a meta-analysis of prevalence, prognosis and effect of latitude. *J Neurol Neurosurg Psychiatry* 2013; 84: 909-14.

Evangelou N, Konz D, Esiri MM, Smith S, Palace J, Matthews PM. Regional axonal loss in the corpus callosum correlates with cerebral white matter lesion volume and distribution in multiple sclerosis. *Brain* 2000; 123 (Pt 9): 1845-9.

Fernandez O, Arroyo-Gonzalez R, Rodriguez-Antiguedad A, et al. [Biomarkers in multiple sclerosis]. *Rev Neurol* 2013; 56: 375-90.

Fernandez V, Valls-Sole J, Relova JL, et al. Recommendations for the clinical use of motor evoked potentials in multiple sclerosis. *Neurologia* 2012. doi: 10.1016/j.nrl.2012.07.007.

Filippi M, Agosta F. Imaging biomarkers in multiple sclerosis. *J Magn Reson Imaging* 2010; 31: 770-88.

Filippi M, Rocca MA. Conventional MRI in multiple sclerosis. *J Neuroimaging* 2007; 17 Suppl 1: 3S-9S.

Filippi M, Rocca MA, Barkhof F, et al. Association between pathological and MRI findings in multiple sclerosis. *Lancet Neurol* 2012; 11: 349-60.

Filippi M, Rocca MA, Benedict RH, et al. The contribution of MRI in assessing cognitive impairment in multiple sclerosis. *Neurology* 2010; 75: 2121-8.

Fischer JS, Rudick RA, Cutter GR, Reingold SC. The Multiple Sclerosis Functional Composite Measure (MSFC): an integrated approach to MS clinical outcome assessment. National MS Society Clinical Outcomes Assessment Task Force. *Mult Scler* 1999; 5: 244-50.

Fisher E, Lee JC, Nakamura K, Rudick RA. Gray matter atrophy in multiple sclerosis: a longitudinal study. *Ann Neurol* 2008; 64: 255-65.

Fisniku LK, Brex PA, Altmann DR, et al. Disability and T2 MRI lesions: a 20-year follow-up of patients with relapse onset of multiple sclerosis. *Brain* 2008; 131: 808-17.

Fisniku LK, Chard DT, Jackson JS, et al. Gray matter atrophy is related to long-term disability in multiple sclerosis. *Ann Neurol* 2008; 64: 247-54.

Forn C, Belenguer A, Belloch V, Sanjuan A, Parcet MA, Avila C. Anatomical and functional differences between the Paced Auditory Serial Addition Test and the Symbol Digit Modalities Test. *J Clin Exp Neuropsychol* 2011; 33: 42-50.

Frischer JM, Bramow S, Dal-Bianco A, et al. The relation between inflammation and neurodegeneration in multiple sclerosis brains. *Brain* 2009; 132: 1175-89.

Frohman EM, Filippi M, Stuve O, et al. Characterizing the mechanisms of progression in multiple sclerosis: evidence and new hypotheses for future directions. *Arch Neurol* 2005; 62: 1345-56.

Fu L, Matthews PM, De Stefano N, et al. Imaging axonal damage of normal-appearing white matter in multiple sclerosis. *Brain* 1998; 121 (Pt 1): 103-13.

Gagliardo A, Galli F, Grippo A, et al. Motor evoked potentials in multiple sclerosis patients without walking limitation: amplitude vs. conduction time abnormalities. *J Neurol* 2007; 254: 220-7.

Gaitan MI, Shea CD, Evangelou IE, et al. Evolution of the blood-brain barrier in newly forming multiple sclerosis lesions. *Ann Neurol* 2011; 70: 22-9.

BIBLIOGRAFÍA

Garcia-Barragan N, Villar LM, Espino M, Sadaba MC, Gonzalez-Porque P, Alvarez-Cermeno JC. Multiple sclerosis patients with anti-lipid oligoclonal IgM show early favourable response to immunomodulatory treatment. *Eur J Neurol* 2009; 16: 380-5.

Geurts JJ, Calabrese M, Fisher E, Rudick RA. Measurement and clinical effect of grey matter pathology in multiple sclerosis. *Lancet Neurol* 2012; 11: 1082-92.

Giovannelli F, Borgheresi A, Balestrieri F, et al. Modulation of interhemispheric inhibition by volitional motor activity: an ipsilateral silent period study. *J Physiol* 2009; 587: 5393-410.

Goodin DS. Magnetic resonance imaging as a surrogate outcome measure of disability in multiple sclerosis: have we been overly harsh in our assessment? *Ann Neurol* 2006; 59: 597-605.

Grassiot B, Desgranges B, Eustache F, Defer G. Quantification and clinical relevance of brain atrophy in multiple sclerosis: a review. *J Neurol* 2009; 256: 1397-412.

Griffin CM, Chard DT, Ciccarelli O, et al. Diffusion tensor imaging in early relapsing-remitting multiple sclerosis. *Mult Scler* 2001; 7: 290-7.

Guo J, Ji Q, Reddick WE. Multi-slice myelin water imaging for practical clinical applications at 3.0 T. *Magn Reson Med* 2012.

Hoppner J, Kunesch E, Buchmann J, Hess A, Grossmann A, Benecke R. Demyelination and axonal degeneration in corpus callosum assessed by analysis of transcallosally mediated inhibition in multiple sclerosis. *Clin Neurophysiol* 1999; 110: 748-56.

Horakova D, Kalincik T, Dusankova JB, Dolezal O. Clinical correlates of grey matter pathology in multiple sclerosis. *BMC Neurol* 2012; 12: 10.

Hutchinson M. Truly benign multiple sclerosis is rare: let's stop fooling ourselves--commentary. *Mult Scler* 2012; 18: 15.

Inusah S, Sormani MP, Cofield SS, et al. Assessing changes in relapse rates in multiple sclerosis. *Mult Scler* 2010; 16: 1414-21.

Invernizzi P, Bertolasi L, Bianchi MR, Turatti M, Gajofatto A, Benedetti MD. Prognostic value of multimodal evoked potentials in multiple sclerosis: the EP score. *J Neurol* 2011; 258: 1933-9.

Joseph FG, Hirst CL, Pickersgill TP, Ben-Shlomo Y, Robertson NP, Scolding NJ. CSF oligoclonal band status informs prognosis in multiple sclerosis: a case control study of 100 patients. *J Neurol Neurosurg Psychiatry* 2009; 80: 292-6.

Jung P, Beyerle A, Humpich M, Neumann-Haefelin T, Lanfermann H, Ziemann U. Ipsilateral silent period: a marker of callosal conduction abnormality in early relapsing-remitting multiple sclerosis? *J Neurol Sci* 2006; 250: 133-9.

Kale N, Agaoglu J, Tanik O. Electrophysiological and clinical correlates of corpus callosum atrophy in patients with multiple sclerosis. *Neurol Res* 2010; 32: 886-90.

Kern KC, Sarcona J, Montag M, Giesser BS, Sicotte NL. Corpus callosal diffusivity predicts motor impairment in relapsing-remitting multiple sclerosis: a TBSS and tractography study. *Neuroimage* 2011; 55: 1169-77.

Killestein J, Polman CH. Determinants of interferon beta efficacy in patients with multiple sclerosis. *Nat Rev Neurol* 2011; 7: 221-8.

Kirov, II, Patil V, Babb JS, Rusinek H, Herbert J, Gonon O. MR spectroscopy indicates diffuse multiple sclerosis activity during remission. *J Neurol Neurosurg Psychiatry* 2009; 80: 1330-6.

Kitzler HH, Su J, Zeineh M, et al. Deficient MWF mapping in multiple sclerosis using 3D whole-brain multi-component relaxation MRI. *Neuroimage* 2012; 59: 2670-7.

Koch-Henriksen N, Sorensen PS. The changing demographic pattern of multiple sclerosis epidemiology. *Lancet Neurol* 2010; 9: 520-32.

Kolasinski J, Stagg CJ, Chance SA, et al. A combined post-mortem magnetic resonance imaging and quantitative histological study of multiple sclerosis pathology. *Brain* 2012; 135: 2938-51.

Kurtzke JF. Rating neurologic impairment in multiple sclerosis: an expanded disability status scale (EDSS). *Neurology* 1983; 33: 1444-52.

Lassmann H. Models of multiple sclerosis: new insights into pathophysiology and repair. *Curr Opin Neurol* 2008; 21: 242-7.

Lassmann H, van Horssen J, Mahad D. Progressive multiple sclerosis: pathology and pathogenesis. *Nat Rev Neurol* 2012; 8: 647-56.

BIBLIOGRAFÍA

Laule C, Kozlowski P, Leung E, Li DK, Mackay AL, Moore GR. Myelin water imaging of multiple sclerosis at 7 T: correlations with histopathology. *Neuroimage* 2008; 40: 1575-80.

Laule C, Vavasour IM, Moore GR, et al. Water content and myelin water fraction in multiple sclerosis. A T2 relaxation study. *J Neurol* 2004; 251: 284-93.

Lenzi D, Conte A, Mainero C, et al. Effect of corpus callosum damage on ipsilateral motor activation in patients with multiple sclerosis: a functional and anatomical study. *Hum Brain Mapp* 2007; 28: 636-44.

Leocani L, Comi G. Neurophysiological markers. *Neurol Sci* 2008; 29 Suppl 2: S218-21.

Leray E, Yaouanq J, Le Page E, et al. Evidence for a two-stage disability progression in multiple sclerosis. *Brain* 2010; 133: 1900-13.

Lin X, Tench CR, Morgan PS, Constantinescu CS. Use of combined conventional and quantitative MRI to quantify pathology related to cognitive impairment in multiple sclerosis. *J Neurol Neurosurg Psychiatry* 2008; 79: 437-41.

Lin X, Tench CR, Morgan PS, Niepel G, Constantinescu CS. 'Importance sampling' in MS: use of diffusion tensor tractography to quantify pathology related to specific impairment. *J Neurol Sci* 2005; 237: 13-9.

Liu Y, Duan Y, He Y, et al. Whole brain white matter changes revealed by multiple diffusion metrics in multiple sclerosis: a TBSS study. *Eur J Radiol* 2012; 81: 2826-32.

Loureiro P, Shirani A, Saeedi J, Oger J, Schreiber WE, Tremlett H. Oligoclonal bands and cerebrospinal fluid markers in multiple sclerosis: associations with disease course and progression. *Mult Scler* 2013; 19: 577-84.

Lucchinetti C, Bruck W, Parisi J, Scheithauer B, Rodriguez M, Lassmann H. Heterogeneity of multiple sclerosis lesions: implications for the pathogenesis of demyelination. *Ann Neurol* 2000; 47: 707-17.

Lucchinetti CF, Altintas A, Wegner C, et al. Magnetic Resonance Imaging Correlates of Multiple Sclerosis Pathologic Subtypes. *Ann Neurol* 2003; 54 (Suppl 7): S37.

Lucchinetti CF, Gavrilova RH, Metz I, et al. Clinical and radiographic spectrum of pathologically confirmed tumefactive multiple sclerosis. *Brain* 2008; 131: 1759-75.

Lukas C, Minneboo A, de Groot V, et al. Early central atrophy rate predicts 5 year clinical outcome in multiple sclerosis. *J Neurol Neurosurg Psychiatry* 2010; 81: 1351-6.

Margaritella N, Mendoza L, Garegnani M, et al. Exploring the predictive value of the evoked potentials score in MS within an appropriate patient population: a hint for an early identification of benign MS? *BMC Neurol* 2012; 12: 80.

Marrie RA. Environmental risk factors in multiple sclerosis aetiology. *Lancet Neurol* 2004; 3: 709-18.

Mesaros S, Rocca MA, Riccitelli G, et al. Corpus callosum damage and cognitive dysfunction in benign MS. *Hum Brain Mapp* 2009; 30: 2656-66.

Miller DH, Barkhof F, Frank JA, Parker GJ, Thompson AJ. Measurement of atrophy in multiple sclerosis: pathological basis, methodological aspects and clinical relevance. *Brain* 2002; 125: 1676-95.

Miller DH, Chard DT, Ciccarelli O. Clinically isolated syndromes. *Lancet Neurol* 2012; 11: 157-69.

Miller DM, Rudick RA, Cutter G, Baier M, Fischer JS. Clinical significance of the multiple sclerosis functional composite: relationship to patient-reported quality of life. *Arch Neurol* 2000; 57: 1319-24.

Mitosek-Szewczyk K, Gordon-Kraicer W, Flis D, Stelmasiak Z. Some markers of neuronal damage in cerebrospinal fluid of multiple sclerosis patients in relapse. *Folia Neuropathol* 2011; 49: 191-6.

Montalban X, Tintore M, Swanton J, et al. MRI criteria for MS in patients with clinically isolated syndromes. *Neurology* 2010; 74: 427-34.

Moore CS, Abdullah SL, Brown A, Arulpragasam A, Crocker SJ. How factors secreted from astrocytes impact myelin repair. *J Neurosci Res* 2011; 89: 13-21.

Morgen K, Jeffries NO, Stone R, et al. Ring-enhancement in multiple sclerosis: marker of disease severity. *Mult Scler* 2001; 7: 167-71.

Morgen K, Sammer G, Courtney SM, et al. Evidence for a direct association between cortical atrophy and cognitive impairment in relapsing-remitting MS. *Neuroimage* 2006; 30: 891-8.

BIBLIOGRAFÍA

Nair A, Frederick TJ, Miller SD. Astrocytes in multiple sclerosis: a product of their environment. *Cell Mol Life Sci* 2008; 65: 2702-20.

Narayana PA. Magnetic resonance spectroscopy in the monitoring of multiple sclerosis. *J Neuroimaging* 2005; 15: 46S-57S.

Oh J, Han ET, Lee MC, Nelson SJ, Pelletier D. Multislice brain myelin water fractions at 3T in multiple sclerosis. *J Neuroimaging* 2007; 17: 156-63.

Onu M, Roceanu A, Sboto-Frankenstein U, et al. Diffusion abnormality maps in demyelinating disease: correlations with clinical scores. *Eur J Radiol* 2012; 81: e386-91.

Otero-Romero S, Roura P, Sola J, et al. Increase in the prevalence of multiple sclerosis over a 17-year period in Osona, Catalonia, Spain. *Mult Scler* 2012.

Ozturk A, Smith SA, Gordon-Lipkin EM, et al. MRI of the corpus callosum in multiple sclerosis: association with disability. *Mult Scler* 2010; 16: 166-77.

Patti F. Cognitive impairment in multiple sclerosis. *Mult Scler* 2009; 15: 2-8.

Pelletier J, Suchet L, Witjas T, et al. A longitudinal study of callosal atrophy and interhemispheric dysfunction in relapsing-remitting multiple sclerosis. *Arch Neurol* 2001; 58: 105-11.

Penny S, Khaleeli Z, Cipolotti L, Thompson A, Ron M. Early imaging predicts later cognitive impairment in primary progressive multiple sclerosis. *Neurology* 2010; 74: 545-52.

Pirko I, Lucchinetti CF, Sriram S, Bakshi R. Gray matter involvement in multiple sclerosis. *Neurology* 2007; 68: 634-42.

Polman CH, Reingold SC, Banwell B, et al. Diagnostic criteria for multiple sclerosis: 2010 revisions to the McDonald criteria. *Ann Neurol* 2011; 69: 292-302.

Popescu BF, Pirko I, Lucchinetti CF. Pathology of multiple sclerosis: where do we stand? *Continuum (Minneapolis Minn)* 2013; 19: 901-21.

Popescu V, Agosta F, Hulst HE, et al. Brain atrophy and lesion load predict long term disability in multiple sclerosis. *J Neurol Neurosurg Psychiatry* 2013.

Portaccio E, Stromillo ML, Goretti B, et al. Neuropsychological and MRI measures predict short-term evolution in benign multiple sclerosis. *Neurology* 2009; 73: 498-503.

Prentice RL. Surrogate endpoints in clinical trials: definition and operational criteria. *Stat Med* 1989; 8: 431-40.

Preziosa P, Rocca MA, Mesaros S, et al. Intrinsic damage to the major white matter tracts in patients with different clinical phenotypes of multiple sclerosis: a voxelwise diffusion-tensor MR study. *Radiology* 2011; 260: 541-50.

Pugliatti M, Rosati G, Carton H, et al. The epidemiology of multiple sclerosis in Europe. *Eur J Neurol* 2006; 13: 700-22.

Rajasekharan S, Bar-Or A. From bench to MS bedside: challenges translating biomarker discovery to clinical practice. *J Neuroimmunol* 2012; 248: 66-72.

Rio J, Rovira A, Tintore M, et al. Relationship between MRI lesion activity and response to IFN-beta in relapsing-remitting multiple sclerosis patients. *Mult Scler* 2008; 14: 479-84.

Rocca MA, Messina R, Filippi M. Multiple sclerosis imaging: recent advances. *J Neurol* 2012.

Roosendaal SD, Geurts JJ, Vrenken H, et al. Regional DTI differences in multiple sclerosis patients. *Neuroimage* 2009; 44: 1397-403.

Rossi F, Giorgio A, Battaglini M, et al. Relevance of brain lesion location to cognition in relapsing multiple sclerosis. *PLoS One* 2012; 7: e44826.

Rovaris M, Bozzali M, Iannucci G, et al. Assessment of normal-appearing white and gray matter in patients with primary progressive multiple sclerosis: a diffusion-tensor magnetic resonance imaging study. *Arch Neurol* 2002; 59: 1406-12.

Rovaris M, Iannucci G, Falautano M, et al. Cognitive dysfunction in patients with mildly disabling relapsing-remitting multiple sclerosis: an exploratory study with diffusion tensor MR imaging. *J Neurol Sci* 2002; 195: 103-9.

Ruiz-Pena JL, Pinero P, Sellers G, et al. Magnetic resonance spectroscopy of normal appearing white matter in early relapsing-remitting multiple sclerosis: correlations between disability and spectroscopy. *BMC Neurol* 2004; 4: 8.

Sajja BR, Wolinsky JS, Narayana PA. Proton magnetic resonance spectroscopy in multiple sclerosis. *Neuroimaging Clin N Am* 2009; 19: 45-58.

BIBLIOGRAFÍA

Sarchielli P, Presciutti O, Pelliccioli GP, et al. Absolute quantification of brain metabolites by proton magnetic resonance spectroscopy in normal-appearing white matter of multiple sclerosis patients. *Brain* 1999; 122 (Pt 3): 513-21.

Sastre-Garriga J, Ingle GT, Chard DT, et al. Metabolite changes in normal-appearing gray and white matter are linked with disability in early primary progressive multiple sclerosis. *Arch Neurol* 2005; 62: 569-73.

Sbardella E, Tomassini V, Stromillo ML, et al. Pronounced focal and diffuse brain damage predicts short-term disease evolution in patients with clinically isolated syndrome suggestive of multiple sclerosis. *Mult Scler* 2011; 17: 1432-40.

Sbardella E, Tona F, Petsas N, Pantano P. DTI Measurements in Multiple Sclerosis: Evaluation of Brain Damage and Clinical Implications. *Mult Scler Int* 2013; 2013: 671730.

Scalfari A, Neuhaus A, Degenhardt A, et al. The natural history of multiple sclerosis: a geographically based study 10: relapses and long-term disability. *Brain* 2010; 133: 1914-29.

Schwartz KM, Erickson BJ, Lucchinetti C. Pattern of T2 hypointensity associated with ring-enhancing brain lesions can help to differentiate pathology. *Neuroradiology* 2006; 48: 143-9.

Sepulcre J, Masdeu JC, Pastor MA, et al. Brain pathways of verbal working memory: a lesion-function correlation study. *Neuroimage* 2009; 47: 773-8.

Sepulcre J, Masdeu JC, Sastre-Garriga J, et al. Mapping the brain pathways of declarative verbal memory: Evidence from white matter lesions in the living human brain. *Neuroimage* 2008; 42: 1237-43.

Sepulcre J, Vanotti S, Hernandez R, et al. Cognitive impairment in patients with multiple sclerosis using the Brief Repeatable Battery-Neuropsychology test. *Mult Scler* 2006; 12: 187-95.

Sigal T, Shmuel M, Mark D, Gil H, Anat A. Diffusion tensor imaging of corpus callosum integrity in multiple sclerosis: correlation with disease variables. *J Neuroimaging* 2012; 22: 33-7.

Simpson S, Jr., Blizzard L, Otahal P, Van der Mei I, Taylor B. Latitude is significantly associated with the prevalence of multiple sclerosis: a meta-analysis. *J Neurol Neurosurg Psychiatry* 2011; 82: 1132-41.

Siritho S, Freedman MS. The prognostic significance of cerebrospinal fluid in multiple sclerosis. *J Neurol Sci* 2009; 279: 21-5.

Song SK, Sun SW, Ju WK, Lin SJ, Cross AH, Neufeld AH. Diffusion tensor imaging detects and differentiates axon and myelin degeneration in mouse optic nerve after retinal ischemia. *Neuroimage* 2003; 20: 1714-22.

Song SK, Sun SW, Ramsbottom MJ, Chang C, Russell J, Cross AH. Dysmyelination revealed through MRI as increased radial (but unchanged axial) diffusion of water. *Neuroimage* 2002; 17: 1429-36.

Song SK, Yoshino J, Le TQ, et al. Demyelination increases radial diffusivity in corpus callosum of mouse brain. *Neuroimage* 2005; 26: 132-40.

Squire LR. Memory systems of the brain: a brief history and current perspective. *Neurobiol Learn Mem* 2004; 82: 171-7.

Stangel M, Fredrikson S, Meinl E, Petzold A, Stuve O, Tumani H. The utility of cerebrospinal fluid analysis in patients with multiple sclerosis. *Nat Rev Neurol* 2013; 9: 267-76.

Stuve O, Cravens PD, Frohman EM, et al. Immunologic, clinical, and radiologic status 14 months after cessation of natalizumab therapy. *Neurology* 2009; 72: 396-401.

Tallantyre EC, Bo L, Al-Rawashdeh O, et al. Clinico-pathological evidence that axonal loss underlies disability in progressive multiple sclerosis. *Mult Scler* 2010; 16: 406-11.

Teunissen CE, Dijkstra C, Polman C. Biological markers in CSF and blood for axonal degeneration in multiple sclerosis. *Lancet Neurol* 2005; 4: 32-41.

Thurtell MJ, Galetta SL. Low-contrast multifocal visual evoked potentials: identifying more shades of gray in MS. *Neurology* 2012; 79: 732-3.

Tintore M, Rovira A, Rio J, et al. Do oligoclonal bands add information to MRI in first attacks of multiple sclerosis? *Neurology* 2008; 70: 1079-83.

Trapp BD, Peterson J, Ransohoff RM, Rudick R, Mork S, Bo L. Axonal transection in the lesions of multiple sclerosis. *N Engl J Med* 1998; 338: 278-85.

Tumani H, Hartung HP, Hemmer B, et al. Cerebrospinal fluid biomarkers in multiple sclerosis. *Neurobiol Dis* 2009; 35: 117-27.

van Waesberghe JH, Kamphorst W, De Groot CJ, et al. Axonal loss in multiple sclerosis lesions: magnetic resonance imaging insights into substrates of disability. *Ann Neurol* 1999; 46: 747-54.

BIBLIOGRAFÍA

Villar LM, Garcia-Sanchez MI, Costa-Frossard L, et al. Immunological markers of optimal response to natalizumab in multiple sclerosis. *Arch Neurol* 2012; 69: 191-7.

Villar LM, Masjuan J, Gonzalez-Porque P, et al. Intrathecal IgM synthesis is a prognostic factor in multiple sclerosis. *Ann Neurol* 2003; 53: 222-6.

Villar LM, Masterman T, Casanova B, et al. CSF oligoclonal band patterns reveal disease heterogeneity in multiple sclerosis. *J Neuroimmunol* 2009; 211: 101-4.

Villoslada P, Baranzini S. Data integration and systems biology approaches for biomarker discovery: challenges and opportunities for multiple sclerosis. *J Neuroimmunol* 2012; 248: 58-65.

Vukusic S, Confavreux C. Prognostic factors for progression of disability in the secondary progressive phase of multiple sclerosis. *J Neurol Sci* 2003; 206: 135-7.

Wattjes MP, Harzheim M, Lutterbey GG, et al. Prognostic value of high-field proton magnetic resonance spectroscopy in patients presenting with clinically isolated syndromes suggestive of multiple sclerosis. *Neuroradiology* 2008; 50: 123-9.

Wilson M, Tench CR, Morgan PS, Blumhardt LD. Pyramidal tract mapping by diffusion tensor magnetic resonance imaging in multiple sclerosis: improving correlations with disability. *J Neurol Neurosurg Psychiatry* 2003; 74: 203-7.

Williams A, Piaton G, Lubetzki C. Astrocytes--friends or foes in multiple sclerosis? *Glia* 2007; 55: 1300-12.

Wolk DA, Dickerson BC. Fractionating verbal episodic memory in Alzheimer's disease. *Neuroimage* 2011; 54: 1530-9.

Yaldizli O, Atefy R, Gass A, et al. Corpus callosum index and long-term disability in multiple sclerosis patients. *J Neurol* 2010; 257: 1256-64.

Yu HJ, Christodoulou C, Bhise V, et al. Multiple white matter tract abnormalities underlie cognitive impairment in RRMS. *Neuroimage* 2012; 59: 3713-22.

Zivadinov R, Pirko I. Advances in understanding gray matter pathology in multiple sclerosis: are we ready to redefine disease pathogenesis? *BMC Neurol* 2012; 12: 9.